

AL-TR-1991-0129

AD-A245 866



VERTICAL IMPACT TESTS OF HUMANS AND ANTHROPOMORPHIC MANIKINS

John R. Buhrman

CREW SYSTEMS DIRECTORATE
BIODYNAMICS AND BIOCOMMUNICATIONS DIVISION

APRIL 1991

DTIC
ELECTE
FEB 12 1992
S B D

INTERIM REPORT FOR PERIOD 29 SEPTEMBER 1987 TO MARCH 1988

92-03306



Approved for public release; distribution is unlimited.

92 2 10 0 8

AIR FORCE SYSTEMS COMMAND
WRIGHT-PATTERSON AIR FORCE BASE, OHIO 45433-6573

ARMSTRONG
LABORATORY

NOTICES

When US Government drawings, specifications, or other data are used for any purpose other than a definitely related Government procurement operation, the Government thereby incurs no responsibility nor any obligation whatsoever, and the fact that the Government may have formulated, furnished, or in any way supplied the said drawings, specifications, or other data, is not to be regarded by implication or otherwise, as in any manner licensing the holder or any other person or corporation, or conveying any rights or permission to manufacture, use or sell any patented invention that may in any way be related thereto.

Please do not request copies of this report from the Armstrong Laboratory. Additional copies may be purchased from:

National Technical Information Service
5285 Port Royal Road
Springfield VA 22161

Federal Government agencies and their contractors registered with Defense Technical Information Center should direct requests for copies of this report to:

Defense Technical Information Center
Cameron Station
Alexandria VA 22314

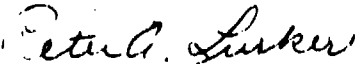
TECHNICAL REVIEW AND APPROVAL

AL-TR-1991-0129

The voluntary informed consent of the subjects used in this research was obtained as required by Air Force Regulation 169-3.

This report has been reviewed by the Office of Public Affairs (PA) and is releasable to the National Technical Information Service (NTIS). At NTIS, it will be available to the general public, including foreign nations.

This technical report has been reviewed and is approved for publication.


PETER A. LURKER, Lt Col, USAF, BSC
Acting Director
Biodynamics and Biocommunications Division
Armstrong Laboratory

REPORT DOCUMENTATION PAGE

Form Approved
OMB No. 0704-0188

Public reporting burden for this collection of information is estimated to average 1 hour per response, including the time for reviewing instructions, searching existing data sources, gathering and maintaining the data needed, and completing and reviewing the collection of information. Send comments regarding this burden estimate or any other aspect of this collection of information, including suggestions for reducing this burden, to Washington Headquarters Services, Directorate for Information Operations and Reports, 1215 Jefferson Davis Highway, Suite 1204, Arlington, VA 22202-4302, and to the Office of Management and Budget, Paperwork Reduction Project (0704-0188), Washington, DC 20503.

1. AGENCY USE ONLY (Leave blank)		2. REPORT DATE April 1991		3. REPORT TYPE AND DATES COVERED Interim - 29 Sep 87 to 19 Apr 91	
4. TITLE AND SUBTITLE Vertical Impact Tests of Humans and Anthropomorphic Manikins				5. FUNDING NUMBERS PE - 62202F PR - 7231 TA - 723131 WU - 72313101	
6. AUTHOR(S) John R. Buhrman					
7. PERFORMING ORGANIZATION NAME(S) AND ADDRESS(ES)				8. PERFORMING ORGANIZATION REPORT NUMBER AL-TR-1991-0129	
9. SPONSORING/MONITORING AGENCY NAME(S) AND ADDRESS(ES)				10. SPONSORING/MONITORING AGENCY REPORT NUMBER	
11. SUPPLEMENTARY NOTES					
12a. DISTRIBUTION/AVAILABILITY STATEMENT Approved for public release; distribution is unlimited				12b. DISTRIBUTION CODE	
13. ABSTRACT (Maximum 200 words) Small and large prototype Advanced Dynamic Anthropomorphic Manikins (ADAMs) along with CG-95 and CG-95 GARD manikins, were subjected to impacts up to +24 Gz on a vertical deceleration tower. Human subjects were also tested at levels of up to +10 Gz. The test variables were acceleration input and rise-time, seat-back angle, restraint harness, and seat cushion. Both the small and large ADAMs were found to be structurally sound at test up to +24 Gz. Data acquisition, however, was often incomplete, due mostly to broken wires, noisy channels, and circuit board failures. Both ADAM manikins demonstrated reasonable good repeatability of acceleration and force data in the direction of impact, although the channel sensitivities appeared to gradually change with repeated tests. The small ADAM appeared to demonstrate relatively consistent simulation of human dynamic response in the z-axis, but the large ADAM had a tendency to generate larger peak acceleration and seat force data than expected. Employing a Confor™ Foam seat cushion appeared to have almost no effect on human dynamic response. The X-Band 90° restraint harness appeared to outperform the PCU-15/P harness in the human tests. Varying the seat-back angle +10° significantly effected only the peak magnitude of the x-axis chest acceleration data.					
14. SUBJECT TERMS ADAM GARD Manikin Impact Seat Cushion Restrain Harness Sensitivity Rise-Time Repeatability				15. NUMBER OF PAGES 148	
				16. PRICE CODE	
17. SECURITY CLASSIFICATION OF REPORT UNCLASSIFIED	18. SECURITY CLASSIFICATION OF THIS PAGE UNCLASSIFIED	19. SECURITY CLASSIFICATION OF ABSTRACT UNCLASSIFIED	20. LIMITATION OF ABSTRACT UL		

GENERAL INSTRUCTIONS FOR COMPLETING SF 298

The Report Documentation Page (RDP) is used in announcing and cataloging reports. It is important that this information be consistent with the rest of the report, particularly the cover and title page. Instructions for filling in each block of the form follow. It is important to *stay within the lines* to meet optical scanning requirements.

Block 1. Agency Use Only (Leave blank).

Block 2. Report Date. Full publication date including day, month, and year, if available (e.g. 1 Jan 88). Must cite at least the year.

Block 3. Type of Report and Dates Covered. State whether report is interim, final, etc. If applicable, enter inclusive report dates (e.g. 10 Jun 87 - 30 Jun 88).

Block 4. Title and Subtitle. A title is taken from the part of the report that provides the most meaningful and complete information. When a report is prepared in more than one volume, repeat the primary title, add volume number, and include subtitle for the specific volume. On classified documents enter the title classification in parentheses.

Block 5. Funding Numbers. To include contract and grant numbers; may include program element number(s), project number(s), task number(s), and work unit number(s). Use the following labels:

C - Contract	PR - Project
G - Grant	TA - Task
PE - Program Element	WU - Work Unit Accession No.

Block 6. Author(s). Name(s) of person(s) responsible for writing the report, performing the research, or credited with the content of the report. If editor or compiler, this should follow the name(s).

Block 7. Performing Organization Name(s) and Address(es). Self-explanatory.

Block 8. Performing Organization Report Number. Enter the unique alphanumeric report number(s) assigned by the organization performing the report.

Block 9. Sponsoring/Monitoring Agency Name(s) and Address(es). Self-explanatory.

Block 10. Sponsoring/Monitoring Agency Report Number. (If known)

Block 11. Supplementary Notes. Enter information not included elsewhere such as: Prepared in cooperation with...; Trans. of...; To be published in.... When a report is revised, include a statement whether the new report supersedes or supplements the older report.

Block 12a. Distribution/Availability Statement. Denotes public availability or limitations. Cite any availability to the public. Enter additional limitations or special markings in all capitals (e.g. NOFORN, REL, ITAR).

DOD - See DoDD 5230.24, "Distribution Statements on Technical Documents."

DOE - See authorities.

NASA - See Handbook NHB 2200.2.

NTIS - Leave blank.

Block 12b. Distribution Code.

DOD - Leave blank.

DOE - Enter DOE distribution categories from the Standard Distribution for Unclassified Scientific and Technical Reports.

NASA - Leave blank.

NTIS - Leave blank.

Block 13. Abstract. Include a brief (Maximum 200 words) factual summary of the most significant information contained in the report.

Block 14. Subject Terms. Keywords or phrases identifying major subjects in the report.

Block 15. Number of Pages. Enter the total number of pages.

Block 16. Price Code. Enter appropriate price code (NTIS only).

Blocks 17. - 19. Security Classifications. Self-explanatory. Enter U.S. Security Classification in accordance with U.S. Security Regulations (i.e., UNCLASSIFIED). If form contains classified information, stamp classification on the top and bottom of the page.

Block 20. Limitation of Abstract. This block must be completed to assign a limitation to the abstract. Enter either UL (unlimited) or SAR (same as report). An entry in this block is necessary if the abstract is to be limited. If blank, the abstract is assumed to be unlimited.

PREFACE

The tests described within this report were accomplished by the Crew Protection Branch, Biodynamics and Bioengineering Division of the Armstrong Laboratory at Wright-Patterson Air Force Base, Ohio. The test program was sponsored by the Crew Escape Technologies (CREST) Advanced Development Program Office (ADPO), Human Systems Division. Lt Col Michael Higgins was the CREST program manager.

Support of the ADAM manikin was provided by the Modeling and Analysis Branch of the Biodynamics and Bioengineering Division and also by Systems Research Laboratories, Inc. of Dayton, Ohio. Mr Roy Rasmussen was the Contract Technical Monitor for the ADAM development program. The program manager for Systems Research Laboratories was Richard P. White, Jr.

The impact facilities, data acquisition equipment, and data processing system were operated by the Scientific Services Division of DynCorp under Air Force contract F33615-86-C-0531. Mr Marshall Miller was the Engineering Supervisor for DynCorp.

Photographic data and documentation services were provided by the Technical Photographic Division of the 4950th Test Wing.

Accession For	
NTIS GRA&I	<input checked="checked" type="checkbox"/>
DTIC TAB	<input type="checkbox"/>
Unannounced	<input type="checkbox"/>
Justification	
By	
Distribution/	
Availability Codes	
Dist	Avail and/or Special
A-1	

TABLE OF CONTENTS

PREFACE	iii
TABLE OF CONTENTS	v
LIST OF FIGURES	vii
LIST OF TABLES	vii
LIST OF ABBREVIATIONS	viii
INTRODUCTION	1
Background	1
Test Objectives	1
ADAM Evaluation Criteria	2
METHODS	3
Test Facilities and Equipment	3
Human Subjects	3
Instrumentation and Data Processing	3
Photogrammetric Data	4
Experimental Design	5
RESULTS	8
Test-by-Test Narrative	8
Structural Adequacy of ADAM	13
ADAM Instrumentation	13
ADAM Sensitivity	14
Repeatability of Manikin Dynamic Response	19
Manikin Simulation of Human Dynamic Response	23
Acceleration Response	23
Seat Forces	28
Manikin Response vs. Sled Acceleration Level	28
Transfer Function Analysis	28
Seat Cushions	36
Human Dynamic Response	36
Manikin Dynamic Response	37
Restraint Harness	38
Human Dynamic Response	38
Manikin Dynamic Response	40
Seat-Back Angle	40
Human Dynamic Response	40
Manikin Dynamic Response	41
Varying Rise-Time	42
Human Dynamic Response	42
Manikin Dynamic Response	42
DISCUSSION	44
ADAM Reliability	44
ADAM Sensitivity	44
Repeatability of Manikin Dynamic Response	45
Manikin Simulation of Human Dynamic Response	45
Seat Cushions	46
Restraint Harness	46
Seat-Back Angle	46
Varying Rise-Time	47
SUMMARY AND CONCLUSIONS	48
Summary	48
Conclusions	48
REFERENCES	50

TABLE OF CONTENTS (continued)

APPENDIX A. Test Configuration and Data Acquisition System	51
APPENDIX B. Anthropometry of Test Subjects	109
APPENDIX C. Numerical Listing of Tests	110
APPENDIX D. Transfer Function Analysis Plots	113
APPENDIX E. Sample Data	118

LIST OF FIGURES

FIGURE		PAGE
1	Resultant Seat Force vs. Subject Weight, Cell A	29
2	Resultant Seat Force vs. Subject Weight, Cell B	29
3	Resultant Seat Force vs. Subject Weight, Cell C	30
4	Resultant Seat Force vs. Subject Weight, Cell D	30
5	Resultant Seat Force vs. Subject Weight, Cell E	31
6	Resultant Seat Force vs. Subject Weight, Cell F	31
7	Head Z Acceleration vs. Carriage Acceleration	32
8	Chest Z Acceleration vs. Carriage Acceleration	32
9	Head X Acceleration vs. Carriage Acceleration	33
10	Resultant Seat Force vs. Carriage Acceleration	33
11	Lumbar Z Force vs. Carriage Acceleration	34
12	Neck Z Force vs. Carriage Acceleration	34
13	Responses of CG-95 Manikin With and Without Confor TM Foam Seat Cushion	39

LIST OF TABLES

TABLE		PAGE
1	Experimental Test Conditions	5
2	Subject Test Summary	6
3	ADAM Low-Level Channel Sensitivity Changes	14
4	ADAM High-Level Channel Sensitivity Changes	15
5	Mean ADAM Low-Level Channel Calibration Voltage Changes	17
6	Mean ADAM High-Level Channel Calibration Voltage Changes	18
7	ADAM-S Dynamic Response Repeatability	20
8	ADAM-L Dynamic Response Repeatability	21
9	CG-5 Dynamic Response Repeatability	22
10	CG-95 Dynamic Response Repeatability	22
11	F-Test Comparison of Manikin Standard Deviations	23
12	Mean Acceleration Data for Cells A, B, and C	24
13	Mean Acceleration Data for Cells D, E, and F	25
14	Wilcoxon Rank Sum Test Summaries of ADAM vs. Human Acceleration Data in Cell C	27
15	Wilcoxon Rank Sum Test Summaries of GARD vs. Human Acceleration Data in Cell C	27
16	Resonant Frequency	35
17	Damping Ratio	36
18	Wilcoxon Signed Rank Test Summaries for Human Subject Confor TM Foam Seat Cushion Comparisons	37
19	Wilcoxon Signed Rank Test Summaries for Human Subject ACES II Seat Cushion Comparisons	37
20	Wilcoxon Signed Rank Test Summaries for Human Subject Restraint Harness Comparisons	40
21	Wilcoxon Signed Rank Test Summaries for Human Subject +10° Seat-Back Angle Comparisons	41
22	Wilcoxon Signed Rank Test Summaries for Human Subject -10° Seat-Back Angle Comparisons	41
23	Wilcoxon Signed Rank Test Summaries for Human Subject Varying Rise-Time Comparisons	42

LIST OF ABBREVIATIONS

ADAM	Advanced Dynamic Anthropomorphic Manikin
ADACS	Automatic Data Acquisition and Control System
CG-5	Center of Gravity GARD 5th Percentile Manikin
CG-95	Center of Gravity GARD 95th Percentile Manikin
DDI	DECOM to DRASS Interface
DECOM	ADAM Decommutator Data Transmission System
DRASS	ADAM Data Retrieval and Storage System
DRI	Dynamic Response Index
FPS	ADAM Field Power Supply
GARD	Grumman-Alderson Research Dummy
NSD	No Significant Difference
RAM	ADAM Internal Data Storage System
RCAL	ADAM Calibration Voltage
SRL	Systems Research Laboratories, Inc.
VDT	Vertical Deceleration Tower
VIP-95	Alderson 95th Percentile Manikin

INTRODUCTION

Background

Tests of human subject dynamic response to impact as well as the use of anthropomorphic manikins to simulate human dynamic response in cockpit ejection tests have become increasingly important with the development of advanced aircraft systems.

This test program was conducted as part of the developmental phase of the Advanced Dynamic Anthropomorphic Manikin (ADAM) program. This program was the first in a series of experiments that were conducted to map the dynamic response properties of ADAM manikins in impact environments, and to compare the ADAM responses to those of human subjects and other manikins currently in use by the Air Force.

The ADAM manikins were designed to withstand high acceleration levels while providing improved simulation of human dynamic response. The ADAM design incorporates an improved spinal system and joint motions, an increased number of sensors and channels, and an internal data storage system as well as an external data transmission link. Small and large ADAM anthropometry approximated the 3rd and 97th percentiles of military flying personnel. (1)

One small and one large ADAM prototype were provided for a series of tests at AAMRL. Tests were conducted using the AAMRL vertical deceleration tower facility. Test data were collected and analyzed to determine the adequacy of the ADAM dynamic responses to +Gz acceleration as well as to test the structural integrity of ADAM. Human subjects were also tested as part of the same program to demonstrate the ability of the ADAM to simulate human dynamic response. In addition, two Grumman-Alderson Research (GARD) Dummies, the CG-5 and CG-95, representative of 5th and 95th percentile Air Force flying personnel, were also tested to provide a means of comparing ADAM dynamic responses to those of other manikins. All subjects were tested at carriage acceleration levels of 10 G with seat-back positions that were aligned at angles of -10, 0, and +10 degrees with respect to the acceleration vector. The dynamic responses were measured under two different restraint conditions and three seat cushion conditions. The two ADAM manikins were also tested at acceleration levels of up to 24 G to provide additional information on their structural integrity.

Test Objectives

The specific objectives of the tests were as follows:

1. To measure the dynamic response of the human body during +z-axis impact with seat-back angles of 10, 0, and -10 degrees.
2. To measure the dynamic response of the ADAM prototypes during +z-axis impact with seat-back angles of 10, 0, and -10 degrees.
3. To measure the dynamic response of the GARD manikins during +z-axis impact with seat-back angles of 10, 0, and -10 degrees.
4. To measure the dynamic response of human subjects, the ADAM prototypes, and the GARD manikins with and without seat cushions.

5. To measure the dynamic response of human subjects, the ADAM prototypes, and the GARD manikins with the CREST X-band 90 and PCU-15/P restraint harnesses.

6. To demonstrate the structural integrity of ADAM prototypes and instrumentation systems.

7. To demonstrate the functional capability of the ADAM instrumentation system.

ADAM Evaluation Criteria

The following evaluation criteria were to be used to evaluate the adequacy of the ADAM:

1. The primary resonance of the ADAM prototypes should be 10 Hz within ± 1 Hz as a goal. If the primary resonance is outside a band of ± 2 Hz about 10 Hz, the ADAM will not be considered adequate for ejection seat testing, and revision of its mechanical response properties will be recommended.

2. The peak force measured on the seat structure during impact tests of the ADAM prototypes shall be representative of the peak force measured with human subjects.

3. The ADAM prototypes shall withstand the 24 G impact without permanent deformation or failure of mechanical structures.

4. The ADAM prototypes shall collect data throughout the +z-axis impact tests without disruption due to the impact environment.

5. The ADAM instrumentation system shall collect data during replicate tests (test cell C) that shall be reproducible within ± 5 percent.

METHODS

Test Facilities and Equipment

All tests were conducted using the AL Vertical Deceleration Tower (VDT) and the VIP seat fixture. The seat-back was positioned at angles of -10, 0, or +10 degrees with respect to the +Gz acceleration vector. Metering pin number 102 was used to control the deceleration profile for all test conditions except cell D, where pin 46 was used. A head rest, which was individually adjusted for each subject, provided head support during the tests. The restraint harnesses used were the CREST X-Band-90 and the PCU-15/P with a lap belt. The harness straps were pretensioned to 20 +5 lbs at each attachment point prior to each test. Additional straps were used to maintain the initial position of the subjects' ankles and thighs during the free-fall phase of the test. The seat cushions used were the ACES II and the CREST Confor™ Foam and were placed on both the seat pan and seat back. See Appendix A for a more detailed description of the test facilities and equipment.

Human Subjects

Volunteer subjects were members of the AAMRL Impact Acceleration Stress Panel. They were selected and used in accordance with the applicable human use guidelines as specified in AFR 169-3 and in Protocol 85-07-02. Anthropometric measurements for each subject are listed in Appendix B. Each subject was provided with an abort switch from the control and safety system of the vertical deceleration tower. The switch was held in the right hand and was required to be depressed by the subject in order for the test to proceed. All subjects wore only cut-off long underwear along with an HGU-26/P USAF flight helmet during these tests. No upper extremity bracing was used in any of the tests. Standing blood pressure measurements were obtained before each test and electrocardiograms were recorded before, during, and after each test. A medical technician administered a post-test questionnaire designed to assess the subject's impressions of the test conditions.

Instrumentation and Data Processing

Accelerometers and load transducers were mounted to the seat fixture. The accelerometers included both linear and angular types. The load transducers included fixed load cells, triaxial load cells, and load links. All transducers were calibrated both before and after the tests. Carriage velocity was measured with a tachometer attached to an aluminum wheel on the carriage in contact with the track rail.

One small and one large ADAM prototype were tested along with one CG-5 and CG-95 GARD manikin. A 95th percentile Alderson manikin, the VIP-95, was used for structural and equipment proof tests. A triaxial linear accelerometer array and an angular accelerometer were used to measure head acceleration in the GARD and VIP-95 manikins and were mounted internally in the manikin heads. For the human subjects, both devices were attached to a bite-block which was individually prepared for each subject by the medical technician. The triaxial accelerometer array was mounted to a plexiglass block to provide electrical isolation of the device from the subject. The entire array was held within the subject's mouth during the impact

experiment. The angular accelerometer was used to measure acceleration about the y-axis. It was mounted on the frame's metal arm which extended from the subject's mouth and located at a fixed position relative to the triaxial translational accelerometer. Chest accelerations were measured by a triaxial linear accelerometer array mounted on an aluminum block and an adjacent angular accelerometer mounted on a bracket. These were attached to the chest of all manikins and human subjects with a velcro harness.

Each of the ADAM manikins contained the following internal sensors: triaxial linear accelerometers mounted in the head and chest, six-component load cells mounted in the head/neck and pelvis, and position sensors mounted in the torso and limbs. Signal amplification, filtering, digitization, and temporary storage of the data were provided by the internal ADAM electronic instrumentation system. Power for the ADAM internal electronics and sensor excitation was provided by the ADAM field power supply (FPS).

The ADAM data were transmitted over its own line in a whip cable via a decommutator and stored in the ADAM data retrieval and storage system (DRASS). Following an ADAM test the decommutated (DECOM) data were downloaded from the DRASS to a Z-100 computer for temporary storage and then transferred to a Vax computer for analysis. Data were also collected over a period of four seconds by the ADAM data acquisition system and stored in the ADAM on-board memory (RAM). The on-board RAM data were then downloaded to the DRASS, downloaded to the Z-100, and transferred to the Vax computer. A list of ADAM channel sensitivities was provided by the ADAM support contractor, Systems Research Laboratories, Inc. (SRL) to allow conversion of the digitized data into engineering units.

Eight ADAM sensors were also tapped at their outputs and coupled to an on-board automatic data acquisition and control system (ADACS) for signal conditioning. These sensors provided data for the following channels: Head X and Z Acceleration, Chest X Acceleration, Lumbar Z Acceleration, Lumbar Z Axial Load, Neck Z Axial Load, Right Knee Flexion Position, and Left Knee Flexion Position. An externally mounted sensor also provided data for Chest X, Y, and Z Acceleration. Data acquisition was controlled by a comparator on the master instrumentation control unit in the instrumentation station of the test facility. Signal conditioning, filtering, and digitization (at a rate of 1000 samples/sec) of the transducer signals was handled by the ADACS. The digitized data were transmitted through a whip cable to the computer room for storage on digital magnetic tape and processing by a Vax computer system. Test data were reviewed immediately after each test by using a "quick look" scan routine which produced plots of data over time. A list of ADACS channel sensitivities allowed conversion of the data to engineering units.

Sections 6 through 8 of Appendix A provide more detailed information on the transducers, instrumentation, and data processing described above.

Photogrammetric Data

Photogrammetric data were recorded on two 16 mm high-speed cameras mounted on the test fixture at oblique and right angles to the subject. Motion of the subjects' head, cheek, mouth, and chest were quantified by tracking the motion of subject-mounted fiducial targets. After processing of the

high-speed film, the data were digitized by an automatic film reader (AFR) system. A high-speed instant analytical replay (INSTARTM) video system was also used to provide coverage for each test. More detailed information on camera specifications, photogrammetric data processing, and subject fiducial targets can be found in section 7.2 of Appendix A.

Experimental Design

The independent variables in both the human and manikin tests were the acceleration of the carriage, the carriage velocity, the seat cushion, the seat-back angle, the restraint system, the metering pin (which controlled the impact rise-time and pulse duration), and the subject population. The dependent variables included the restraint-strap forces, seat-pan forces, seat-back forces, head and chest accelerations, and displacement of body segments. Tables 1 and 2 list the experimental conditions of each test cell as well as the number of tests of each subject, excluding proof tests. A complete listing by test number is given in Appendix C.

TABLE 1. EXPERIMENTAL TEST CONDITIONS

TEST CELL	ACCELERATION LEVEL (G)	SEAT CUSHIONS	SEAT-BACK ANGLE (°)	RESTRAINT HARNES
X	8	Confor TM Foam	0	X-Band 90
Y	8	Confor TM Foam	10	X-Band 90
A	10	Confor TM Foam	0	X-Band 90
B	10	Confor TM Foam	10	X-Band 90
C	10	None	0	X-Band 90
D	10	None	0	X-Band 90
E	10	None	0	PCU-15/P
F	10	ACES II	0	PCU-15/P
G	10	ACES II	-10	PCU-15/P
H	15	Confor TM Foam	0	X-Band 90
I	20	Confor TM Foam	0	X-Band 90
J	24	Confor TM Foam	0	X-Band 90
K	10	None	0	X-Band 90
L	10	Confor TM Foam	-10	X-Band 90
M	15	None	0	X-Band 90
N	20	None	0	X-Band 90
O	24	None	0	X-Band 90

TABLE 2. SUBJECT TEST SUMMARY

CELL	HUMAN	ADAM-S	ADAM-L	CG-5	CG-95
X	9	0	0	0	0
Y	6	0	0	0	0
A	14	1	1	1	1
B	14	3	4	1	1
C	14	6	8	6	6
D	14	1	1	2	1
E	14	2	8	1	1
F	14	1	5	1	1
G	0	1	1	1	1
H	0	4	5	3	5
I	0	1	3	1	1
J	0	1	2	1	1
K	0	0	0	0	0
L	10	0	0	1	1
M	0	0	0	1	0
N	0	0	0	1	0
O	0	0	0	1	0

A structural and equipment proof test was conducted at 15 G at the beginning of the test program to insure the integrity of the test apparatus for human tests. This test was accomplished with the Alderson VIP-95 anthropomorphic manikin. Additionally, a fully instrumented test was conducted with the VIP-95 manikin at each orientation and experimental test level prior to human subject tests. These tests were reviewed by the program investigators before proceeding with the human tests. As an added precaution, an uninstrumented manikin test was accomplished each day prior to human testing.

An initial series of tests was conducted with human subjects for orientation purposes. These tests were conducted at an acceleration level of 8 G with a Confor™ Foam seat cushion and an X-Band 90 restraint harness. Tests were conducted with both 0° and 10° seat-back angles (cells X and Y respectively).

For comparative evaluation and statistical analysis, the following null hypotheses were developed:

1. The dynamic responses of the human body during +z-axis impact are not different with seat-back angles of 0° and 10°.
2. There are no differences between the human responses when either seat cushions or no seat cushions are used for the +z-axis impact tests.
3. There are no differences between the manikin responses when either seat cushions or no seat cushions are used for the +z-axis impact tests.
4. The dynamic responses of the ADAM and the human body are not different during +z-axis impact.
5. The dynamic responses of the GARD manikin and the human body during +z-axis are not different.
6. The dynamic responses of the ADAM and the GARD manikin during +z-axis impact are not different.
7. The dynamic responses of the human body, the ADAM, and the GARD manikins during +z-axis impact are not different when the X-Band 90 harness or the PCU-15/P harness are used.

RESULTS

Test-by-Test Narrative

1. TEST 1419 ADAM-L CELL A

No data were present on the RAM/DECOM Lumbar Z Force channel. The conversion program developed by SRL incorrectly identified channel numbers instead of multiplexer numbers. The data were correctly reprocessed. The ADAM's arms and legs were not properly adjusted for stiffness by SRL before the test.

2. TEST 1420 ADAM-L CELL A

ADAM received three false start signals as the carriage was hoisted.

3. TEST 1433 ADAM-S CELL C

Noise was present in the Left Vertical Anchor X data. Repairing a connection did not alleviate the problem. False ADAM starts occurred.

4. TEST 1434 ADAM-S CELL C

Noise was present in the Left Vertical Anchor X data.

5. TEST 1438A ADAM-L CELL C

Wire insulation melted against a hot resistor inside ADAM. A dead battery cell was found in the right leg.

6. TEST 1438 ADAM-L CELL C

No RAM/DECOM data were present except in the Lumbar Z Acceleration channel. The cause was a failed component in the ADAM signal conditioning board power supply. Noise was present in the Left Vertical Anchor Z data.

7. TEST 1439 ADAM-L CELL C

A spike was present in the Left Vertical Z Anchor Force data. The cause was a faulty connection in the transducer line. Noise was again present in the Left Vertical Anchor Z data. ADAM shifted seat to right and head to left upon impact.

8. TEST 1452 ADAM-L CELL C

A spike was present in the Left Elbow Flexion data in both ADACS and RAM/DECOM. Noise was present in the RAM/DECOM Left Flexion Knee data.

9. TEST 1453 ADAM-L CELL C

The Left Elbow Flexion data was offset in both ADACS and RAM/DECOM.

10. TEST 1467 ADAM-L CELL C

The RAM data did not transfer to the DRASS. The cause was determined to be an IC chip on the digital I/O board involved in parallel port data transfer.

11. TEST 1494 ADAM-L CELL B

A false start caused ADAM to go into the data collection mode prematurely. ADAM was reset and the test proceeded normally. No RAM data were present. This was caused by a broken wire to the event marker channel. DECOM data could not be decoded by the computer (see test 1495).

12. TEST 1495 ADAM-S CELL B

The computer could not decode the DECOM data. The cause was incorrect frame sync codes. No effective solution was found.

13. TEST 1499 ADAM-L CELL B

DECOM data were noisy with incorrect sync codes. This problem, also observed on earlier tests, was still uncorrected.

14. TEST 1500 ADAM-S CELL B

Bad DECOM data as observed on earlier tests.

15. TEST 1501 ADAM-S CELL E

Noise was still present on six of eight DECOM channels. Prior to this test a filter was placed on the DECOM line. A negative spike was present on the Right Seat Z load channel.

16. TEST 1502 ADAM-L CELL E

Six of eight DECOM channels were still bad. Prior to this test a shield on the DECOM line was re-connected. An ADACS wire to the Left Knee Flexion channel was broken in the large ADAM and remained broken through test 1545.

17. TEST 1515 ADAM-L CELL E

Noise was present in the DECOM data, caused by wrong frame sync codes. The cameras and lights were purposely not operated during this test, which demonstrated that they were not causing the DECOM noise.

18. TEST 1516 ADAM-L CELL E

Bad DECOM data. See further testing.

19. TEST 1538 ADAM-L CELL F

No ADAM data was present except DECOM Lumbar Z Acceleration.

20. TEST 1539 ADAM-L CELL F

A common ground was installed between the DDI (DECOM to DRASS Interface) and DRASS, and connected to the DDI "pull-up" resistors, which were originally added to improve data transmission. It was thought that this would eliminate the noise in the DECOM data. The seat force transducers were mistakenly zeroed with ADAM in the seat.

21. TEST 1545 ADAM-L CELL F

The ADACS Left Knee Flexion data was zero. This problem appears to have been occurring in the large ADAM since test 1502. The cause was a broken line between the ADAM and the ADACS connector.

22. TEST 1546 ADAM-S CELL E

The A/D board failed prior to the test due to an IC shorting to a feed-through. The ICs were later removed and reinserted using an improved assembly procedure.

23. TEST 1551 ADAM-L CELL D

Noise was present in the Left Vertical Anchor Z data. The cause was a defective sensor line.

24. Additional Procedures

Incorrect channel numbering and sensitivity polarities, which were causing incorrect elbow and knee flexions RAM/DECOM data, were corrected. An open negative excitation line to one of the leg sensors was repaired. This may have occurred during the inspection.

25. TEST 1572 ADAM-L CELL B

The ADAMS were initially weighed without batteries, then correctly reweighed with batteries.

26. TEST 1582 ADAM-L CELL E

The 90° camera jammed on the first attempt. On the second attempt, the carriage was released before the countdown reached zero. This was caused by a faulty switch in the medical monitor. No ADACS or RAM/DECOM data were processed.

27. TEST 1583 ADAM-L CELL E

The cameras were turned off during the test. No RAM/DECOM data were processed.

28. TEST 1584 ADAM-L CELL E

The 90° camera jammed on the first attempt. The camera was replaced with a new one.

29. TEST 1585 ADAM-L CELL F

The RAM data did not download from the ADAM. The cause was a faulty IC chip on the digital I/O board. This same IC chip had also failed in test 1467.

30. Additional Procedures

A checkout of the large ADAM revealed the following problems: The Left Sternoclavicular Pronation/Retraction, Left Knee Medial/Lateral, and the Left and Right Hip Flexion position sensors had wires broken at the sensors. These wires were repaired and the strain reliefs improved. The Right Knee Medial/Lateral position sensor and the Right and Left Lower Leg Torque Negative load cells had wires broken at the analog mother board. The wires in the Right and Left Lower Leg Torque Positive channels were broken at the sensor connector. The breaks appeared to be due to improper handling and insufficient strain relief on the sensor wiring. All four Lower Leg Torque channels were recalibrated as required.

31. TEST 1590 ADAM-S CELL C

Noise was present in the RAM Chest Z Acceleration data. Additional ADAM channels were added prior to this test. The test revealed a defective Head Y accelerometer and a broken positive excitation wire on the Right Knee Flexion position sensor causing bad data on these two channels.

32. TEST 1601 ADAM-S CELL H

The Lumbar Z Moment channel was noisy. Wires in the Left Knee Medial/Lateral Rotation and the Right Lower Leg Torque Positive channels were broken. The parallel wire to the ADACS from the Left Knee Flexion transducer was broken away from the PC board and the wire clip screw was missing from the wire bundle. All appropriate repairs were made prior to the test. Sensor offsets were increased for tests 1601-1603.

33. TEST 1604 ADAM-L CELL H

Faulty DECOM data was again present. No corrective action was taken at this time. Noise was present on the RAM Chest Z Acceleration data.

34. TEST 1605 ADAM-L CELL I

A data dropout occurred on all ADACS and RAM/DECOM channels just after peak acceleration. The cause was determined to be a solder splash on a connector between a signal conditioning board and its mother board. The spinal yaw-stop was damaged from impact.

35. Additional Procedures

A complete sensor check of the large manikin showed that the Pelvis Y accelerometer was not functioning. The cause was a broken wire at the body of the accelerometer which became free of its strain relief.

36. TEST 1606 ADAM-S CELL H

No RAM/DECOM data were collected per instructions of test conductor.

37. TEST 1607 ADAM-S CELL H

The seat force transducers were mistakenly zeroed while ADAM was turned off. No RAM/DECOM data were collected in accordance with the instructions of the test conductor.

38. TEST 1608 ADAM-S CELL H

No RAM/DECOM data were collected as in test 1607.

39. TEST 1618 ADAM-L CELL I

A data dropout occurred as in test 1605. The spinal yaw-stop was impacted. A negative spike was present in the Lumbar Z Acceleration channel. No RAM/DECOM data were collected, reason unknown.

40. Additional Procedures ADAM-S

Wiring problems in the ADACS Head Z accelerometer, and Lumbar Z Force connections internal to ADAM, were repaired.

41. TEST 1634 ADAM-L CELL H

The Pelvis Y accelerometer was defective. The Left Arm Supination/Pronation wire was broken. The Left Lower Leg Torque Positive connector was bad. The DECOM data had sync code errors. The spinal yaw-stop was impacted. Two square waves were present on the Left Sternoclavicular Elevation channel. Sensor offsets were increased for tests 1634-1636. Spikes were present in the RAM Right Sternoclavicular Elevation data.

42. TEST 1635 ADAM-L CELL I

The DECOM Chest X Acceleration channel data was faulty. The Chest Z Acceleration wire was broken. The yaw-stop was impacted. The test conductor recommended proceeding with testing despite the DECOM problems.

43. TEST 1636 ADAM-L CELL J

The 90° camera jammed on the first and second test attempts. It was determined that both cameras had been swapped from their original positions in the initial camera solutions. The DECOM data had sync errors. The yaw-stop was impacted. The Left Knee Flexion voltage was zero for tests 1637-1639.

44. TESTS 1637-1639 ADAM-L CELL H

The wire from the Left Flexion sensor pulled away from the PC board. The yaw-stop was impacted. The test conductor had recommended proceeding with the tests despite the separated wire. No RAM/DECOM data was processed in accordance with the instructions of the test conductor.

Structural Adequacy of ADAM

There were no major delays in the test program due to failures of any ADAM structural components. After completion of the test program, both ADAM manikins were inspected to assess structural damage and determine what repairs and modifications were necessary. Below is a list of component damage along with the recommended corrective actions.

SMALL ADAM:

1. Gouges in the shoulder clevis were discovered. The corrective action will be to add a steel plate to the affected area. The aluminum clevis will be machined down to allow for the plate to be installed.
2. Cocking of stop retaining rings in the elbow and knee was observed. The corrective action will be to place washers between the rings and the clevis. They will be of varying thickness and will limit the motion of the stop within the clevis holes.
3. Gouges in the aluminum wrist clevis were noted. The corrective action will be to machine the aluminum clevis and install steel or plastic material which can be replaced in case of damage.
4. Overstressed upper arm thrust bearings were discovered. The corrective action will be replacement of the damaged bearings. It was also recommended that the torque in this area be limited to a maximum of 10 lb/in. This should be documented in the operations manual.

LARGE ADAM:

1. Gouges in the aluminum wrist clevis were discovered as in the small ADAM.
2. Overstressed upper arm thrust bearings were also present as in the small ADAM.
3. Damage to the outer spine tube yaw stop was found. The motion of the viscera box or the viscera box damper piston must be limited such that when full vertical displacement of the two pieces is reached, there is still clearance between the inner tube stop and the outer tube. A polyurethane disc will be placed in the top of the outer tube. This will limit the distance of vertical motion of the inner and outer tubes. This disk will be placed in both the large and small ADAM.

ADAM Instrumentation

The data acquisition systems of the ADAM manikins were able to measure transducer generated dynamic responses at carriage acceleration levels up to +24 Gz. Although individual problems occurred in some channels, the ADAM internal instrumentation system was able to condition and digitize the data during the impact tests. Data was successfully downloaded to the DRASS during the tests (DECOM system) and after the tests (RAM system), and later downloaded to the Vax computer system. A list of instrumentation failures and problems in individual tests is contained in the Test-by-Test

Narrative. The main areas of concern were noisy data (especially in the DECOM system), broken wires in the position sensor paths, and circuit board failures. A thorough analysis of the ADAM instrumentation systems has been reported by Strzelecki and Buhrman (4).

ADAM Sensitivity

The sensitivity of the internal ADAM channels is the product of the transducer sensitivity times the gain of the individual channel signal conditioning circuits, and is specified in engineering units per volt. Tables 3 and 4 list the percent changes between the initial and final sensitivities of both low-level (requiring amplification) and high-level (no amplification required) ADAM channels. These occurred during a total of 21 small ADAM and 38 large ADAM tests which were run over a period of three months, with a total time between initial and final calibration of about four and one-half months. The low-level channel sensitivity variations ranged from -11.5% to 30.5% in the small ADAM with a mean magnitude change of 9.3%, and from -17.9% to 23.3% in the large ADAM with a mean magnitude change of 9.7%. The high-level sensitivity variations ranged from -21.8% to 34.1% in the small ADAM with a mean magnitude change of 5.0%, and from -10.1% to 110.6% in the large ADAM with a mean magnitude change of 4.9%.

TABLE 3. ADAM LOW-LEVEL CHANNEL SENSITIVITY CHANGES

CHANNEL NO./NAME	INITIAL SENS.	SMALL ADAM % CHANGE	LARGE ADAM % CHANGE
1 NECK Z FORCE	666.6 lb/volt	6.8	6.1
2 NECK Y FORCE	444.4 lb/volt	4.0	7.2
3 NECK X FORCE	444.4 lb/volt	-9.2	23.3
5 NECK Z MOMENT	555.6 lb-in	10.0	-4.0
6 NECK Y MOMENT	555.6 lb-in	13.7	-0.1
7 NECK X MOMENT	555.6 lb-in	15.1	17.8
9 HEAD Z ACCEL	11.1 G/volt	3.2	2.8
10 HEAD Y ACCEL	11.1 G/volt	1.1	1.6
11 HEAD X ACCEL	22.2 G/volt	-11.5	2.0
13 CHEST Z ACCEL	11.1 G/volt	-9.5	12.4
14 CHEST Y ACCEL	11.1 G/volt	9.3	15.6
15 CHEST X ACCEL	22.2 G/volt	9.7	-3.9
34 LUMBAR Y FORCE	666.6 lb/volt	-8.9	14.2

TABLE 3. ADAM LOW-LEVEL CHANNEL SENSITIVITY CHANGES (continued)

CHANNEL NO./NAME	INITIAL SENS.	SMALL ADAM % CHANGE	LARGE ADAM % CHANGE
35 LUMBAR X FORCE	666.6 lb/volt	10.7	-14.9
38 LUMBAR X MOMENT	666.6 lb-in	6.4	13.0
39 LUMBAR Z FORCE	1111.1 lb/volt	7.6	21.0
42 LUMBAR Z MOMENT	666.6 lb-in	-7.0	-17.9
43 LUMBAR Y MOMENT	666.6 lb-in	30.5	-4.1
79 PELVIS X ACCEL	20.0 G/volt	-8.5	---
79 PELVIS X ACCEL	22.2 G/volt	---	-8.1
98 PELVIS Z ACCEL	11.1 G/volt	-1.0	-4.0
99 PELVIS Y ACCEL	11.1 G/volt	11.2	---
COMBINED DATA MEAN		9.3	9.7

TABLE 4. ADAM HIGH-LEVEL CHANNEL SENSITIVITY CHANGES

CHANNEL NO./NAME	INITIAL SENS.	SMALL ADAM % CHANGE	LARGE ADAM % CHANGE
18 RT SHLDR TRANS ABD	-18.2°/volt	-5.2	1.5
19 LFT SHLDR TRANS ABD	18.2°/volt	0.0	-4.5
22 RT SHLDR FLEXION	23.5°/volt	-5.7	110.6*
23 LFT SHLDR FLEXION	-23.5°/volt	1.9	-1.3
30 RT SHLDR MED/LAT	-13.0°/volt	-0.8	10.2
31 LFT SHLDR MED/LAB	13.0°/volt	3.2	9.3
50 RT STERNO ELEV/DEPR	13.3°/volt	-0.6	-0.3
51 LFT STERNO ELEV/DEPR	13.3°/volt	0.2	-4.6
54 RT STERNO PRON/RETR	13.3°/volt	-0.4	1.1
55 LFT STERNO PRON/RETR	13.3°/volt	-0.2	-4.6
58 RT KNEE FLEXION	-13.3°/volt	0.9	-4.0
59 LFT KNEE FLEXION	-13.3°/volt	3.4	3.4

TABLE 4. ADAM HIGH-LEVEL CHANNEL SENSITIVITY CHANGES (continued)

CHANNEL NO./NAME	INITIAL SENS.	SMALL ADAM % CHANGE	LARGE ADAM % CHANGE
62 RT KNEE MED/LAT	-13.3°/volt	-1.6	2.3
63 LFT KNEE MED/LAT	-13.3°/volt	-5.2	-0.3
82 RT ARM CORONAL ABD	-17.0°/volt	1.9	-9.5
83 LFT ARM CORONAL ABD	17.0°/volt	-0.4	-1.2
86 RT ELBOW FLEXION	-14.0°/volt	4.9	0.0
87 LFT ELBOW FLEXION	-14.0°/volt	-9.3	-1.6
90 RT FOREARM SUP/PRON	17.0°/volt	1.3	2.7
91 LFT FOREARM SUP/PRON	-17.0°/volt	-9.4	-10.1
114 RT HIP SUPINE ABD	-13.3°/volt	2.8	16.3
115 LFT HIP SUPINE ABD	-13.3°/volt	9.1	17.9
118 RT HIP FLEXION	-13.3°/volt	-1.5	-0.6
119 LFT HIP FLEXION	13.3°/volt	-9.7	-3.3
122 RT HIP MED/LAT	-13.3°/volt	-4.0	1.0
123 LFT HIP MED/LAT	13.3°/volt	-0.3	5.2
126 LUMBAR ROLL	-13.3°/volt	34.1	14.2
127 LUMBAR PITCH	-13.3°/volt	-21.8	-1.9
COMBINED DATA MEAN		5.0	4.9

* excluded from mean calculations

In addition to the percent changes from the initial to the final sensitivities, the means of individual test calibration voltage changes were computed for 14 selected tests for each manikin and are shown in Tables 5 and 6. These calibration voltages were obtained by applying a voltage called the RCal value to the signal conditioning circuit and taking the difference between this value and the initial or nonRCal voltage. These difference voltages were then measured before and after impact. The low-level mean voltage changes for both ADAMs were nearly all less than + 0.04 volts with a mean of 0.02 volts, which translates to a mean percent change in calibration voltage of about 1% per test. In the ADAM high-level channels, most mean voltage changes were less than + 0.18 volts with a mean of 0.08 volts, which translates to a mean change in calibration voltage of 13.8% per test.

TABLE 5. MEAN ADAM LOW-LEVEL CHANNEL CALIBRATION VOLTAGE CHANGES

CHANNEL NO./NAME	SMALL ADAM		LARGE ADAM	
	PRE-IMPACT CAL VOLTAGE	VOLTAGE CHANGE	PRE-IMPACT CAL VOLTAGE	VOLTAGE CHANGE
1 NECK Z FORCE	3.51	0.04	4.02	0.03
2 NECK Y FORCE	2.47	0.03	2.52	0.01
3 NECK X FORCE	2.89	0.02	2.20	0.01
5 NECK Z MOMENT	2.43	0.01	2.48	0.03
6 NECK Y MOMENT	2.55	0.02	2.80	0.02
7 NECK X MOMENT	2.50	0.01	2.56	0.01
9 HEAD Z ACCEL	1.26	0.01	1.17	0.01
10 HEAD Y ACCEL	0.28	0.00	1.18	0.02
11 HEAD X ACCEL	1.22	0.01	1.29	0.01
13 CHEST Z ACCEL	1.34	0.03	1.32	0.02
14 CHEST Y ACCEL	1.24	0.03	1.14	0.01
15 CHEST X ACCEL	1.45	0.01	1.35	0.01
34 LUMBAR Y FORCE	2.55	0.01	2.18	0.01
35 LUMBAR X FORCE	2.29	0.02	2.46	0.01
38 LUMBAR X MOMENT	2.87	0.02	2.71	0.02
39 LUMBAR Z FORCE	4.73	0.03	4.88	0.02
42 LUMBAR Z MOMENT	1.95	0.04	3.08	0.02
43 LUMBAR Y MOMENT	2.15	0.04	2.86	0.08
79 LUMBAR X ACCEL	1.33	0.08	1.33	0.04
98 LUMBAR Z ACCEL	1.40	0.02	1.24	0.01
99 LUMBAR Y ACCEL	1.32	0.01	1.00	0.01
COMBINED DATA MEAN	2.08	0.02	2.18	0.02

TABLE 6. MEAN ADAM HIGH-LEVEL CHANNEL CALIBRATION VOLTAGE CHANGES

CHANNEL NO./NAME	SMALL ADAM		LARGE ADAM	
	PRE-IMPACT CAL VOLTAGE	VOLTAGE CHANGE	PRE-IMPACT CAL VOLTAGE	VOLTAGE CHANGE
18 RT SHLDR ABD	-1.31	0.04	-0.89	0.18
19 LFT SHLDR ABD	1.38	0.03	1.11	0.01
22 RT SHLDR FLEXION	-0.84	0.02	-0.38	0.04
23 LFT SHLDR FLEXION	1.48	0.02	0.93	0.08
30 RT SHLDR MED/LAT	0.74	0.09	-0.02	0.29
31 LFT SHLDR MED/LAT	-0.65	0.12	-0.78	0.12
50 RT STERN ELEV/DEP	0.40	0.21	0.43	0.01
51 LFT STERN ELEV/DEP	-0.14	0.03	0.10	0.08
54 RT STERN PRO/RET	0.05	0.09	0.00	0.04
55 LFT STERN PRO/RET	0.02	0.05	1.18	0.03
58 RT KNEE FLEXION	0.07	0.12	1.05	0.23
59 LFT KNEE FLEXION	0.46	0.13	0.94	0.05
62 RT KNEE MED/LAT	-0.03	0.05	-0.14	0.06
63 LFT KNEE MED/LAT	1.04	0.03	0.38	0.03
82 RT ARM CORONAL ABD	-1.00	0.08	-0.59	0.05
83 LFT ARM CORONAL ABD	0.95	0.10	1.22	0.16
86 RT ELBOW FLEXION	-0.31	0.06	0.61	0.11
87 LFT ELBOW FLEXION	-0.18	0.09	-0.09	0.05
90 RT FOREARM SUP/PRO	-1.58	0.09	-1.42	0.14
91 LFT FOREARM SUP/PRO	1.26	0.09	1.50	0.12
114 RT HIP SUPINE ABD	0.47	0.15	0.74	0.07
115 LFT HIP SUPINE ABD	-0.46	0.15	0.52	0.07
118 RT HIP FLEXION	1.02	0.08	1.03	0.06
119 LFT HIP FLEXION	-0.92	0.18	0.05	0.07
122 RT HIP MED/LAT	0.01	0.03	0.16	0.01
123 LFT HIP MED/LAT	-0.03	0.06	-0.10	0.04
126 LUMBAR ROLL	0.02	0.02	0.28	0.06
127 LUMBAR PITCH	-0.06	0.12	-0.25	0.07
COMBINED DATA MEAN	0.60	0.08	0.60	0.08

Repeatability of Manikin Dynamic Response

The repeatability tests consisted of five consecutive tests for each manikin, with the exception of one non-consecutive large ADAM test. (All the data taken from this test, however, fell within one standard deviation of the mean). The parameters for these tests were as follows:

Test cell: C
Acceleration input: +10 Gz
Seat cushion: None
Seat-back angle: None
Restraint system: X-Band 90 harness

The standard deviation within each group of tests was used to measure repeatability since this result is determined by the sum of the individual deviations from the mean. Plus or minus two standard deviations indicates the distance from the mean within which approximately 95% of all results would be expected to occur. This value as a percent of the mean is referred to in this study as the repeatability index.

Tables 7 and 8 give the mean peak magnitude (accelerations were offset-adjusted) and time-to-peak values along with two standard deviations and their percentage of the mean value, for selected ADAM channels. The small ADAM manikin showed reasonably good repeatability indexes for peak magnitudes of the z-axis acceleration data, with values of +6.8% to +13.6% for the head and chest respectively, but much higher x-axis indexes of +23.7% and +83.5%. The small ADAM demonstrated excellent repeatability in the Resultant Seat Force peak magnitude data with a repeatability index of +3.0%, while the Lumbar Z Force and Neck Z Force data had moderately high repeatability indexes of +14.5% and +15.7%, respectively. The small ADAM had relatively low repeatability indexes for all time-to-peak values, ranging from +9.1% to +11.6%, with the only exception being the Lumbar Z Force channel with an index of +19.8%.

The large ADAM demonstrated excellent repeatability in the peak magnitudes of the z-axis acceleration data, with repeatability indexes of +4.4% and +7.2% for the head and chest, respectively. The repeatability of the x-axis acceleration data, as in the small ADAM, showed poor repeatability, with indexes of +16.9% and +72.8%. The large ADAM demonstrated good repeatability in the Resultant Seat Force, Lumbar Z Force, and Neck Z Force data, with indexes of +6.1%, +9.6%, and +8.5%, respectively. The large ADAM also demonstrated relatively good repeatability of time-to-peak data, with repeatability indexes ranging from +3.1% to +14.8%.

Tables 9 and 10 indicate that the GARD manikins showed similar trends to the ADAM manikins in repeatability, with low z-axis acceleration peak magnitude repeatability indexes, ranging from +1.7% to +8.1%, and high x-axis peak magnitude indexes ranging from +27.1% to +91.3%. Both GARD manikins demonstrated excellent repeatability in the Resultant Seat Force peak magnitude data, with indexes of +2.2% for the CG-5 and +2.3% for the CG-95. The time-to-peak repeatability indexes for the acceleration data ranged from +9.9% to +18.4% for the z-axis, but were much higher for the x-axis, ranging from +61.1% to +99.9%.

TABLE 7. ADAM-S DYNAMIC RESPONSE REPEATABILITY

CHANNEL	MEAN	2 SD	2 SD %
HEAD Z ACCEL (G)	11.33	0.77	<u>+6.8%</u>
CHEST Z ACCEL (G)	13.25	1.81	<u>+13.6%</u>
HEAD X ACCEL (G)	-5.13	1.21	<u>+23.7%</u>
CHEST X ACCEL (G)	4.42	3.69	<u>+83.5%</u>
RES SEAT FORCE (LB)	1911.8	58.12	<u>+3.0%</u>
LUMBAR Z FORCE (LB)	572.9	82.98	<u>+14.5%</u>
NECK Z FORCE (LB)	120.4	18.97	<u>+15.7%</u>
HEAD Z ACCEL (ms)	72.0	5.1	<u>+7.1%</u>
CHEST Z ACCEL (ms)	72.0	8.4	<u>+11.6%</u>
HEAD X ACCEL (ms)	125.2	12.3	<u>+9.8%</u>
CHEST X ACCEL (ms)	75.2	6.8	<u>+9.1%</u>
RES SEAT FORCE (ms)	70.0	3.7	<u>+5.3%</u>
LUMBAR Z FORCE (ms)	64.4	12.8	<u>+19.8%</u>
NECK Z FORCE (ms)	67.8	7.8	<u>+11.5%</u>

TABLE 8. ADAM-L DYNAMIC RESPONSE REPEATABILITY

CHANNEL	MEAN	2 SD	2 SD %
HEAD Z ACCEL (G)	15.32	0.68	<u>+4.4%</u>
CHEST Z ACCEL (G)	18.21	1.32	<u>+7.2%</u>
HEAD X ACCEL (G)	-5.19	0.88	<u>+16.9%</u>
CHEST X ACCEL (G)	1.62	1.18	<u>+72.8%</u>
RES SEAT FORCE (LB)	3358.7	203.9	<u>+6.1%</u>
LUMBAR Z FORCE (LB)	1291.2	124.0	<u>+9.6%</u>
NECK Z FORCE (LB)	186.6	15.84	<u>+8.5%</u>
HEAD Z ACCEL (ms)	73.4	5.4	<u>+7.4%</u>
CHEST Z ACCEL (ms)	74.2	11.0	<u>+14.8%</u>
HEAD X ACCEL (ms)	120.8	8.9	<u>+7.3%</u>
CHEST X ACCEL (ms)	78.6	9.2	<u>+11.7%</u>
RES SEAT FORCE (ms)	72.4	2.3	<u>+3.1%</u>
LUMBAR Z FORCE (ms)	71.8	3.8	<u>+5.4%</u>
NECK Z FORCE (ms)	73.6	6.3	<u>+8.5%</u>

TABLE 9. CG-5 DYNAMIC RESPONSE REPEATABILITY

CHANNEL	MEAN	2 SD	2 SD %
HEAD Z ACCEL (G)	11.60	0.37	<u>+3.2%</u>
CHEST Z ACCEL (G)	12.41	0.61	<u>+4.9%</u>
HEAD X ACCEL (G)	-0.92	0.84	<u>+91.3%</u>
CHEST X ACCEL (G)	1.43	0.54	<u>+37.8%</u>
RES SEAT FORCE (LB)	1610.2	35.74	<u>+2.2%</u>
HEAD Z ACCEL (ms)	64.2	7.7	<u>+11.9%</u>
CHEST Z ACCEL (ms)	64.6	11.9	<u>+18.4%</u>
HEAD X ACCEL (ms)	47.6	29.1	<u>+61.1%</u>
CHEST X ACCEL (ms)	56.8	37.0	<u>+65.2%</u>
RES SEAT FORCE (ms)	66.6	11.8	<u>+17.7%</u>

TABLE 10. CG-95 DYNAMIC RESPONSE REPEATABILITY

CHANNEL	MEAN	2 SD	2 SD %
HEAD Z ACCEL (G)	12.13	0.20	<u>+1.7%</u>
CHEST Z ACCEL (G)	13.46	1.09	<u>+8.1%</u>
HEAD X ACCEL (G)	-0.86	0.27	<u>+31.9%</u>
CHEST X ACCEL (G)	1.32	0.36	<u>+27.1%</u>
RES SEAT FORCE (LB)	2463.8	57.84	<u>+2.3%</u>
HEAD Z ACCEL (ms)	66.2	6.5	<u>+9.9%</u>
CHEST Z ACCEL (ms)	73.6	10.3	<u>+13.9%</u>
HEAD X ACCEL (ms)	113.6	113.5	<u>+99.9%</u>
CHEST X ACCEL (ms)	79.0	57.0	<u>+72.2%</u>
RES SEAT FORCE (ms)	69.2	3.6	<u>+5.2%</u>

Direct statistical comparisons of the standard deviations between the peak magnitude and time-to-peak mean test data of the manikins were performed using the F-test ($\alpha = 0.05$). The results are listed in Table 11, with a significantly smaller standard deviation indicating better manikin repeatability. Instances where no significant differences were found are indicated by the abbreviation "NSD". There was only one significant difference in the standard deviations between the small and large ADAM, but several differences between the ADAM and GARD manikins. The significant differences which were present indicated smaller standard deviations in the peak magnitudes of the GARD manikin responses, and smaller standard deviations in the time-to-peak of the ADAM responses.

TABLE 11. F-TEST COMPARISON OF MANIKIN STANDARD DEVIATIONS ($\alpha = 0.05$)

CHANNEL	ADAM-S vs. CG-5	ADAM-L vs. CG-95	ADAM-L vs. ADAM-S
HEAD Z ACCEL (G)	NSD	CG-95 < A-L	NSD
CHEST Z ACCEL (G)	CG-5 < A-S	NSD	NSD
HEAD X ACCEL (G)	NSD	CG-95 < A-L	NSD
CHEST X ACCEL (G)	CG-5 < A-S	CG-95 < A-L	A-L < A-S
RES SEAT FORCE (LB)	NSD	CG-95 < A-L	---
HEAD Z ACCEL (ms)	NSD	NSD	NSD
CHEST Z ACCEL (ms)	NSD	NSD	NSD
HEAD X ACCEL (ms)	A-S < CG-5	A-L < CG-95	NSD
CHEST X ACCEL (ms)	A-S < CG-5	A-L < CG-95	NSD
RES SEAT FORCE (ms)	A-S < CG-5	NSD	---

Manikin Simulation of Human Dynamic Response

Acceleration response

Means of human and manikin dynamic response test data for acceleration peak magnitude (offset-adjusted) and time-to-peak values in cells A-F are listed in Tables 12 and 13. All data is taken from the ADACS measurements. Mean values of manikin test data which are more than ± 2 standard deviations from the mean of the corresponding human data are marked with an asterisk. Observations of the Chest X Acceleration data in all cells show a tendency for the large ADAM to generate larger peak magnitudes and for the other manikins to generate lower peak magnitudes than predicted by the corresponding human data. In the Chest Z Acceleration data, the large ADAM and the CG-95 showed a tendency to generate larger peak magnitudes than the human data. The large ADAM also showed a strong tendency to generate

larger peak magnitudes in the Head Z Acceleration data than the corresponding human data. In the time-to-peak data, all four manikins, especially the CG-95, demonstrated a tendency to generate higher Chest X values than the human data. The small ADAM and CG-5 showed a tendency to produce lower than expected time-to-peak values in the Chest Z, while the CG-5 showed a strong tendency to generate lower than expected time-to-peak values in the Head Z Acceleration data.

The Wilcoxon Rank Sum test was used to statistically compare the human and manikin data in cell C for the three acceleration measurements referred to above. Cell C provided a good data set for comparison since it had a sample size of at least six tests per manikin, along with the use of standard impact test parameters. These included a half-sinusoidal acceleration input pulse with 66 ms rise time, a seat-back angle of 0°, and no seat cushion.

TABLE 12. MEAN ACCELERATION DATA FOR CELLS A, B, AND C

	CELL A					
CHANNEL	HUMAN n=15 2 SD		ADAM-S n=1	ADAM-L n=1	CG-5 n=1	CG-95 n=1
HEAD Z ACCEL (G)	11.97	0.96	11.23	15.01*	12.37	12.52
CHEST Z ACCEL (G)	13.84	1.90	13.60	13.74	13.54	15.45
CHEST X ACCEL (G)	4.23	1.90	1.95*	9.63*	1.64*	1.87*
HEAD Z ACCEL (ms)	71.9	7.6	77.	77.	63.*	70.
CHEST Z ACCEL (ms)	83.3	16.3	70.	78.	64.*	77.
CHEST X ACCEL (ms)	70.1	13.7	107.*	78.	95.*	91.*
	CELL B					
CHANNEL	HUMAN n=14 2 SD		ADAM-S n=3	ADAM-L n=4	CG-5 n=1	CG-95 n=1
HEAD Z ACCEL (G)	12.33	1.46	12.59	15.48*	12.48	13.01
CHEST Z ACCEL (G)	14.08	4.70	14.50	17.70	12.83	17.51
CHEST X ACCEL (G)	5.73	2.04	3.37*	3.59*	4.56	5.97
HEAD Z ACCEL (ms)	75.6	7.8	72.7	76.7	63.*	72.
CHEST Z ACCEL (ms)	79.7	12.9	75.3	79.8	63.*	81.
CHEST X ACCEL (ms)	68.9	12.0	74.0	73.3	85.*	95.*

TABLE 12. MEAN ACCELERATION DATA FOR CELLS A, B, AND C (continued)

	CELL C					
CHANNEL	HUMAN n=14	2 SD	ADAM-S n=6	ADAM-L n=8	CG-5 n=6	CG-95 n=6
HEAD Z ACCEL (G)	11.57	1.68	11.35	15.65*	11.75	12.21
CHEST Z ACCEL (G)	13.49	2.56	13.45	17.90*	12.56	14.13
CHEST X ACCEL (G)	3.70	3.22	4.01	2.62	1.72	1.44
HEAD Z ACCEL (ms)	71.1	9.6	71.0	72.9	64.2	67.0
CHEST Z ACCEL (ms)	78.1	14.6	70.8	74.6	64.5	73.7
CHEST X ACCEL (ms)	65.1	13.8	73.8	75.8	60.0	81.7*

* Values outside ± 2 std. dev.

TABLE 13. MEAN ACCELERATION DATA FOR CELLS D, E, AND F

	CELL D					
CHANNEL	HUMAN n=14	2 SD	ADAM-S n=1	ADAM-L n=1	CG-5 n=2	CG-95 n=1
HEAD Z ACCEL (G)	17.23	4.52	24.72*	20.35	22.80*	17.58
CHEST Z ACCEL (G)	13.78	5.30	20.39*	18.75	25.97*	21.92*
CHEST X ACCEL (G)	6.36	3.30	7.86	5.93	3.91	2.96*
HEAD Z ACCEL (ms)	40.8	9.1	31.*	35.	31.*	31.*
CHEST Z ACCEL (ms)	46.4	21.4	33.	39.	36.5	42.
CHEST X ACCEL (ms)	40.0	11.7	43.	47.	45.5	56.*

TABLE 13. MEAN ACCELERATION DATA FOR CELLS D, E, AND F (continued)

CHANNEL	CELL E					
	HUMAN n=14	2 SD	ADAM-S n=2	ADAM-L n=6	CG-5 n=1	CG-95 n=1
HEAD Z ACCEL (G)	12.99	2.82	12.57	17.29*	13.22	12.90
CHEST Z ACCEL (G)	14.18	3.14	13.77	16.31	14.21	13.69
CHEST X ACCEL (G)	5.13	2.26	6.88	12.92*	3.25	2.73*
HEAD Z ACCEL (ms)	70.8	10.9	58.0*	65.8	63.	72.
CHEST Z ACCEL (ms)	75.3	7.4	68.5	71.7	66.*	76.
CHEST X ACCEL (ms)	68.4	10.7	61.5	71.8	73.	94.*
CHANNEL	CELL F					
	HUMAN n=14	2 SD	ADAM-S n=1	ADAM-L n=5	CG-5 n=1	CG-95 n=1
HEAD Z ACCEL (G)	14.51	1.50	13.85	16.99*	14.31	14.17
CHEST Z ACCEL (G)	15.49	2.90	13.86	14.58	14.80	15.72
CHEST X ACCEL (G)	5.45	3.42	8.61	13.86*	2.42	2.55
HEAD Z ACCEL (ms)	76.8	7.70	71.	77.	69*	71.
CHEST Z ACCEL (ms)	79.6	7.96	75.	76.2	76.	77.
CHEST X ACCEL (ms)	76.6	4.06	73.	78.8	79.	91.*

* Values outside ± 2 std. dev.

Summaries of comparisons between the means of human and ADAM acceleration peak magnitude and time-to-peak test data using the Wilcoxon Rank Sum test are given in Table 14. The acceleration measurements of the small ADAM were closer to the corresponding human test data than were the other three manikins. There were no significant differences between the small ADAM and the human data in any of the peak magnitude measurements, with only small differences occurring in the time-to-peak measurements of the Chest X Acceleration (+13%) and the Chest Z Acceleration (-9%). Both of these variations were within two standard deviations of the corresponding mean of the human test data. The peak magnitude measurements of the large ADAM responses, however, were significantly larger than the human subjects for the Chest Z Acceleration (+33%) and Head Z Acceleration (+35%), with a longer time-to-peak value of the Chest X Acceleration (+16%). Of these large ADAM values, however, only the Head Z Acceleration peak magnitude deviated more than two standard deviations from the corresponding mean of the human test data.

TABLE 14. WILCOXON RANK SUM TEST SUMMARIES OF ADAM VS. HUMAN
ACCELERATION DATA IN CELL C ($\alpha=0.05$)

CHANNEL	HUMAN MEAN	ADAM-S		ADAM-L	
		MEAN	% CHANGE	MEAN	% CHANGE
HEAD Z ACCEL (G)	11.57	11.35	NSD	15.65	+35%
CHEST Z ACCEL (G)	13.49	13.45	NSD	17.90	+33%
CHEST X ACCEL (G)	3.70	4.01	NSD	2.62	NSD
HEAD Z ACCEL (ms)	71.1	71.0	NSD	72.9	NSD
CHEST Z ACCEL (ms)	78.1	70.8	-9%	74.6	NSD
CHEST X ACCEL (ms)	65.1	73.8	+13%	75.8	+16%

Results of the Wilcoxon analysis of the human versus the GARD manikin responses are shown in Table 15. Both the CG-5 and CG-95 GARD manikins showed a large decrease in mean peak magnitude in the Chest X Acceleration data as compared to the corresponding mean of the human test data, with differences of -54% and -61% for the CG-5 and CG-95, respectively. However, due to the relatively large variation in the human test data, neither value varied by more than two standard deviations. There were no significant differences from the mean of the human test data in either GARD manikin in the peak magnitudes of the Head Z or Chest Z acceleration data. However, both GARD manikins each had two acceleration time-to-peak values which were significantly different from the human data. In the CG-5, the Chest Z Acceleration time-to-peak varied by -17% and the Head Z Acceleration time-to-peak by -10%. The CG-95 Chest X Acceleration time-to-peak varied by +26% and the Head Z Acceleration time-to-peak by -6%. Of these values, however, only the CG-95 Chest X Acceleration time-to-peak varied by more than two standard deviations from the corresponding mean of the human data. Effects of individual cell parameters on manikin response are discussed in Sections 3.7 thru 3.10 of Results.

TABLE 15. WILCOXON RANK SUM TEST SUMMARIES OF GARD VS. HUMAN
ACCELERATION DATA IN CELL C ($\alpha=0.05$)

CHANNEL	HUMAN MEAN	CG-5		CG-95	
		MEAN	% CHANGE	MEAN	% CHANGE
HEAD Z ACCEL (G)	11.57	11.75	NSD	12.21	NSD
CHEST Z ACCEL (G)	13.49	12.56	NSD	14.13	NSD
CHEST X ACCEL (G)	3.70	1.72	-54%	1.44	-61%
HEAD Z ACCEL (ms)	71.1	64.2	-10%	67.0	-6%
CHEST Z ACCEL (ms)	78.1	64.5	-17%	73.7	NSD
CHEST X ACCEL (ms)	65.1	60.0	NSD	81.7	+26%

Seat forces

Regression lines computed for the human data set, with intervals evaluated to two standard deviations, are plotted for Resultant Seat Force peak magnitudes versus subject weight, and are shown in Figures 1-6. All corresponding data points for the four manikins are also shown on the graphs (plots for Cell D are included, but since an input pulse with a rapid rise-time was employed, they will not be referenced in this section). The plotted measurements of the small ADAM show the closest fit to the human test data, with all points being located within or just outside the two standard deviations interval of the human data regression line. Both the CG-5 and CG-95 data also show a good fit with the exception of Cell E, where both manikins show a somewhat lower value than the human data. The large ADAM peak magnitude responses, however, are consistently larger than the corresponding human test data in all cells. It should be noted, however, that the regression line was extrapolated for weights over 194 pounds since no human test data was available at heavier subject weights.

Manikin response vs. carriage acceleration level

Figures 7-9 show plots of acceleration mean peak magnitudes as a function of carriage (sled) acceleration level for all four manikins. All tests utilized the Confor™ Foam seat cushion and the X-Band 90 restraint harness. The Head Z and Chest Z acceleration plots all demonstrated fairly linear increases in peak magnitude with increasing carriage acceleration levels, with the large ADAM plots showing magnitudes consistently larger than the other three manikins. In addition, the slopes of the large ADAM data plots were about twice as high as the slopes of the other three manikins. With the exception of the small ADAM, the increases in Head X Acceleration mean peak magnitudes were somewhat non-linear, with the ADAM manikins showing larger peak magnitudes at all carriage acceleration levels than the GARD manikins.

Figures 10-12 show plots of manikin Resultant Seat Force, Lumbar Z Force, and Neck Z Force mean peak magnitude versus carriage acceleration level (only the small and large ADAM plots were available for the Lumbar Z and Neck Z responses). All plots show linear increases in peak magnitude with increasing carriage acceleration level. The plots also demonstrate increasing peak magnitude and slope with increasing manikin weight at all carriage acceleration levels.

Transfer function analysis

A computer program was employed to solve Chest Z Acceleration/Seat Z Acceleration and Head Z Acceleration/Seat Z Acceleration dynamic response transfer function equations for resonant frequencies and damping ratios of all human tests, as well as one test with each manikin for cells A-F. The program utilized the Dynamic Response Index (DRI) a mathematical model developed by AL which describes the human body as a mechanical system. (2) The fit of the model was demonstrated by using the computed values to solve for the acceleration response magnitudes over time and comparing these plots to the actual empirical response data of two small ADAM and two large ADAM tests. The results of the plots are shown in Appendix D. All curves show a reasonably good fit, although the large ADAM empirical acceleration peak magnitude is somewhat higher than predicted by the model. The human mean resonant frequency for all cells including both acceleration ratios

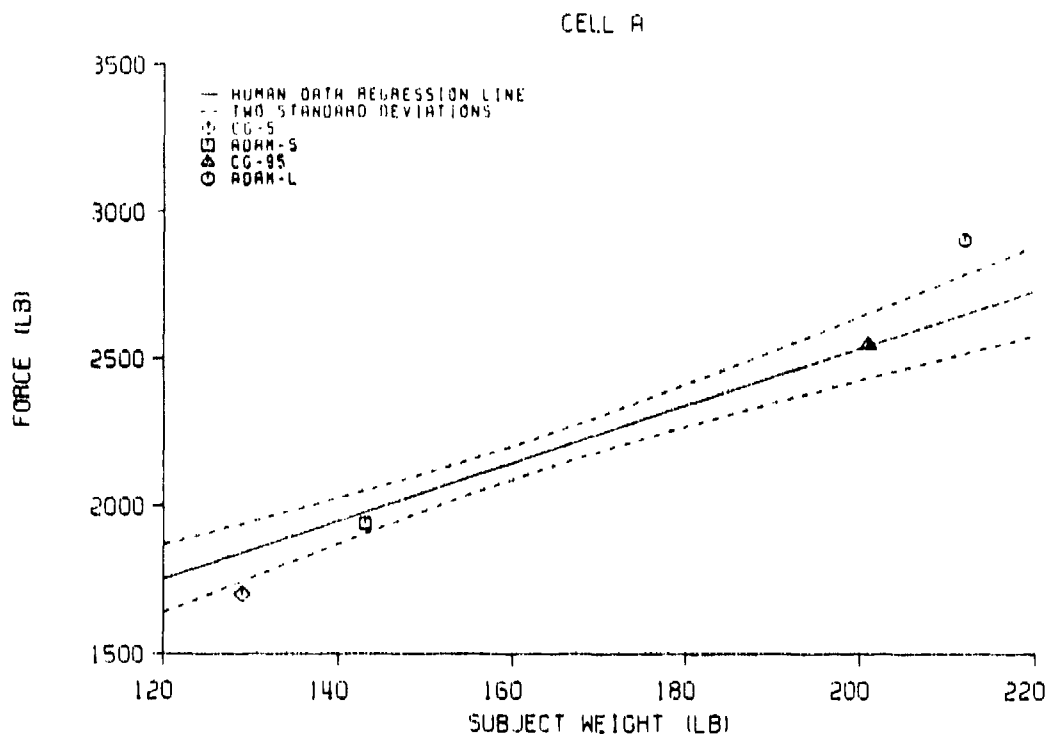


FIGURE 1. RESULTANT SEAT FORCE VS. SUBJECT WEIGHT, CELL A

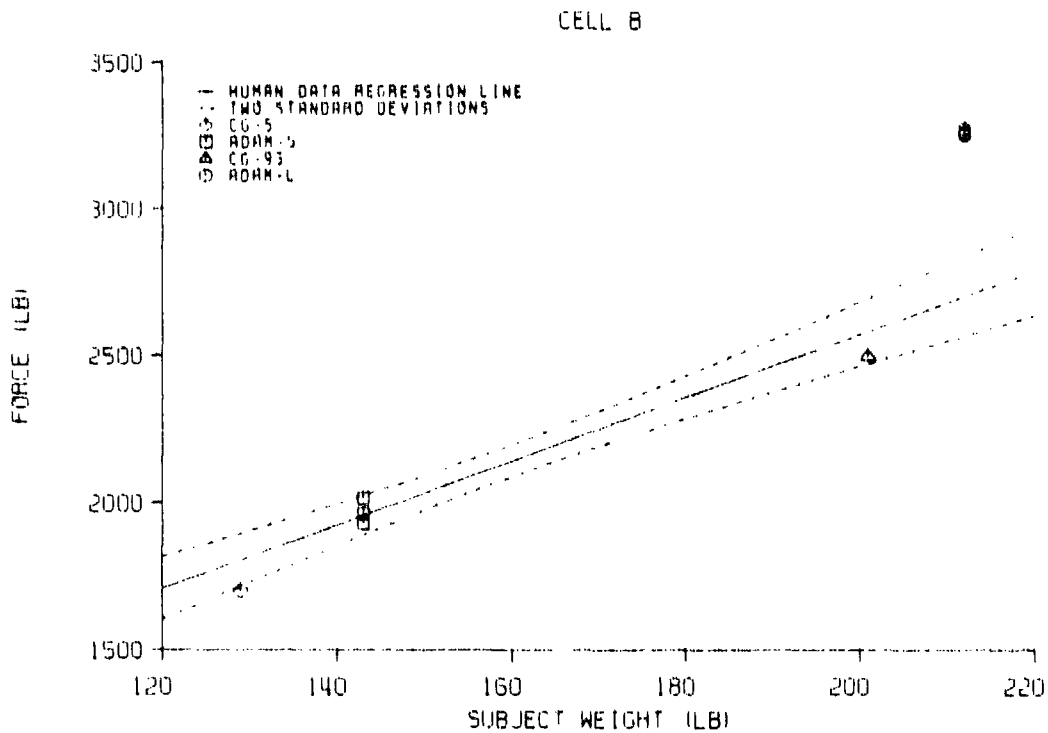


FIGURE 2. RESULTANT SEAT FORCE VS. SUBJECT WEIGHT, CELL B

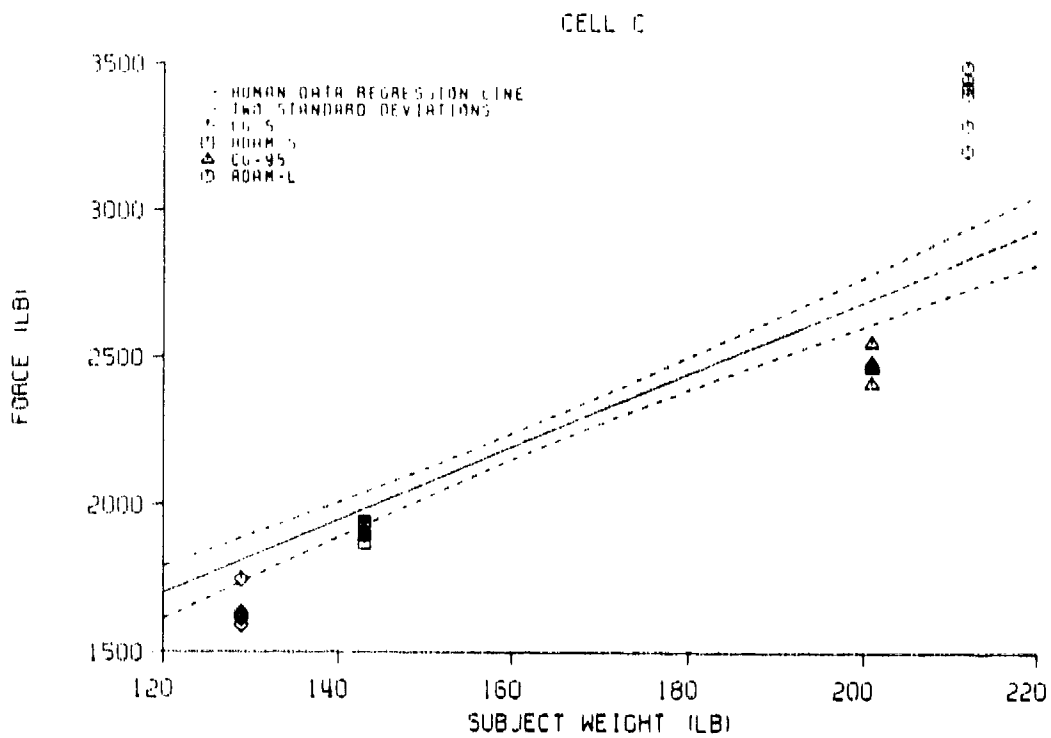


FIGURE 3. RESULTANT SEAT FORCE VS. SUBJECT WEIGHT, CELL C

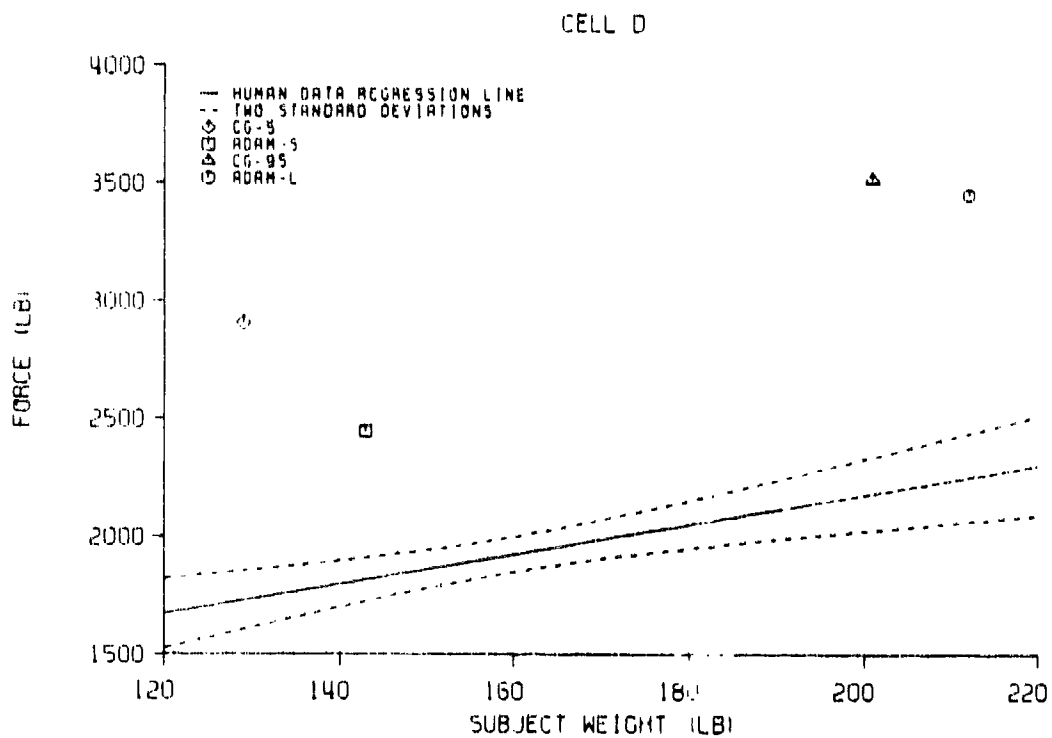


FIGURE 4. RESULTANT SEAT FORCE VS. SUBJECT WEIGHT, CELL D

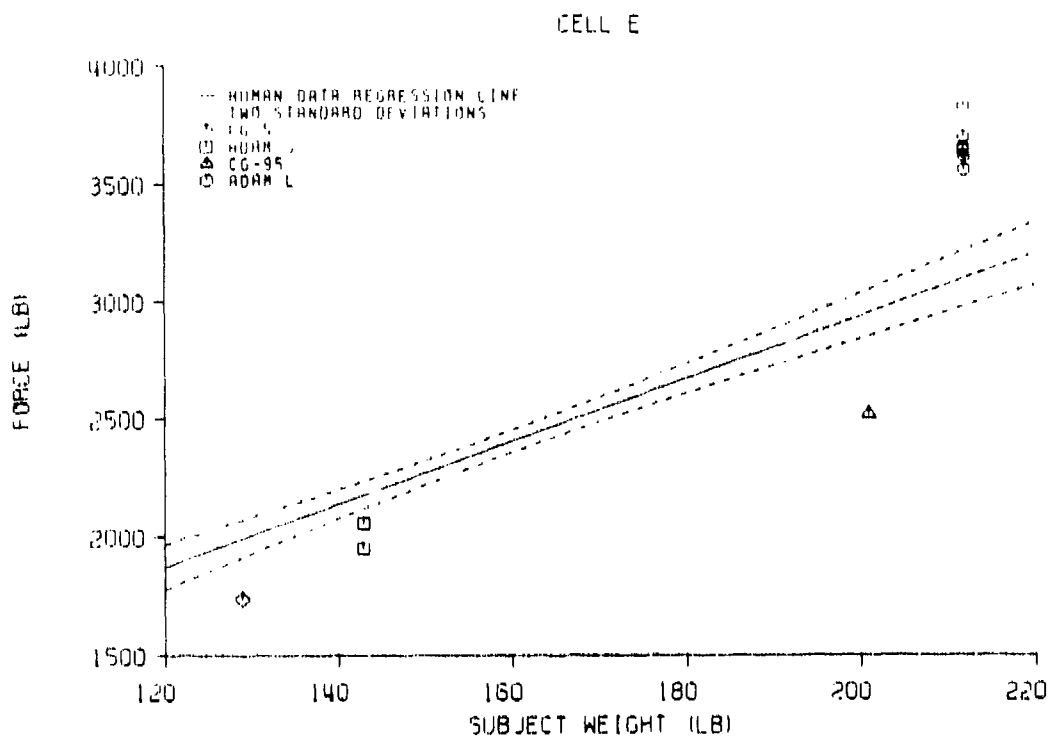


FIGURE 5. RESULTANT SEAT FORCE VS. SUBJECT WEIGHT, CELL E

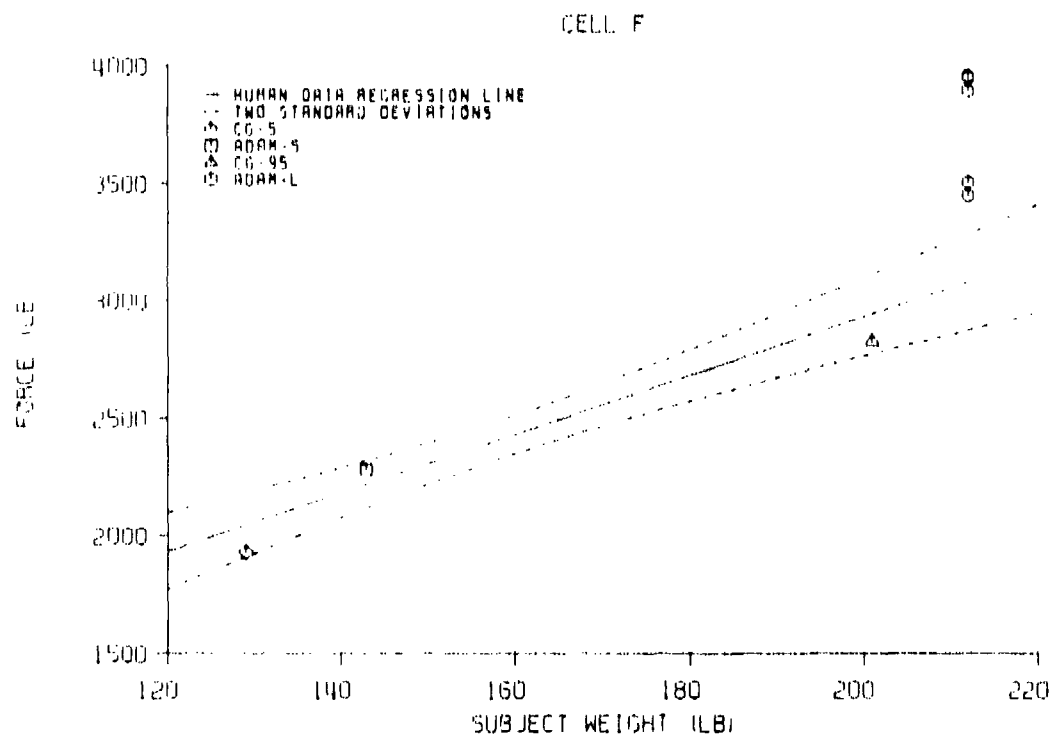


FIGURE 6. RESULTANT SEAT FORCE VS. SUBJECT WEIGHT, CELL F

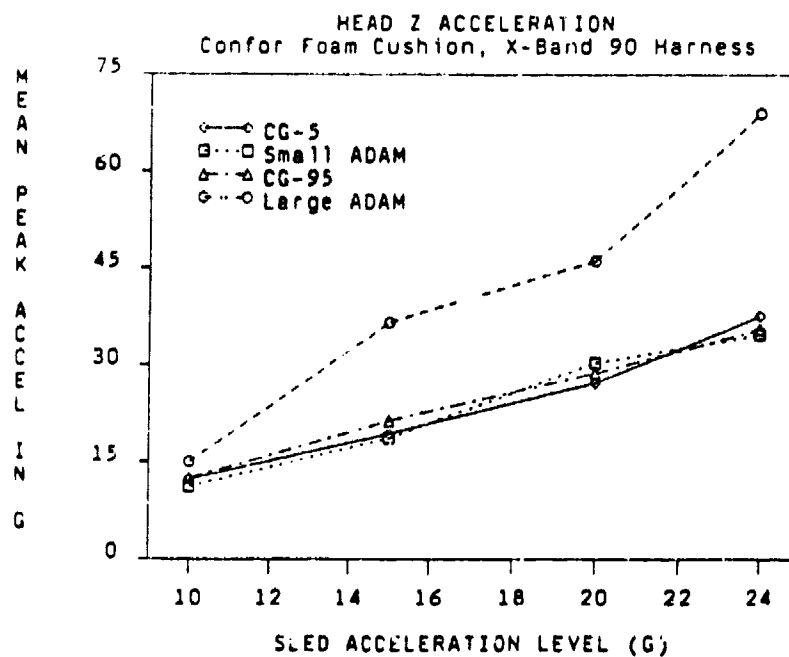


FIGURE 7. HEAD Z ACCELERATION VS. CARRIAGE ACCELERATION

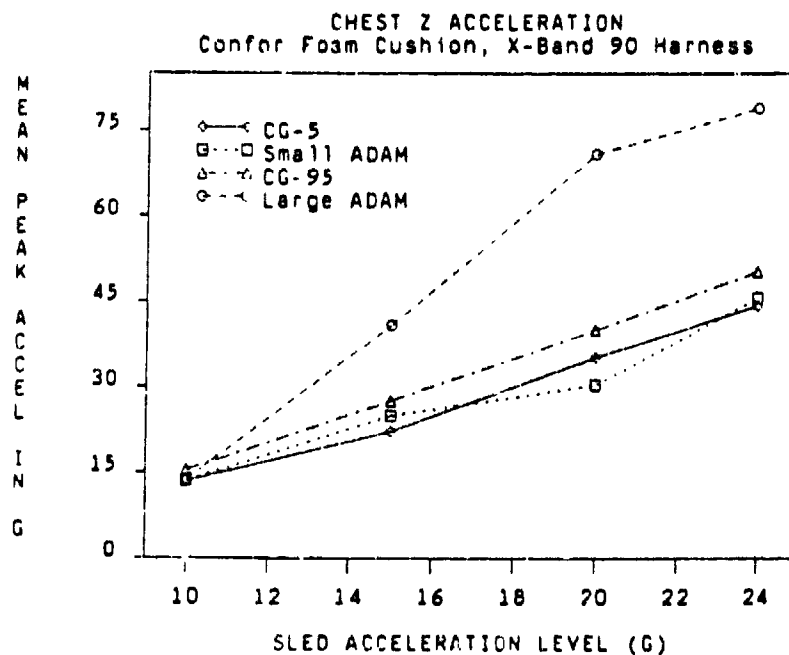


FIGURE 8. CHEST Z ACCELERATION VS. CARRIAGE ACCELERATION

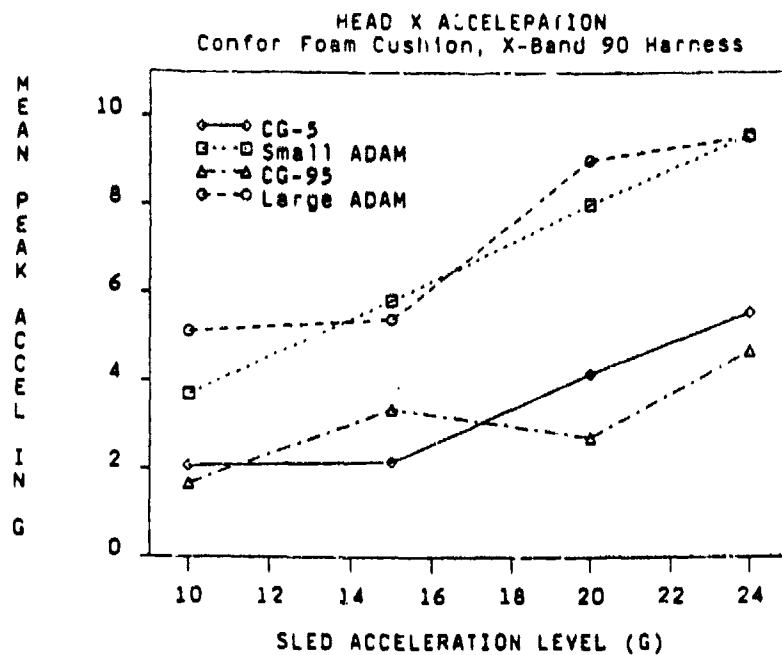


FIGURE 9. HEAD X ACCELERATION VS. CARRIAGE ACCELERATION

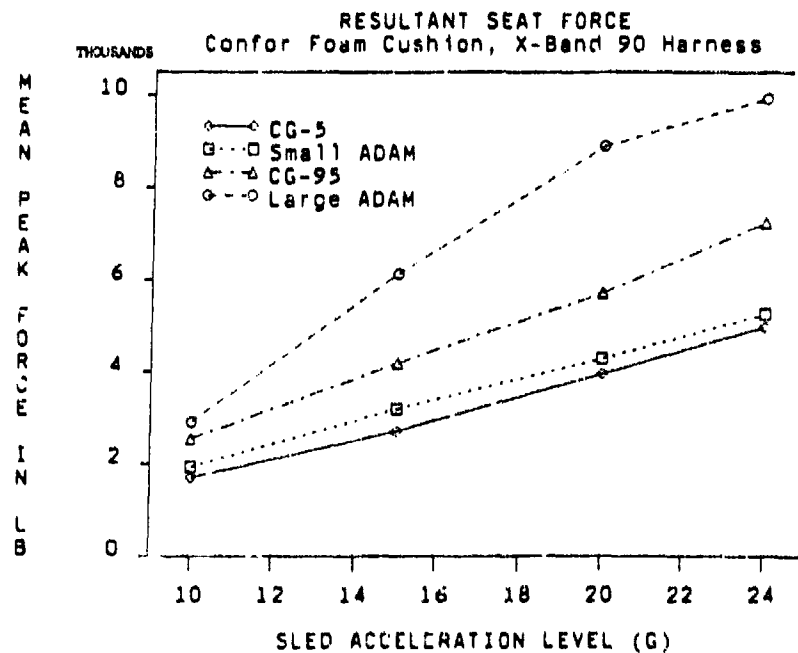


FIGURE 10. RESULTANT SEAT FORCE VS. CARRIAGE ACCELERATION

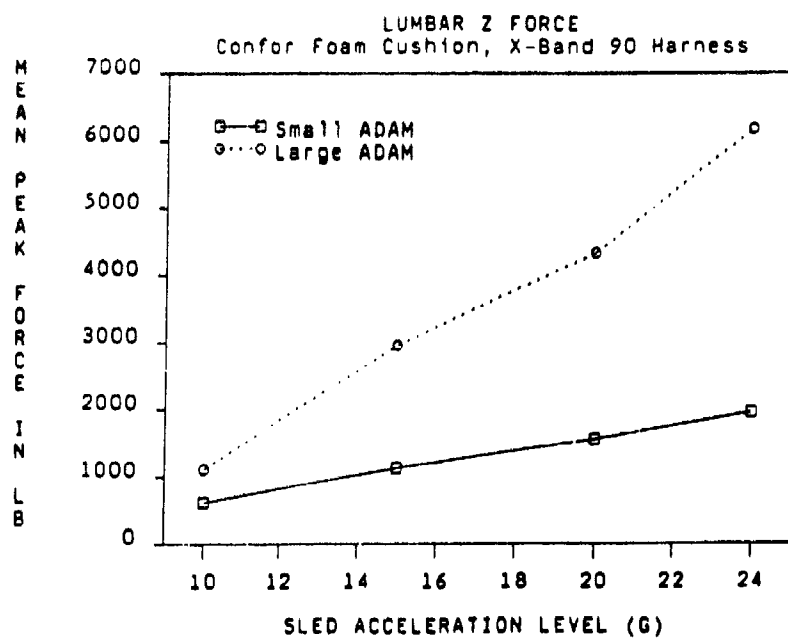


FIGURE 11. LUMBAR Z FORCE VS. CARRIAGE ACCELERATION

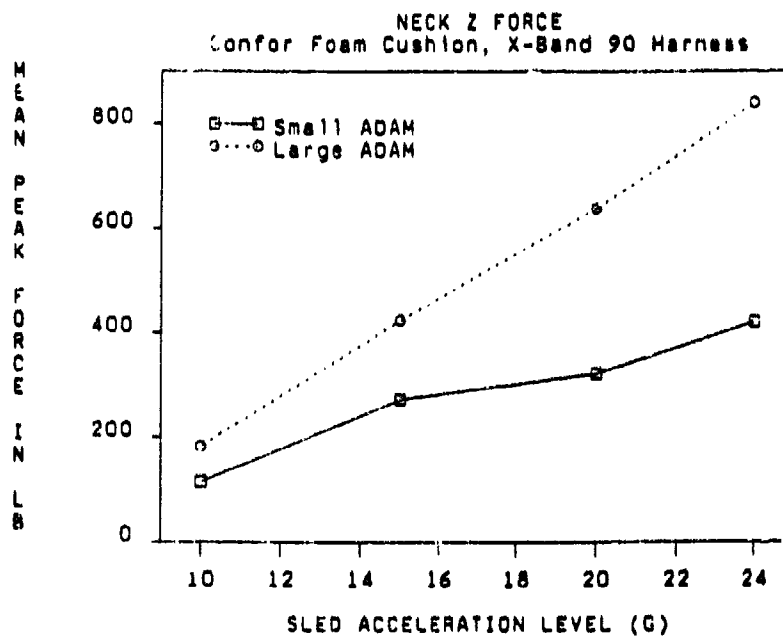


FIGURE 12. NECK Z FORCE VS. CARRIAGE ACCELERATION

was computed at 12 Hz with a damping ratio of 0.35. These results are similar to those obtained by Wittman (9) who used a spring-mass-damper model to analyze tests performed on the same vertical drop facility and obtained a resonant frequency of 10 Hz and a damping ratio of 0.3.

The results of the resonant frequency computations are shown in Table 16, with asterisks indicating manikin data lying more than two standard deviations outside the mean of the corresponding human test data. The resonant frequencies of all four manikins were reasonably close to the human data in all six cells. Although some of the manikin values were slightly outside of the two standard deviations interval, even those values were nearly all within the expected frequency range of 10-12 Hz.

The results of the damping ratio computations are shown in Table 17. All of the damping ratios for both GARD manikins were within two standard deviations of the mean of the human test data. The large ADAM results show two damping ratios slightly outside the lower two standard deviations boundary. The small ADAM results for the Head Z Acceleration/Seat Z Acceleration computations show damping ratios of 0.718 and 0.740 for cells A and C respectively, which are much higher than predicted by the human test data.

TABLE 16. RESONANT FREQUENCY

Head Z Accel/Seat Z Accel						
CELL	HUMAN	2 SD	ADAM-S	ADAM-L	CG-5	CG-95
A	12.55	1.86	10.65*	10.46*	13.75	11.71
B	12.11	1.40	11.65	12.36	11.64	13.58*
C	11.72	2.60	12.88	12.18	12.16	11.58
D	11.44	3.08	11.32	10.46	12.86	12.77
E	12.31	1.80	12.43	12.16	11.36	11.20
F	12.03	1.44	12.38	11.95	11.11	10.94
Chest Z Accel/Seat Z Accel						
CELL	HUMAN	2 SD	ADAM-S	ADAM-L	CG-5	CG-95
A	12.51	1.15	10.95*	10.68*	13.13	12.61
B	12.60	0.98	11.05*	12.16	11.47*	12.29
C	12.87	0.94	12.81	12.09	11.71*	12.90
D	9.91	3.52	10.84	10.48	12.73	12.55
E	12.54	0.94	12.49	12.33	11.22*	12.69
F	12.34	0.60	12.47	12.11	10.86*	10.73*

* Values outside ± 2 std. dev.

TABLE 17. DAMPING RATIO

Head Z Accel/Seat Z Accel						
CELL	HUMAN	2 SD	ADAM-S	ADAM-L	CG-5	CG-95
A	0.401	0.169	0.718*	0.226*	0.520	0.506
B	0.343	0.309	0.419	0.245	0.490	0.491
C	0.431	0.220	0.740*	0.221	0.594	0.477
D	0.338	0.128	0.425	0.228	0.362	0.344
E	0.353	0.295	0.276	0.216	0.433	0.399
F	0.240	0.146	0.266	0.161	0.381	0.343
Chest Z Accel/Seat Z Accel						
CELL	HUMAN	2 SD	ADAM-S	ADAM-L	CG-5	CG-95
A	0.315	0.329	0.346	0.284	0.412	0.313
B	0.310	0.209	0.313	0.222	0.479	0.276
C	0.360	0.179	0.352	0.199	0.504	0.368
D	0.592	0.350	0.322	0.232*	0.336	0.301
E	0.323	0.115	0.290	0.256	0.403	0.328
F	0.254	0.128	0.285	0.204	0.326	0.295

* Values outside ± 2 std. dev.

Seat Cushions

Human dynamic response

Wilcoxon Signed Rank tests were performed in order to compare the effects of using two different seat cushions on human dynamic response. The results of comparing impact tests with the Confor™ Foam seat cushion to tests using no seat cushion (Cell A vs. C), and tests comparing the ACES II cushion to tests using no seat cushion (Cell F vs. E), for mean Head Z, Chest Z, and Chest X accelerations, and Resultant Seat Force, are shown in Tables 18 and 19. The Confor™ Foam seat cushion had a negligible effect on all responses, with only slight differences occurring in the data between the cushion and the no seat cushion conditions. The ACES II seat cushion condition, however, showed small increases in the Chest Z Acceleration (+9%), Head Z Acceleration (+12%), and Resultant Seat Force (+1%) mean peak magnitudes, and increases ranging from +6% to +12% in all four mean time-to-peak values.

TABLE 18. WILCOXON SIGNED RANK TEST SUMMARIES FOR HUMAN SUBJECT
CONFORTM FOAM SEAT CUSHION COMPARISONS ($\alpha = 0.05$)

CHANNEL	NO CUSHION CELL C	CONFOR TM FOAM CELL A	% CHANGE
HEAD Z ACCEL (G)	11.57	11.97	+3%
CHEST Z ACCEL (G)	13.49	13.84	NSD
CHEST X ACCEL (G)	3.70	4.23	NSD
RES SEAT FORCE (lb)	2216	2161	NSD
HEAD Z ACCEL (ms)	71.1	71.9	NSD
CHEST Z ACCEL (ms)	78.1	83.3	+7%
CHEST X ACCEL (ms)	65.1	70.1	NSD
RES SEAT FORCE (ms)	76.7	76.8	NSD

TABLE 19. WILCOXON SIGNED RANK TEST SUMMARIES FOR HUMAN SUBJECT
ACES II SEAT CUSHION COMPARISONS ($\alpha = 0.05$)

CHANNEL	NO CUSHION Cell E	ACES II Cell F	% CHANGE
HEAD Z ACCEL (G)	12.99	14.51	+12%
CHEST Z ACCEL (G)	14.18	15.49	+9%
CHEST X ACCEL (G)	5.13	5.45	NSD
RES SEAT FORCE (lb)	2398	2425	NSD
HEAD Z ACCEL (ms)	70.8	76.8	+8%
CHEST Z ACCEL (ms)	75.3	79.6	+6%
CHEST X ACCEL (ms)	68.4	76.6	+12%
RES SEAT FORCE (ms)	73.8	78.1	+6%

Manikin dynamic response

The effects of the ConforTM Foam seat cushion on the ability of the manikins to simulate human dynamic response were varied. Table 12 shows that all manikins in Cell A except the large ADAM, demonstrated decreased human response simulation with the ConforTM Foam cushion. This was evidenced by the larger number of data means in Cell A outside the two

standard deviations interval of the mean of the corresponding human data, as compared to Cell C, which used no seat cushion. The CG-5 showed the poorest performance of the four manikins, with all of its time-to-peak measurements occurring outside the interval. Effects on seat forces can be seen in comparing the Resultant Seat Force peak magnitude versus subject weight plots in Figure 1 for tests with the ConforTM Foam seat cushion (Cell A), and Figure 3, without the cushion (Cell C). The data for all four manikins show a slightly closer fit to the corresponding human data regression line in Cell A, with the ConforTM Foam seat cushion, than in Cell C, with no seat cushion.

Effects of the ConforTM Foam seat cushion on manikin dynamic response at increasing G-levels are shown in Figure 13. Mean peak magnitudes versus carriage acceleration level are plotted for Head Z, Chest Z, and Head X accelerations, and Resultant Seat Force, with and without the seat cushion for the CG-5 manikin (only the CG-5 data was available for this test condition). The plots show a close fit between the seat cushion and no seat cushion conditions for both Head Z and Chest Z acceleration data. The Head X Acceleration plots show larger peak magnitude values at all G-levels with the ConforTM Foam cushion than in the no seat cushion condition. The plots for the Resultant Seat Force show a close fit of the data for the two conditions, with the exception of the 20 G carriage acceleration level, which shows a smaller peak magnitude force in tests using the ConforTM Foam seat cushion.

Employing the ACES II seat cushion did not appear to have a significant effect on the simulation of human dynamic acceleration responses by any of the manikins. The response data in Cell E (without ACES II) and Cell F (with ACES II) of Table 13 are fairly similar, with slightly more data means occurring outside the two standard deviations interval of the corresponding human data in Cell E than in Cell F. The small ADAM and the CG-5 had fewer data means outside the interval (1 and 2 respectively) overall in both cells than the large ADAM and the CG-95 (4 and 3 respectively). Effects on seat forces can be seen in comparing the Resultant Seat Force peak magnitude versus subject weight plots in Figure 5 for tests with no seat cushions (Cell E), and Figure 6, with the ACES II seat cushion (Cell F). The manikin data in Cell F, with the ACES II, show a closer fit to the corresponding human regression line in nearly all instances.

Restraint Harness

Human dynamic response

Wilcoxon Signed Rank tests were performed in order to compare the effects of the two restraint harnesses on human dynamic response. The results of comparing the X-Band 90 with the PCU-15/P (Cell C vs. E) for Head Z, Chest Z, and Chest X accelerations, and Resultant Seat Force, are shown in Table 20. The mean peak magnitude of the Chest X Acceleration data was substantially greater (+38%) with the PCU-15/P restraint harness than with the X-Band 90 restraint harness. Smaller increases in the peak magnitude data occurred in the PCU-15/P condition in the Chest Z Acceleration (+5%), Head Z Acceleration (+11%), and Resultant Seat Force (+10%). There were no significant differences between the two harnesses in any of the time-to-peak response data.

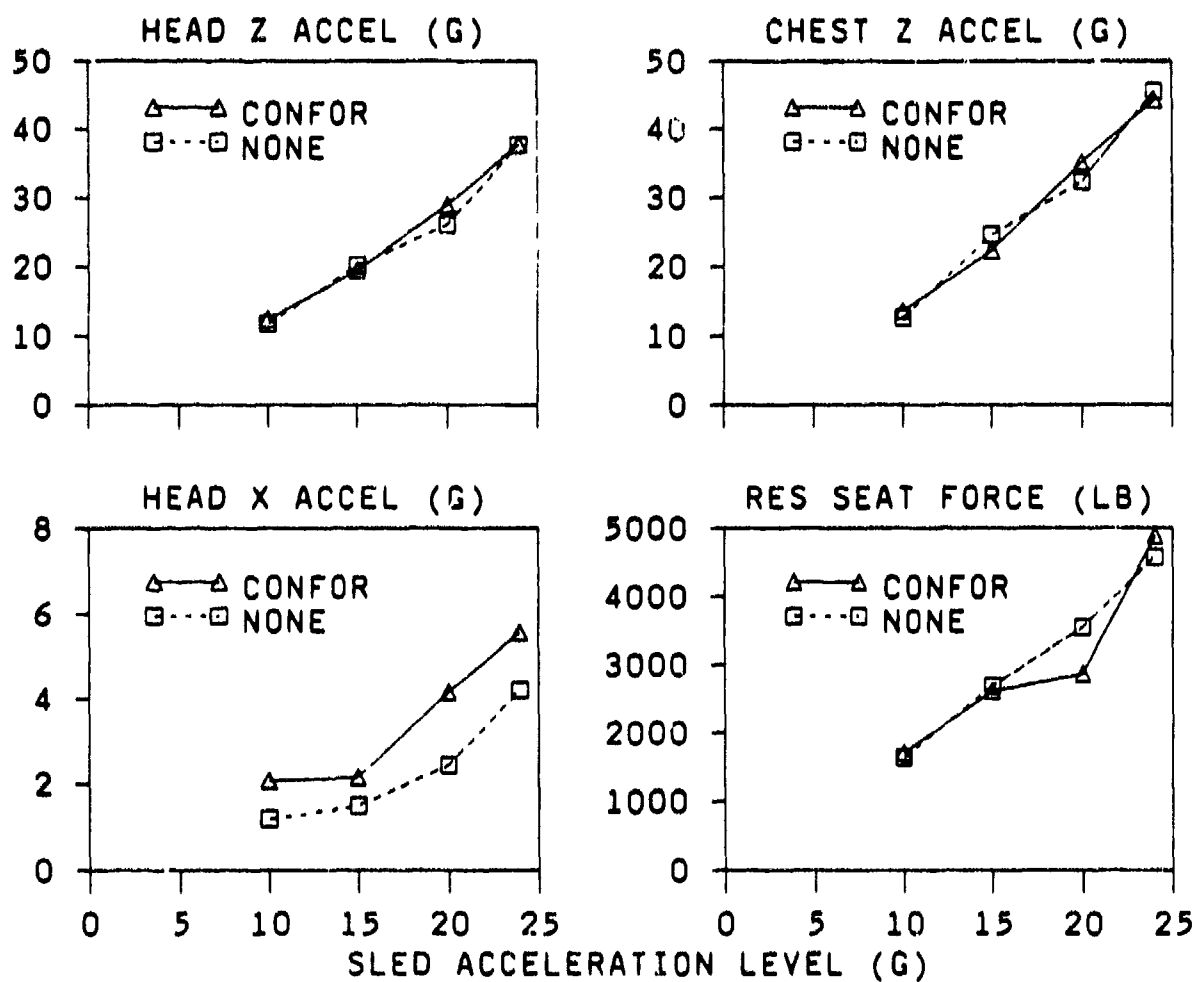


FIGURE 13. RESPONSES OF CG-5 MANIKIN WITH AND WITHOUT CONFOR™ FOAM SEAT CUSHION

TABLE 20. WILCOXON SIGNED RANK TEST SUMMARIES FOR HUMAN SUBJECT RESTRAINT HARNESS COMPARISONS ($\alpha = 0.05$)

CHANNEL	X-BAND 90 Cell C	PCU-15/P Cell E	% CHANGE
HEAD Z ACCEL (G)	11.68	12.99	+11%
CHEST Z ACCEL (G)	13.47	14.18	+5%
CHEST X ACCEL (G)	3.73	5.13	+38%
RES SEAT FORCE (lb)	2188	2398	+10%
HEAD Z ACCEL (ms)	70.7	70.8	NSD
CHEST Z ACCEL (ms)	77.9	75.3	NSD
CHEST X ACCEL (ms)	64.7	68.4	NSD
RES SEAT FORCE (ms)	75.5	73.8	NSD

Manikin dynamic response

Summaries of mean peak magnitude and time-to-peak of acceleration data for tests performed with the X-Band 90 restraint harness are shown in Cell C of Table 12, and results of tests with the PCU-15/P harness are shown in Cell E of Table 13. All manikins except the large ADAM demonstrated slightly better simulation of human response in Cell C, with the X-Band 90 harness, as indicated by fewer data means outside the two standard deviations interval of the corresponding human data. However, it should be noted that with the exception of the large ADAM, the manikin sample size in Cell C was much larger than that of Cell E, so differences in the two cells' standard deviations would be expected.

Resultant Seat Force peak magnitude values vs. subject weight are plotted for tests with the X-Band 90 harness in Figure 3 (Cell C) and with the PCU-15/P harness in Figure 5 (Cell E). The data for the CG-5, CG-95, and small ADAM manikins all show a slightly closer fit to the corresponding human data regression line in Cell C, with the X-Band 90 harness, while the data for the large ADAM shows a slightly closer fit in Cell E, with the PCU-15/P harness.

Seat-Back Angle

Human dynamic response

Wilcoxon Signed Rank tests were performed in order to determine the effects of varying the seat-back angle on human dynamic response. The results of comparing a seat-back angle of +10° and 0° (Cell B vs. A) and a seat-back angle of -10° and 0° (Cell L vs. A) for Head Z, Chest Z, and Chest X accelerations, and Resultant Seat Force, are shown in Tables 21 and 22. The effects of both seat-back angles were negligible with the exception of the Chest X Acceleration data, whose peak magnitude increased by 38% with the +10° seat-back angle and decreased by 24% with the -10° seat-back angle.

TABLE 21. WILCOXON SIGNED RANK TEST SUMMARIES FOR HUMAN SUBJECT +10°
SEAT-BACK ANGLE COMPARISONS ($\alpha = 0.05$)

CHANNEL	0° SEAT-BACK Cell A	+10° SEAT-BACK Cell B	% CHANGE
HEAD Z ACCEL (G)	12.03	12.33	NSD
CHEST Z ACCEL (G)	13.80	14.08	NSD
CHEST X ACCEL (G)	4.16	5.73	+38%
RES SEAT FORCE (lb)	2145	2135	NSD
HEAD Z ACCEL (ms)	71.8	75.6	+5%
CHEST Z ACCEL (ms)	82.2	79.7	NSD
CHEST X ACCEL (ms)	69.7	68.9	NSD
RES SEAT FORCE (ms)	77.0	76.6	NSD

TABLE 22. WILCOXON SIGNED RANK TEST SUMMARIES FOR HUMAN SUBJECT -10°
SEAT-BACK ANGLE COMPARISONS ($\alpha = 0.05$)

CHANNEL	0° SEAT-BACK Cell A	-10° SEAT-BACK Cell L	% CHANGE
HEAD Z ACCEL (G)	12.01	11.89	NSD
CHEST Z ACCEL (G)	13.91	14.07	NSD
CHEST X ACCEL (G)	4.12	3.12	-24%
RES SEAT FORCE (lb)	2205	2250	NSD
HEAD Z ACCEL (ms)	71.3	72.5	NSD
CHEST Z ACCEL (ms)	82.5	78.1	NSD
CHEST X ACCEL (ms)	69.7	72.0	NSD
RES SEAT FORCE (ms)	77.6	80.7	NSD

Manikin dynamic response

Table 12 shows the effects of variation in seat-back angle on the simulation of acceleration response by the manikins. The results obtained in Cell A, with a seat-back angle of 0°, were similar to cell B, with a seat-back angle of +10°. In both cells, the poorest simulation of human response as evidenced by a greater number of mean acceleration data lying

outside the corresponding two standard deviations interval of the human data, occurred in the large ADAM peak magnitude values and the CG-5 time-to-peak values. Resultant Seat Force peak magnitude data are plotted for tests with a seat-back angle of 0° in Figure 1 (Cell A) and a seat-back angle of +10° in Figure 2 (Cell B). The manikin data in both cells show a similarly close fit to the corresponding human data regression line, with the exception of the large ADAM, whose data show a closer fit to the human data in Cell A than in Cell B.

Varying Rise-Time

Human dynamic response

The effect on human dynamic response of employing a deceleration input pulse with a rapid rise-time was demonstrated by a series of tests which used metering pin number 46 on the VDT facility (Cell D). This pin generates a half-sinusoidal 24 ms rise-time input pulse, as opposed to pin 102 (66 ms rise-time), which was used for all other test cells. Wilcoxon Signed Rank tests comparing Cell C with Cell D were performed in order to compare the effects of the rapid rise-time pulse on human response, and are shown in Table 23. Employing the rapid rise-time pulse resulted in increases in the peak magnitudes of the Head Z Acceleration and the Chest X Acceleration data of 48% and 71% respectively, with no significant change in the Chest Z Acceleration. In addition, the peak magnitude of the Resultant Seat Force data decreased by 12%. Also, all four of the corresponding time-to-peak values decreased by 38-50%.

TABLE 23. WILCOXON SIGNED RANK TEST SUMMARIES FOR HUMAN SUBJECT
VARYING RISE-TIME COMPARISONS ($\alpha = 0.05$)

CHANNEL	66 MS Cell C	24 MS Cell D	% CHANGE
HEAD Z ACCEL (G)	11.68	17.23	+48%
CHEST Z ACCEL (G)	13.47	13.78	NSD
CHEST X ACCEL (G)	3.73	6.36	+71%
RES SEAT FORCE (lb)	2188	1920	-12%
HEAD Z ACCEL (ms)	70.7	40.8	-42%
CHEST Z ACCEL (ms)	77.9	46.4	-40%
CHEST X ACCEL (ms)	64.7	40.0	-38%
RES SEAT FORCE (ms)	75.5	37.5	-50%

Manikin dynamic response

As seen in a comparison of cells C and D in Tables 12 and 13, employing an input pulse with a rapid rise-time caused large increases in the peak

magnitudes of the acceleration data and large decreases in the time-to-peak measurements in all four manikins. The small sample size in Cell D, however, precludes statistical significance. In Table 13, Cell D, the mean peak magnitudes of the Chest Z and Head Z Acceleration data in all four manikins demonstrates a decrease in their ability to simulate z-axis human dynamic response in the rapid rise-time condition. This is evidenced by the peak magnitudes of the data being much greater than the mean of the corresponding human data for those measurements. In the Chest X Acceleration data, however, all manikin peak magnitude values except the CG-95 were within two standard deviations of the mean of the corresponding human data. The mean time-to-peak values of all four manikins were larger for the Chest X Acceleration and smaller for the Chest Z and Head Z accelerations than the corresponding human data. As in the peak magnitude data, not all the variations were greater than two standard deviations from the mean of the corresponding human data. Overall, the large ADAM most closely approximated the human response data for the rapid rise-time condition, with no mean peak magnitude values nor time-to-peak values outside the two standard deviations interval of the human data.

The effects of the rapid rise-time input pulse on the peak magnitude of the Resultant Seat Force for the manikins can be seen in Figure 4. The seat forces of all four manikins were much greater than two standard deviations from the regression line of the corresponding human data, as compared to Figure 3 (Cell C), where only the large ADAM mean peak magnitude was well outside the two standard deviations interval.

DISCUSSION

ADAM Reliability

Both the small and large ADAM were found to be structurally sound, with no major damage occurring in any tests at impact levels up to 24 G in the z-axis direction. Data acquisition, however, was often incomplete, due mostly to broken wires, noisy channels, and circuit board failures. The DECOM system was plagued with excessive noise throughout much of the testing until a grounding problem in the data link was discovered and corrected. Although the ADAM sensors appeared to perform well during impact, the internal ADAM paths providing signal transmission and sensor excitation were sometimes interrupted due to breaks in the wiring or sensor connections.

ADAM Sensitivity

The sensitivity of the ADAM channels is the product of the transducer sensitivity times the gain of the individual channel signal conditioning circuits, and is specified in engineering units per volt. Since the transducer sensitivity is normally a constant value as specified by the manufacturer, the variations in sensitivity would be due to changes in the amplification properties of the ADAM signal conditioning circuits. These changes probably occurred slowly over time as the ADAM power was turned on and off and as the instrumentation was subjected to impacts. This would appear to be the case since only small changes in sensitivity were found when comparisons of several channels were made after a much shorter period of time with a small number of impacts. Also, the mean low-level calibration voltages for both ADAMs varied by less than 1% per test, which is also indicative of relatively gradual changes in the sensitivities. In summary, the ADAM channel sensitivities appear to be relatively stable for individual impact tests. Periodic recalibration is recommended, however, for multiple tests over extended periods of time.

The mean variations per test in the calibration voltages for the low-level channels were much less than for the high-level channels (+0.02 volts vs. +0.08 volts). The differences between these values would appear to be attributable to differences between the two channel systems. Both systems use a potentiometer to shunt the calibration voltage across the sensors, but the low-level system uses adjustable resistors as compared to fixed resistors for the high-level system. The low-level system accelerometer and load cell sensors have a relatively constant impedance while the high-level system position sensors vary their resistance with movement of body segments. Also, the applied calibration voltages receive additional amplification in the low-level system before being filtered. The differences in calibration voltage variations between the high- and low-level systems, therefore, appear to be caused by the variations in loading of the applied calibration voltages due to one or more of these circuit differences. It should be noted that the calibration check system was designed only to provide an indication of defects in channel operation either before or during the test. Although it does give some information on channel stability for individual tests, this information does not necessarily correlate with long term channel sensitivity.

Repeatability of Manikin Dynamic Response

Both the ADAM and GARD manikins demonstrated reasonably good repeatability in the +Gz direction for both acceleration and force data. Some variation between tests would normally be expected due to slight differences in the harness tensions, manikin positioning, and acceleration input profiles. For manikin test programs concerned with repeatability of peak magnitude z-axis impact test data, a good rule of thumb would be small ADAM $\pm 15\%$, large ADAM $\pm 10\%$, CG-95 $\pm 8\%$, and CG-5 $\pm 5\%$.

Both the ADAM and the GARD manikins appeared to demonstrate poor repeatability in the x-axis acceleration data. The poor x-axis repeatability was not unexpected since the carriage acceleration input pulse in the z-axis direction resulted in smaller peak magnitudes of the x-axis acceleration response data. Standard deviations used to measure x-axis repeatability therefore appear as larger percentages of the means. Direct comparisons between the ADAM and GARD manikins for both axes show a general trend of better repeatability of peak magnitude data in the GARD manikins and better repeatability of the time-to-peak data in the ADAM manikins.

Manikin Simulation of Human Dynamic Response

The small ADAM was most consistently able to simulate human dynamic response, as evidenced by a closer fit of the small ADAM response data with the corresponding human data than the other three manikins. This was true in both numbers of mean acceleration response data within the two standard deviations interval of the mean of the corresponding human data, as well as in comparisons of manikin and human responses in Wilcoxon Rank Sum tests. The small ADAM seat force peak magnitudes were also consistently very close to the predicted human mean values as demonstrated by linear regression analysis. Results consistent with the human data were also obtained in the transfer function analysis computations of the resonant frequencies and damping ratios, although two of the small ADAM damping ratios were higher than expected.

The large ADAM demonstrated inconsistent simulation of human dynamic response, as demonstrated by the analysis techniques discussed above. The measured peak magnitudes of the acceleration data, particularly in the z-axis, tended to be greater than the corresponding human data, although the large ADAM was able to accurately simulate the human responses in measuring the acceleration time-to-peak. Linear regression analysis showed the large ADAM seat force measurements to be substantially larger than those predicted by the human data. However, it should be noted that the corresponding human regression data was interpolated since no human data was available at weights as great as the weight of the large ADAM. Transfer function analysis showed large ADAM resonant frequencies and damping ratios to be reasonably close to the mean of the human data.

Both GARD manikins demonstrated inconsistent simulation of human dynamic response. Peak magnitude measurements of the CG-5 and CG-95 acceleration data in the z-axis were reasonably close to the corresponding human data, but time-to-peak measurements and the Chest X Acceleration peak magnitude

data were not as close to the human data as were the ADAM manikins. Linear regression analysis showed that the measured peak seat forces of the GARD manikins were not as close to the corresponding human data as were the small ADAM, but were closer than the large ADAM values. The computed resonant frequencies and damping ratios were found to be reasonably close to the human data for both GARD manikins.

Seat Cushions

Employing the ConforTM Foam seat cushion appeared to have almost no effect on the human acceleration and force data which were analyzed with Wilcoxon Signed-Rank tests. Analysis of manikin acceleration data, however, demonstrated decreased simulation of human dynamic response in all four manikins when using the cushion. Manikin simulation of human response in measuring seat force data, however, actually improved when using the ConforTM Foam cushion. This was evidenced by the closer fit to the human data regression line of the manikin response data obtained while using the seat cushion, as opposed to the no seat cushion condition. The seat cushion appeared to have very little effect on manikin (only the CG-5 measurements were available) peak magnitude acceleration and seat force data at higher impact levels up to 24 G, with the exception of the Head X Acceleration data, where the peak magnitudes were larger when using the cushion.

Use of the ACES II seat cushion in human tests resulted in slight increases in the z-axis acceleration peak magnitude data and slight increases in all time-to-peak data. The ACES II cushion did not appear to have any noticeable effect on the simulation of human acceleration response by the manikins. However, as with the ConforTM Foam cushion, use of the ACES II seat cushion did result in improved manikin simulation of human seat force response data.

Restraint Harnesses

The X-Band 90 restraint harness appeared to outperform the PCU-15/P harness in both human and manikin tests. Employing the X-Band 90 harness in human tests resulted in lower peak magnitudes in the acceleration and seat force data than the PCU-15/P. Also, all manikins demonstrated better simulation of human acceleration response with the X-Band 90 harness than with the PCU-15/P. In regression analysis of the seat forces, three of the four manikins showed a closer fit to the human data when using the X-Band 90 harness.

Seat-Back Angle

Variation in the seat-back angle in human tests significantly affected only the peak magnitude of the Chest X Acceleration data. Tests with a seat-back angle of +10° demonstrated an increase in peak magnitude, while tests with an angle of -10° showed a decrease in peak magnitude. The seat-back angle of +10° did not appear to have any significant effect on the ability of the manikins to simulate human dynamic response.

Varying Rise-Time

Employing an acceleration input pulse with a rapid rise-time (24 ms) in human tests resulted in increases in the peak magnitudes of the acceleration data and a decrease in the peak seat force. The manikin tests demonstrated similar increases in the peak magnitudes of the acceleration data, but showed increases in the peak seat forces. The manikins also demonstrated decreased simulation of human dynamic response in the rapid rise-time condition, since the peak magnitudes of the z-axis acceleration data as well as the peak seat forces were substantially higher than the means of the corresponding human data taken from the same cell. Both the human subjects and the manikins demonstrated substantial decreases in time-to-peak measurements in the rapid rise-time condition. This was as expected since the 24 ms rise-time input pulse of the carriage was being translated into more rapid rise-times for the individual time-to-peak responses.

SUMMARY AND CONCLUSIONS

Summary

Small and large prototype ADAM manikins, along with CG-5 and CG-95 GARD manikins, were subjected to impacts of up to 24 G on the AAMRL Vertical Deceleration Tower. Human subjects were also tested at levels of up to 10 G using the same facility. The variables tested were impact level, seat cushion, restraint harness, seat-back angle, and rise-time of carriage acceleration input pulse. Data was recorded for carriage acceleration and velocity, harness anchor loads, head acceleration, chest acceleration, lumbar acceleration, neck force, lumbar force, seat force, and arm and leg motions. The test data was analyzed to evaluate ADAMs' structural adequacy, instrumentation reliability, repeatability of response, and ability to simulate human dynamic response. The results of the ADAM tests were also compared to tests with other manikins currently in use by the Air Force.

Conclusions

Both the small and large ADAM manikins were found to be structurally sound at tests up to 24 G in the z-axis. Data acquisition, however, was often incomplete, due mostly to broken wires, noisy channels, and circuit board failures. Both ADAM manikins demonstrated reasonably good repeatability of acceleration and force data in the direction of impact, although the sensitivities of the ADAM channels appeared to gradually change with repeated tests, thus demonstrating the need for periodic recalibration.

An important criteria in evaluating the usefulness of manikins in impact testing is their ability to simulate human dynamic response. By demonstrating that a strong correlation exists in the measured external accelerations and forces between humans and manikins, internal human response and injury predictions can then be inferred from manikin tests at high-impact levels. Although the small ADAM appeared to demonstrate relatively consistent simulation of human dynamic response in z-axis impact tests, the large ADAM had a tendency to generate larger peak magnitude acceleration and seat force data than predicted by the corresponding human data. Therefore, the large ADAM can not be used to accurately simulate human dynamic response unless basic design changes in its mechanical response properties are implemented.

In summary, the performance of the ADAM prototype manikins did not appear to meet the expectations of the Air Force or the ADAM designers. While the ADAM manikins offered improved data acquisition technology and proved to be structurally sound, the instrumentation systems were found to be unreliable over a long series of impact tests. However, with improvements to the instrumentation wiring and the correction of failure-prone components, the small ADAM could be useful in providing data in impact and ejection testing. The large ADAM, however, would require more extensive design modifications in order to be expected to generate accurate impact data.

In addition to evaluation of the ADAM manikins, the effects of several other variables during the impact tests were analyzed. In seat cushion

comparisons, the ConforTM Foam cushion appeared to outperform the ACES II cushion when measuring human dynamic response. This was demonstrated by the negligible effect of the ConforTM Foam cushion on acceleration and seat force data, compared to the slight increases in the peak magnitudes of the z-axis acceleration data observed in tests with the ACES II. The ACES II seat cushion, however, did appear to have less effect on the manikins' ability to simulate human response than the ConforTM Foam cushion.

Restraint harness evaluations indicated that the X-Band 90 harness appeared to outperform the PCU-15/P harness in both the human and manikin tests. This was evidenced by the lower peak magnitudes observed in the human acceleration and seat force data when using the X-Band 90, as well as the improved ability of the manikins to simulate human dynamic response.

Variations in the seat-back angle significantly affected only the peak magnitude of the chest acceleration data in the x-axis direction. Since the effects on the larger z-axis accelerations and seat forces were negligible, it would appear that the seat-back angle can be adjusted up to + 10° without increased risk of spinal injury in +Gz impact tests up to 10 G.

Impact tests employing a rapid rise-time half-sinusoidal input pulse resulted in a significant increase in the peak magnitude of the head acceleration in the z-axis direction, in both human and manikin tests. This may pose an increased risk of head/neck spinal injury in ejection systems at higher G-levels with similar rapid acceleration profiles. Caution should be observed in correlating manikin tests with human response using these acceleration parameters, since all manikins showed a decrease in their ability to simulate human dynamic response in the rapid rise-time condition.

REFERENCES

1. Bartol, A. M., Hazen, V. L., Kowalski, J. F., Murphy, B. P., and White Jr., R. P. Advanced Dynamic Anthropomorphic Manikin (ADAM) Final Design Report. AAMRL-TR-90-023, 1990.
2. Brinkley, J. W., Mosher, S. E., and Specker, L. J. Development of Acceleration Exposure Limits for Advanced Escape Systems. AGARD Conference Proceedings, No. 472 (1990).
3. Chase, W. and Brown, F. General Statistics. New York NY: John Wiley and Sons, 1986.
4. Strzelecki, J. and Buhrman, J. R. Horizontal Impact Tests of the Anthropomorphic Dynamic Manikin (ADAM). October 1990.
5. Systems Research Laboratories, Inc. Operation and Maintenance Manual for Advanced Dynamic Anthropomorphic Manikin. Prepared for Armstrong Laboratory, 1988.
6. Tse, F. S., Morse, I. E., and Hinkle, R. T. Mechanical Vibrations. Boston: Allyn and Bacon, Inc., 1978.
7. Walpole, R. E. and Myers, R. H. Probability and Statistics for Engineers and Scientists (3rd ed.). New York NY: Macmillan Publishing Co., 1985.
8. Wilcoxon, F. and Wilcox, R. A. Some Rapid Approximate Statistical Procedures. New York NY: Lederle Laboratories, 1964.
9. Wittman, T. J. An Analytical Model to Duplicate Human Dynamic Force Response to Impact. AMRL-TR-66-126, 1966.

TEST CONFIGURATION AND
DATA ACQUISITION SYSTEM FOR THE
VERTICAL IMPACT OF HUMANS AND
ANTHROPOMORPHIC MANIKINS (VIHAM)
DURING +Gz IMPACT ACCELERATION
TEST PROGRAM

Prepared under
Contract F33615-86-C-0531

July 1988

Prepared by
Marshall Z. Miller
and
Stephen E. Mosher

DynCorp
Scientific Support Division
Building 824, Area B
Wright-Patterson AFB, Ohio 45433

TABLE OF CONTENTS

	<u>PAGE</u>
INTRODUCTION.....	A-4
1. TEST FACILITY.....	A-4
2. SEAT FIXTURE.....	A-4
3. RESTRAINT CONFIGURATIONS.....	A-5
4. SEAT CUSHIONS.....	A-5
5. TEST SUBJECTS.....	A-5
6. INSTRUMENTATION.....	A-6
6.1 ACCELEROMETERS.....	A-7
6.2 LOAD TRANSDUCERS.....	A-8
6.3 CALIBRATION.....	A-10
7. DATA ACQUISITION.....	A-11
7.1 AUTOMATIC DATA ACQUISITION AND CONTROL SYSTEM (ADACS)....	A-11
7.2 PHOTOGRAMMETRIC DATA ACQUISITION.....	A-12
8. PROCESSING PROGRAMS.....	A-13
8.1 ADACS PROGRAM OPERATION.....	A-13
8.2 ADAM PROCESSING PROGRAMS.....	A-14

LIST OF TABLES

<u>TABLE</u>	<u>PAGE</u>
A-1. INSTRUMENTATION REQUIREMENTS	
A-1a. PAGE 1 OF 6.....	A-15
A-1b. PAGE 2 OF 6.....	A-16
A-1c. PAGE 3 OF 6.....	A-17
A-1d. PAGE 4 OF 6.....	A-18
A-1e. PAGE 5 OF 6.....	A-19
A-1f. PAGE 6 OF 6.....	A-20
A-2. TYPICAL TRANSDUCER SPECIFICATIONS.....	A-21
A-3. LIST OF TRANSDUCER FIGURES.....	A-10
A-4. TRANSDUCER PRE- AND POST-CALIBRATION	
A-4a. PAGE 1 OF 7.....	A-22
A-4b. PAGE 2 OF 7.....	A-23
A-4c. PAGE 3 OF 7.....	A-24
A-4d. PAGE 4 OF 7.....	A-25
A-4e. PAGE 5 OF 7.....	A-26
A-4f. PAGE 6 OF 7.....	A-27
A-4g. PAGE 7 OF 7.....	A-28

LIST OF ILLUSTRATIONS

<u>FIGURE</u>	<u>PAGE</u>
A-1. AAMRL VERTICAL DECELERATION TOWER.....	A-29
A-2. VIP SEAT POSITIONS.....	A-30
A-3. PLUS 10 DEGREE SEAT POSITION.....	A-31
A-4. 0 DEGREE SEAT POSITION.....	A-32
A-5. MINUS 10 DEGREE SEAT POSITION.....	A-33
A-6. X-BAND-90 DEGREE HARNESS.....	A-34
A-7. PCU-15/P HARNESS.....	A-35
A-8. SUBJECT LEG AND THIGH RESTRAINTS.....	A-36
A-9. ACES II SEAT CUSHION.....	A-37
A-10. CREST CONFORT TM SEAT CUSHION.....	A-38
A-11. AAMRL/BBP COORDINATE SYSTEM.....	A-39
A-12. CARRIAGE VELOCITY WHEEL.....	A-40
A-13. HUMAN HEAD ACCELEROMETER PACKAGE.....	A-41
A-14. CHEST ACCELEROMETER PACKAGE.....	A-42
A-15. TRANSDUCER LOCATIONS AND DIMENSIONS	
A-15a. PAGE 1 OF 4.....	A-43
A-15b. PAGE 2 OF 4.....	A-44
A-15c. PAGE 3 OF 4.....	A-45
A-15d. PAGE 4 OF 4.....	A-46
A-16. LOAD LINK INSTRUMENTATION.....	A-9
A-17. SEAT PAN INSTRUMENTATION.....	A-47
A-18. SEAT PAN INSTRUMENTATION.....	A-48
A-19. SEAT PAN INSTRUMENTATION.....	A-49
A-20. SEAT PAN AND SEAT BACK INSTRUMENTATION.....	A-50
A-21. HEADREST AND SHOULDER LOAD CELL INSTRUMENTATION.....	A-51
A-22. ADACS INSTALLATION.....	A-52
A-23. AUTOMATIC DATA ACQUISITION AND CONTROL SYSTEM.....	A-53
A-24. DATA ACQUISITION AND STORAGE SYSTEM BLOCK DIAGRAM.....	A-54
A-25. ONBOARD CAMERA LOCATIONS.....	A-55
A-26. FIDUCIAL TARGET LOCATIONS	
A-26a. PAGE 1 OF 2.....	A-56
A-26b. PAGE 2 OF 2.....	A-57
A-27. AUTOMATIC FILM READER.....	A-58

INTRODUCTION

This report was prepared by DynCorp for the Harry G. Armstrong Aerospace Medical Research Laboratory (AAMRL/BBP) under Air Force Contract F33615-86-C-0531.

The information provided herein describes the test facility, seat fixture, restraint configurations, seat cushions, test subjects, data acquisition, instrumentation procedures and the test configurations that were used in The Vertical Impact of Humans and Anthropomorphic Manikins (VIHAM) During +Gz Impact Acceleration Test Program. Two hundred eighty tests were conducted from September 1987 through March 1988 on the Vertical Deceleration Tower Test Facility.

1. TEST FACILITY

The AAMRL Vertical Deceleration Tower, as shown in Figure A-1, was used for all of the tests.

The facility consists of a 60 foot vertical steel tower which supports a guide rail system, an impact carriage supporting a plunger, a hydraulic deceleration device and a test control and safety system. The impact carriage can be raised to a maximum height of 42 feet prior to release. After release, the carriage free falls until the plunger, attached to the undercarriage, enters a water filled cylinder mounted at the base of the tower. The deceleration profile produced as the plunger displaces the water in the cylinder is determined by the free fall distance, the carriage and test specimen mass, the shape of the plunger and the size of the cylinder orifice. A rubber bumper is used to absorb the final impact as the carriage stops. For these tests, plunger number 102 was mounted under the carriage for all test cells except cell D. Plunger number 46 was used for test cell D. The cell D final impact had a severe rebound when the normal rubber bumper was used. For cell D only, a new bumper was designed and used consisting of two layers of Confor Cushion (blue, 7 3/4" x 9" x 3" high) sandwiched between three layers of 3/16" gray/blue honeycomb. This new bumper was taped together and covered with plastic so as not to absorb water from the impact. Drop height varied depending on the test cell requirements which ranged from 3'6" to 31'0".

2. SEAT FIXTURE

The VIP seat fixture, as shown in Figure A-1, was used for all of the tests. The seat was designed to withstand vertical impact accelerations up to 50 G. Its adjustable seat back and seat pan allowed the subject to sit in one of three positions, as shown in Figure A-2. When positioned in the seat, the subject's upper legs were bent 90 degrees outward to a horizontal position with his lower legs bent 90 degrees downward to a vertical position. The subject was secured in the seat with a lap belt and shoulder strap. The lap belt and shoulder strap were preloaded to 20 ±5 pounds as required in the test plan.

Figures A-3, A-4 and A-5 further illustrate the plus 10 degree seat position, 0 degree seat position and the minus 10 degree seat position respectively. Note that the seat pan is horizontal for the 0 and minus 10 degree seat-back positions. For the plus 10 degree seat-back position, the seat pan is positioned at a plus 10 degree angle from the horizontal.

The coordinate system (shown in Figure A-2) is left-handed and oriented so that the x and y axes are parallel to the plane of the seat pan and the z axis is perpendicular to the seat pan. For the 0 and plus 10 degree seat positions, the seat back is perpendicular to the seat pan and thus the z axis is parallel to the seat back. For the minus 10 degree seat position the seat pan is horizontal, the seat back inclines 10 degrees forward of the vertical reference, and the z axis is parallel to the vertical reference.

3. RESTRAINT CONFIGURATIONS

Two restraint configurations were tested. The X-Band-90 degree harness and the PCU-15/P and PCU-16/P torso harnesses with a conventional lap belt were used. Figures A-6 and A-7 illustrate the X-Band-90 degree harness and PCU-15/P harness respectively.

Each of the subject's legs were restrained by a strap that encircled the subject's ankle and was attached to the carriage. Another strap crossed the subject's thighs and attached to the seat pan posterior to the knees. The subject's hands were placed under the thigh restraint. These restraints are illustrated by Figure A-8.

4. SEAT CUSHIONS

The ACES II and the CREST cushions were tested during this test program. The ACES II cushion fits on the seat pan only as illustrated by Figure A-9. The CREST cushion is a one-inch thick Confor™ foam cushion. The CREST cushion was used on both the seat pan and seat back as illustrated in Figure A-10.

5. TEST SUBJECTS

Both manikins and human test subjects were used during this test program.

A 95th percentile Alderson manikin, designated VIP-95, was used for structural and equipment proof tests.

Two ADAM prototype manikins representative of the "large" and "small" flying population were used during this test program.

Two GARD manikins were also tested. They were designated as the CG-95 and CG-5 manikins.

6. INSTRUMENTATION

The electronic data collected during this test program is described in Sections 6.1 and 6.2. Section 6.1 discusses accelerometers while Section 6.2 discusses load transducers. Section 6.3 discusses the calibration procedures that were used. The measurement instrumentation used in this test program is listed in Tables A-1a through A-1f. These figures designate the manufacturer, type, serial number, sensitivity and other pertinent data on each transducer used. Table A-2 lists the manufacturer's typical transducer specifications.

Accelerometers and load transducers were chosen to provide the optimum resolution over the expected test load range. Full scale data ranges were chosen to provide the expected full scale range plus 50% to assure the capture of peak signals. All transducer bridges were balanced for zero output prior to the start of each test. Those accelerometers which were in line with the force of gravity were adjusted for a 1 G offset using computer processing software. The accelerometer and load transducer coordinate systems are shown in Figure A-11.

The linear accelerometers were wired to provide a positive output voltage when accelerations were applied in the +x, +y and +z directions, as shown in Figure A-11.

The angular Ry accelerometers were wired to provide a positive output voltage when the angular accelerations were applied in the +y direction according to the right hand rule, as shown in Figure A-11.

The load transducers included three types of load measurement devices. All were wired as follows:

Fixed Load Cells - were wired to provide a positive output when force is applied in the indicated direction (Figure A-11).

Triaxial Load Cells - were wired to provide a positive output when the belt was pulled towards the center of the seat.

Load Links - were wired to provide a positive output when force is applied in the direction indicated (Figure A-11).

Carriage velocity was measured using a Globe Industries tachometer Model 22A672-2. The rotor of the tachometer was attached to an aluminum wheel with a rubber O-ring around its circumference to assure good rail contact. The wheel contacted the track rail and rotated as the carriage moved, producing an output voltage proportional to the velocity. Figure A-12 shows the location of the carriage velocity wheel which is located on top of the carriage.

For the large and small ADAM manikins, left elbow and left knee angles were measured using SPL 6886-16-6869-10 and 6886-16-6869-30 flexion potentiometers respectively. The left knee and left elbow flexion angles are defined to be zero degrees when the knee and arm are fully extended. The flexion angle increases as the leg or arm is retracted. The left knee potentiometer was wired to output 5 volts at 0 degrees, 0 volts at 62.5 degrees and minus 5 volts at 125 degrees. The left elbow flexion potentiometer was wired to provide 5 volts at 0 degrees, 0 volts at 70 degrees and minus 5 volts at 140 degrees.

6.1 Accelerometers

This section describes the accelerometer instrumentation as required in the AAMRL/BBP test plan.

Human head accelerations were measured using three Endevco Model 7264-200 linear accelerometers and one Endevco model 7302A angular (Ry) accelerometer. The accelerometers were mounted to the external edge of a plastic dental bite block. Each subject had his own set of custom fitted dental inserts that were used to support the bite block in his mouth. An aluminum tube extended from the bite block and located a fiducial target used for photo tracking purposes. Figure A-13 illustrates the human head accelerometer package.

The chest accelerometer package consisted of three Endevco Model 2264-150 linear accelerometers mounted to a 1/2 x 1/2 x 1/2 inch aluminum block. An Endevco Model 7302A angular (Ry) accelerometer was mounted on a bracket adjacent to the triaxial chest block. The accelerometer packages were inserted into a steel protection shield to which a length of Velcro fastener strap was attached. The package was placed over the subject's sternum at the level of the xyphoid and was held there by fastening the Velcro strap around the subject's chest. A chest fiducial target was attached directly on top of the chest accelerometer package. Figure A-14 illustrates the chest accelerometer package attached to the Large ADAM manikin.

Carriage z acceleration was measured using an Endevco linear accelerometer model 2262A-200. The accelerometer was located behind the seat on the VIP seat structure.

Seat accelerations were measured using three Endevco Model 2264-200 accelerometers for accelerations in the x, y and z directions. Seat angular (Ry) acceleration was measured using an Endevco Model 7302B angular accelerometer. The three linear accelerometers were attached to a 1 x 1 x 3/4 inch acrylic block and were mounted near the center of the load cell mounting plate. The angular accelerometer was attached to an aluminum bracket and was mounted just behind the linear seat accelerometer package.

Head accelerations for manikin tests were measured using three Endevco Model 2264-200 linear accelerometers and one Endevco Model 7302 angular (Ry) accelerometer. These accelerometers were internally mounted in the head of the VIP 95 and Gard manikins.

For Large and Small ADAM manikin tests, head x and z acceleration, chest x acceleration, and Lumbar z acceleration were each measured using Entran Model EGA-125-100D linear accelerometers. These accelerometers were internally mounted in the manikins.

6.2 Load Transducers

This section describes the load transducer instrumentation as required in the AAMRL/BBP test plan.

The load transducer locations and dimensions are shown in Figures A-15a through A-15d.

Lap/vertical anchor forces and shoulder strap forces were each measured using GM3D-SW triaxial load cells, each capable of measuring forces in the x, y and z directions. The lap/vertical anchor force parameters are indicated below for their respective restraint harness configuration:

X-Band-90 Degree Harness:

- left vertical anchor x, y and z forces
- right vertical anchor x, y and z forces

PCU-15/P Harness:

- left lap x, y and z forces
- right lap x, y and z forces

The lap/vertical anchor force triaxial load cells were located on separate brackets mounted on the side of the seat frame parallel to the seat pan.

The shoulder strap force triaxial load cell was mounted on the seat frame between the seat back support plate and the headrest.

Left and right Horizontal anchor x forces were each measured using Strainert FL1U-2SG load cells for the X-Band-90 degree restraint harness configuration only. The load cells were located on separate brackets mounted on the side of the seat frame parallel to the seat back.

Left, right and center seat forces were measured using three load cells and three load links. The three load cells were Strainert Model FL2.5U-2SPKT load cells. The three load links, as shown in Figure A-16, were fabricated by DynCorp using Micro Measurement Model EA-06-062TJ-350 strain gages. All six measurement devices were located under the seat pan support plate. The load links were used for measuring loads in the x and y directions, two in the x direction and one in the y direction. Each load link housed a swivel ball which acted as a coupler between the seat pan and load cell mounting plate. The Strainert load cells were used for measuring loads in the z direction.

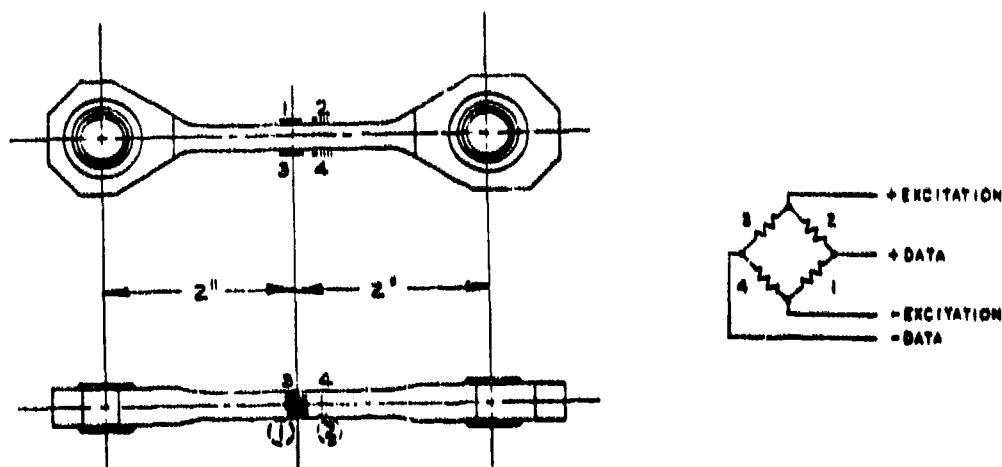


FIGURE A-16: LOAD LINK INSTRUMENTATION

Left, right and center seat back forces were measured using three load cells and three load links. Two load cells were Strainert Model FL1U-2SGKT load cells and the other was a Strainert Model FL1U-2SPKT. The three load links, as shown in Figure A-16, were fabricated by DynCorp using Micro Measurement Model EA-06-062TJ-350 strain gages. All six measurement devices were located behind the seat back support plate. The load links were used for measuring loads in the y and z directions, two in the z direction and one in the y direction. Each load link housed a swivel ball which acted as a coupler between the seat back and load cell mounting plate. The Strainert load cells were used for measuring loads in the x direction.

Upper and lower headrest x forces were each measured using two Strainert Model FL1U-2SG load cells. The load cells were mounted on a rectangular mounting plate which was attached to the upper seat back. The headrest was attached directly to the load cells. The mounting plate/load cells/headrest was adjusted up or down depending on the location of the subjects head.

For large and small ADAM manikin tests, Lumbar z and Neck z forces were each measured using Denton Model 1914 and 1716 load cells respectively. These load cells were internally mounted in the manikins.

Although Figures A-15a through A-15d illustrates the load transducer locations and dimensions, photos can more accurately depict the transducers. Table A-3 lists the reference figures (photos), their descriptions, restraint configuration and seat positions:

FIGURE	DESCRIPTION	CONFIGURATION	SEAT POSITION
A-17	Seat Pan Instrumentation	X-Band-90 Harness	0 and -10 degrees
A-18	Seat Pan Instrumentation	PCU-15/P Harness	0 and -10 degrees
A-19	Seat Pan Instrumentation	X-Band-90 Harness	0 and -10 degrees
A-20	Seat Pan and Seat Back Instrumentation Load Cell	X-Band-90 Harness	+10 degrees
A-21	Headrest and Shoulder Load Cell Instrumentation	N/A	N/A

TABLE A-3: LIST OF TRANSDUCER FIGURES

6.3 Calibration

Calibrations were performed before and after testing to confirm the accuracy and functional characteristics of the transducers. Pre-program and post-program calibrations are given in Tables A-4a through A-4g.

The calibration of all Strainert load cells was performed by the Precision Measurement Equipment Laboratories (PMEL) at Wright-Patterson Air Force Base. PMEL calibrated these devices on a periodic basis and provided current sensitivity and linearity data.

The calibration of the accelerometers was performed by DynCorp using the comparison method (Ensor, 1970). A laboratory standard accelerometer, calibrated on a yearly basis by Endevco with standards traceable to the National Bureau of Standards, and a test accelerometer were mounted on a shaker table. The frequency response and phase shift of the test accelerometer were determined by driving the shaker table with a random noise generator and analyzing the outputs of the accelerometers with a PDP 11/15 computer and 1923 Time Data Unit using Fourier analysis. The natural frequency and the damping factor of the test accelerometer were determined, recorded and compared to previous calibration data for that test accelerometer. Sensitivities were calculated at 40 G and 100 Hertz. The sensitivity of the test accelerometer was determined by comparing its output to the output of the standard accelerometer.

The angular accelerometers were calibrated by DynCorp by comparing their output to the output of a linear standard accelerometer. The angular accelerometer is mounted parallel to the axis of rotation of a Honeywell low inertia D. C. motor. The standard accelerometer is mounted perpendicular to the axis of rotation at a radius of one inch to measure the tangential acceleration. The D. C. motor motion is driven at a constant sinusoidal angular acceleration of 100 Hertz and the sensitivity is calculated by comparing the rms output voltages of the angular and linear accelerometers.

The load links and GM load cells were calibrated by DynCorp. These transducers were calibrated to a laboratory standard load cell in a special test fixture. The sensitivity and linearity of each test load

cell were obtained by comparing the output of the test load cell to the output of the laboratory standard under identical loading conditions. The laboratory standard load cell, in turn, is calibrated by PMEL on a periodic basis.

The velocity wheel is calibrated periodically by DynCorp by rotating the wheel at approximately 2000, 4000 and 6000 revolutions per minute (RPM) and recording both the output voltage and the RPM.

7. DATA ACQUISITION

Data acquisition was controlled by a comparator on the Master Instrumentation Control Unit in the Instrumentation Station. The test was initiated when the comparator countdown clock reached zero. The comparator was set to start data collection at a preselected time.

A reference mark pulse was generated to mark the ADACS electronic data at a preselected time after test initiation to place the reference mark close to the impact point. At the same time, the reference mark pulse triggered a strobe light to mark the test photogrammetric data. The reference mark time was used as the start time for data processing of the electronic and photogrammetric data.

Prior to each test and prior to placing the subject in the seat, data were recorded to establish a zero reference for all data transducers. These data were stored separately from the test data and were used in the processing of data.

7.1 Automatic Data Acquisition and Control System (ADACS)
Installation of the ADACS instrumentation is shown in Figure A-22. The three major components of the ADACS system are the power conditioner, signal conditioners and the encoder. A block diagram of the ADACS is shown in Figure A-23. The signal conditioners contain forty-eight amplifiers with programmable gain and filtering.

Bridge excitation for load cells and accelerometers was 10 VDC. Bridge completion and balance resistors were added as required to each module input connector.

The forty-eight module output data signals were digitized and encoded into forty-eight 11-bit digital words. Two additional 11-bit synchronization (sync) words were added to the data frame making a fifty word capability.

Three synchronization pulse trains (bit sync, word sync and frame sync) were added to the data frame and sent to the computer via a junction box data cable.

The PDP 11/34 minicomputer received serial data from the ADACS. The serial data coming from the carriage are converted to parallel data in

the data formatter. The data formatter inputs data by direct memory access (DMA) into the computer memory via a buffered data channel where data are temporarily stored on disk and later transferred to magnetic tape for permanent storage.

The interrelationships among the data acquisition and storage equipment are shown in Figure A-24.

Test data could be reviewed immediately after each test by using the "Quick Look" SCAN routine. SCAN was used to produce a plot of the data stored on any channel as a function of time. The routine determined the minimum and maximum values of any data plot. It was also used to calculate the rise time, pulse duration and carriage acceleration.

7.2 Photogrammetric Data Acquisition

Two onboard high-speed LOCAM cameras, operating at 500 frames per second, were used to produce the photogrammetric data. Each camera used a 9mm lens. The two camera locations, as shown in Figure A-25, are identified as the side and 45 degree camera.

Motion of the subjects' head, cheek, mouth and chest were quantified by tracking the motion of subject-mounted fiducials. Reference fiducials were placed on the test fixture. The fiducial used was a .75" diameter black circle on a 1.25" diameter white target. The locations of the fiducials generally followed the guidelines provided in "Film Analysis Guides for Dynamic Studies of Test Subjects, Recommended Practice" (SAE J138, March 1980). Figures A-26a and A-26b identify the fiducial target locations.

All cameras were automatically started at a preset time in the test sequence by a signal from the camera and lighting control station.

The photogrammetric data were time correlated in each test. Immediately prior to impact, a reference mark signal triggered the flash unit to mark the camera film frame. At that time, a 100 PPS signal activated the camera light emitting diode (LED) driver which activated the camera LED, producing a time mark at the film edge. This reference mark was then used to correlate the photogrammetric data with the electronically measured data.

The photogrammetric data will be processed as required on the Automatic Film Reader (AFR) system, shown in the clock diagram in Figure A-27. The fiducial tracking routine is initiated via the Data General terminal. The tracking routine is booted from a floppy disk into the Nova 3/12 memory. The system is capable of tracking fiducials manually or automatically. The Nova 3/12 outputs an x-y film coordinate position to magnetic tape for each fiducial being tracked. Data are transferred from magnetic tape to the DEC PDP 11/34 disk file and then transferred to the DEC VAX 11/750 disk file for processing.

An Instant Analytical Replay (INSTAR) video system was also used to provide coverage of each test. This video recorder and display unit is capable of recording high-speed motion at a rate of 120 frames per second. Immediate replay of the impact is possible in real time or in slow motion.

8. PROCESSING PROGRAMS

Test data for the +Gz VIHAM Study was collected using two separate data collection systems. The facility instrumentation and the standard subject instrumentation were monitored using the ADACS data collection system. During tests where the ADAM manikin was the subject, additional test data was collected using the ADAM internal data collection system.

The executable images for the ADACS processing programs are located in directory PROCESS of the VAX 11/750 and the test data is assumed to be stored in directory DATA1. All plots are output to the Tektronix hardcopy unit and the test summary sheet is listed to the Printronix P300 line printer. The test base file is output to directory PROCESS.

The executable images for the ADAM processing programs are located in directory PROCESS of the VAX 11/750. The plots and the test summary sheet are output to the Tektronix hardcopy unit. No test base file is created for the ADAM test data.

8.1 ADACS Program Operation

The two Fortran programs that process the ADACS test data are named VIHAMVDT0A and VIHAMVDT0B. The DCL file which controls the execution of these programs is named VIHAMVDT. The character string 'VIHAM' identifies the study (+Gz VIHAM Study), 'VDT' identifies the facility (Vertical Deceleration Tower), '0' is the revision number and the last character determines the program order of execution.

VIHAMVDT0A creates a temporary DCL file which controls the sequential batch processing of a specified number of tests. VIHAMVDT0A requests the user to enter the total number of tests to be processed and the test number of each test. Directory DATA1 is assumed to contain a zero reference file named '<test no>Z.VDT,' a test data file named '<test no>D.VDT' and a sensitivity file named '<test no>S.VDT.' The user enters the test number and specifies whether the default test parameters are to be used for processing. If the default parameters are selected, then the test number, subject identification, weight, height, sitting height and sex are read in from the first block of the test data file. The cell type, nominal G level and belt preload values are also read in. If the default parameters are not selected, they must be entered by the user.

VIHAMVDT0B does the actual data processing of the test data. The test data includes the carriage, seat, head and chest linear accelerations and the seat, head and chest Ry angular accelerations. The forces consist of the shoulder, headrest, anchor (or lap), back and seat loads. The

carriage velocity and bias voltages are also analyzed. The impact rise time, duration and velocity change, and the seat, head and chest acceleration resultants are computed based on the test data. Also computed are the shoulder, anchor (or lap), back and seat load resultants and the headrest load sum.

The output of VIHAMVDT08 consists of a base file, summary sheet and plots. The base file contains the extrema for the individual channels and the derived quantities. The summary sheet displays the extrema in a more readable format. The time histories of the parameters are plotted on the Tektronix terminal and hardcopied.

8.2 ADAM Processing Programs

The two Fortran programs that process the ADAM test data are named ADAM_DATA and ADAM_DECOM. ADAM_DATA is an interactive program which converts data collected in internal ram memory into engineering units and plots or lists the resulting time histories. ADAM_DECOM is an interactive program which converts data transmitted real time during the test into engineering units and plots or lists the results. The Fortran library ADAM_PLOTS provides subroutine support for both programs.

ADAM_DATA request the user to enter the ADAM test data filename, the test number and the reference mark voltage. The reference mark is used to correlate the ADAM data with the ADACS data. The user also specifies whether the output is to be plotted or listed. The channel numbers, descriptions, sensitivities, offsets and plotting parameters are read in from file CHSPEC in directory PROCESS. Time histories of the channels are plotted or listed for 600 ms starting from the reference mark time. Time zero corresponds to the start of impact.

ADAM_DECOM request the user to enter both the test data filename (internal ram) and the test decom filename (transmitted). This is necessary because the information required to determine the position of the channels in the frame is not transmitted and must be determined from the internal ram data. ADAM_DECOM also displays the number of frames containing bad sync patterns and requests the user to indicate whether to continue processing the corrupted data. Aside from these differences, ADAM_DECOM is functionally equivalent to ADAM_DATA.

Flowcharts of the ADAM processing programs were not included because DynCorp modified an existing program supplied by the customer.

DIGITAL INSTRUMENTATION REQUIREMENTS										DYNALLECTRON CORPORATION				
PROGRAM TITLE														
JACOBY VERTICAL DECELERATION TEST														
DATE 29 SEP 1971										PAGE 1360				
PAGES 1360										PAGE 1360				
DATA POINT	INSTR. TYPE	Q/A	INSTR. RANGE	INSTR. RANGE	INSTR. RANGE	INSTR. RANGE	INSTR. RANGE	INSTR. RANGE	INSTR. RANGE	INSTR. RANGE	INSTR. RANGE	INSTR. RANGE	INSTR. RANGE	INSTR. RANGE
15	08-30-00	15X	5.10 w/1/2	10.03	10.03	10.03	10.03	10.03	10.03	10.03	10.03	10.03	10.03	10.03
16	08-30-00	15X	5.30 w/1/2	10.03	10.03	10.03	10.03	10.03	10.03	10.03	10.03	10.03	10.03	10.03
17	08-30-00	15X	6.30 w/1/2	10.03	10.03	10.03	10.03	10.03	10.03	10.03	10.03	10.03	10.03	10.03
18	08-30-00	21X	5.11 w/1/2	10.03	10.03	10.03	10.03	10.03	10.03	10.03	10.03	10.03	10.03	10.03
19	08-30-00	21X	4.09 w/1/2	10.03	10.03	10.03	10.03	10.03	10.03	10.03	10.03	10.03	10.03	10.03
20	08-30-00	21X	6.12 w/1/2	10.03	10.03	10.03	10.03	10.03	10.03	10.03	10.03	10.03	10.03	10.03
21	08-30-00	20X	6.31 w/1/2	10.03	10.03	10.03	10.03	10.03	10.03	10.03	10.03	10.03	10.03	10.03
22	08-30-00	20X	5.00 w/1/2	10.03	10.03	10.03	10.03	10.03	10.03	10.03	10.03	10.03	10.03	10.03
23	08-30-00	20X	5.66 w/1/2	10.03	10.03	10.03	10.03	10.03	10.03	10.03	10.03	10.03	10.03	10.03
25	08-30-00	15X	2.001 w/1/2	10.03	10.03	10.03	10.03	10.03	10.03	10.03	10.03	10.03	10.03	10.03
26	08-30-00	15X	2.908 w/1/2	10.03	10.03	10.03	10.03	10.03	10.03	10.03	10.03	10.03	10.03	10.03
27	08-30-00	15X	2.023 w/1/2	10.03	10.03	10.03	10.03	10.03	10.03	10.03	10.03	10.03	10.03	10.03
28	08-30-00	5	10.06 w/1/2	10.03	10.03	10.03	10.03	10.03	10.03	10.03	10.03	10.03	10.03	10.03
LEFT AND RIGHT VERT. ACC. X AND Y LOAD CELLS MOVED TEST 1360 THROUGH 1366														
LEFT VERT. ACC. X BECAUSE Y-Z BECAUSE X; RIGHT VERT. ACC. X BECAUSE Y-Z BECAUSE X;														
LEFT AND RIGHT Y AND POLARITY REVERSED.														

TABLE A-1b: INSTRUMENTATION REQUIREMENTS

DYNALECTRON CORPORATION

DIGITAL INSTRUMENTATION REQUIREMENTS

DATE 29 SEP 1967 FROM 23 MAR 1968

132

附一： 附錄

WHEEL INVESTIGATION

INTEL **386**

Abstract

THE UNITED STATES OF AMERICA

[illegible]

PAGE 3 OF 6

TABLE A-1c: INSTRUMENTATION REQUIREMENTS

DIGITAL INSTRUMENTATION REQUIREMENTS										DYNAL ELECTRON CORPORATION				
PROGRAM TITLE														
DATE 20 SEP 1967										23 MAR 1968				
FACILITY										RPM 1360				
VERTICAL INSTRUMENTATION TUBES										RPM 1639				
DATA CHANNEL	DATA POINT	INSTR. INFO. & TYPE	QPM	INSTR. SENS.	INSTR. V. TUBES	FILTER	AMP	SAMPLE RATE	P.A. SENS.	FILTER Hz	INSTR. SENS.	INSTR. BALANCE	INSTR. COMPENSATION	SPECIAL NOTATIONS
13	CHERT BY ANG.	IMBROVO T302A	AMB15	6.80 uv/rad/ SEC ²	10.00	60	100	1K	3577 RAD/SEC ²	120	2.5 5.0 0.0	40K -1m Gal.	-	TYPE 1360-1370 GAIN 201. P.A. 1829 RAD/SEC ²
14	CHERT BY ANG.	IMBROVO T302B	PCH7	3.719 uv/rad/ SEC ²	10.00	60	102	1K	1672 RAD/SEC ²	120	2.5 5.0 0.0	-	-	
15	LEFT SIDE ANG. X FORCE	IMBROVO T302B	209	19.89 uv/rad/ SEC ²	10.00	60	120	1K	125710	120	2.5 5.0 0.0	-	-	X RAD BURNING ONLY
16	RIGHT SIDE ANG. X FORCE	IMBROVO T302B	210	19.95 uv/rad/ SEC ²	10.00	60	100	1K	125310	120	2.5 5.0 0.0	-	-	X RAD BURNING ONLY
17	2.5 VOLT BIAS	-	-	-	-	100	1	1K	2.57063	360	2.5 5.0 0.0	-	-	
18	2.5 VOLT BIAS	-	-	-	-	100	1	1K	2.57063	360	2.5 5.0 0.0	-	-	
19	LEFT LAP X FORCE	-	-	-	-	100	1	1K	-	-	-	-	-	
20	LEFT LAP Y FORCE	-	-	-	-	100	1	1K	-	-	-	-	-	
21	LEFT LAP Z FORCE	-	-	-	-	100	1	1K	-	-	-	-	-	
22	RIGHT LAP X FORCE	-	-	-	-	100	1	1K	-	-	-	-	-	
23	RIGHT LAP Y FORCE	-	-	-	-	100	1	1K	-	-	-	-	-	
24	RIGHT LAP Z FORCE	-	-	-	-	100	1	1K	-	-	-	-	-	

TABLE A-14: INSTRUMENTATION REQUIREMENTS

DYNALLECTRON CORPORATION													
DIGITAL INSTRUMENTATION REQUIREMENTS													
PROGRAM		TITLE		DATE 29 SEP 1987		REV 23 MAR 1988		PAGE 1539					
FACILITY		VERTICAL ACCELERATION TESTER		RUN 1360		PAGE 1539							
DATA CHANNEL	DATA POINT	ACCELERATION TYPE	WAVEFORM	AMPLITUDE	PERIOD	WAVEFORM	AMPLITUDE	PERIOD	WAVEFORM	AMPLITUDE	PERIOD	WAVEFORM	AMPLITUDE
2	HEAD & ACCEL.	1250T-1000	1250T-1000	2.5	120	1250T-1000	2.5	120	1250T-1000	2.5	120	1250T-1000	2.5
3	CHUBB & INTERNAL	1250T-1000	1250T-1000	2.5	120	1250T-1000	2.5	120	1250T-1000	2.5	120	1250T-1000	2.5
4	HEAD & ACCEL.	1250T-1000	1250T-1000	2.5	120	1250T-1000	2.5	120	1250T-1000	2.5	120	1250T-1000	2.5
5	LAUNCH & ACCEL.	1250T-1000	1250T-1000	2.5	120	1250T-1000	2.5	120	1250T-1000	2.5	120	1250T-1000	2.5
6	LAUNCH & FORCE	1250T-1000	1250T-1000	2.5	120	1250T-1000	2.5	120	1250T-1000	2.5	120	1250T-1000	2.5
30	LEFT SIDE PLACEMENT	1250T-1000	1250T-1000	2.5	120	1250T-1000	2.5	120	1250T-1000	2.5	120	1250T-1000	2.5
31	LEFT SIDE PLACEMENT	1250T-1000	1250T-1000	2.5	120	1250T-1000	2.5	120	1250T-1000	2.5	120	1250T-1000	2.5
33	HEAD & FORCE	1250T-1000	1250T-1000	2.5	120	1250T-1000	2.5	120	1250T-1000	2.5	120	1250T-1000	2.5
* LARGE AREA REQUIREMENT													

PROGRAM

TITLE

DATE 29 SEP 1987

REV 23 MAR 1988

PAGE 1539

PAGE 3 OF 6

TABLE A-1e: INSTRUMENTATION REQUIREMENTS

MANUFACTURER	MODEL	RANGE	SENSITIVITY (mV)	RESONANCE FREQ (Hz)	FREQUENCY RESPONSE (Hz.)	EXCITATION (Volt)	2 ARM or 4 ARM	ADDITIONAL NOTES
Endevco	Z264-150	± 150 G	2.5/G	3400	0-800	10	2 arm	Linear accelerometer
Endevco	Z264-200	± 200 G	2.5/G	4700	0-1200	10	2 arm	Linear accelerometer
Endevco	Z264-200	± 200 G	2.5/G	6000	0-1000	10	2 arm	Linear accelerometer, 1000 G overrange
Endevco	Z262A-200	± 200 G	2.5/G	7000	0-1800	10	4 arm	Linear accelerometer, .7 damping ratio
Endevco	7302	± 50,000 Rad/Sec ²	.006 /Rad/Sec ²	2250	1-600	10	4 arm	Angular Accelerometer, X10 overrange; Housing connector
Endevco	7302A	± 50,000 Rad/Sec ²	.055 /Rad/Sec ²	2570	1-600	10	4 arm	Angular accelerometer, X10 overrange
Endevco	7302B	± 50,000 Rad/Sec ²	.004 /Rad/Sec ²	3000	1-600	10	4 arm	Angular accelerometer, X10 overrange
Entran	EA-125 -1000	± 100 G	2.5/G	1500	0-800	15	4 arm	Linear accelerometer; 500 G overrange, .7 damping ratio
Strainert	FL2.5U- 29PKT	± 2500 Lb	.008/Lb	3600	0-2000	10	4 arm	Load cell; 15 V max exc.; 5 K LB max. overrange
Strainert	FL1U-29PKT and -29PKT	± 1000 Lb	.020/Lb	3600	0-2000	10	4 arm	Load cell; 15 V max exc.; 2 K LB max. overrange
Denton	1914-Fz	± 5000 Lb	.0017/Lb	N/A	N/A	10	4 arm	6 axis Load Cell; 15V max exc.
Denton	1716-Fz	± 3000 Lb	.0033/Lb	N/A	N/A	10	4 arm	6 axis neck load cell; 15 V max exc.

TABLE A-2: TYPICAL TRANSDUCER SPECIFICATIONS

PROGRAM CALIBRATION LOG

PROGRAM: VIKAM
 FACILITY: VERTICAL DECELERATION TOWER
 DATES: 29 SEP 87 - 23 MAR 88
 RUN NUMBERS: 1360 - 1639

DATA POINT	TRANSDUCER MFG. & MODEL	SERIAL NUMBER	PRE-CAL		POST-CAL		NOTES
			DATE	SENS mv/g	DATE	SENS mv/g	
CARRIAGE z	EMDEWCO 2262A-200	FR42	04SEP87	4.171 mv/g	11APR88	4.199 mv/g	+ .7
HEAD x	EMDEWCO 726A-200	BH58H	03SEP87	2.594 mv/g	08APR88	2.608 mv/g	+ .5
HEAD y	EMDEWCO 726A-200	BH60H	03SEP87	2.823 mv/g	08APR88	2.817 mv/g	- .2
HEAD z	EMDEWCO 726A-200	BH63H	03SEP87	2.487 mv/g	08APR88	2.494 mv/g	+ .3
CHEST x	EMDEWCO 226A-150	BC26	04SEP87	2.792 mv/g	07APR88	2.791 mv/g	0
CHEST y	EMDEWCO 226A-150	CD13	03SEP87	2.476 mv/g	07APR88	2.465 mv/g	- .4
CHEST z	EMDEWCO 226A-150	2A.0	04SEP87	2.677 mv/g	07APR88	2.709 mv/g	+1.2
SEAT x	EMDEWCO 226A-200	BK17	04SEP87	2.801 mv/g	11APR88	2.746 mv/g	-2.0

TABLE A-4a: TRANSDUCER PRE- AND POST-CALIBRATION (PAGE 1 OF 7)

PROGRAM CALIBRATION LOG

PROGRAM: VIKAM
DATES: 29 SEP 87 - 23 MAR 88
FACILITY: VERTICAL DECELERATION TOWER
RUN NUMBERS: 1460 - 1639

DATA POINT	TRANSDUCER MFG. & MODEL	SERIAL NUMBER	PRE-CAL		POST-CAL		B. CHANGE	NOTES
			DATE	SENS MV/G	DATE	SENS MV/G		
SEAT Y	ENDEVCO 2264-200	BV95	04SEP87	2.985 MV/G	11APR88	2.961 MV/G	- .9	
SEAT Z	ENDEVCO 2264-200	BW07	04SEP87	2.823 MV/G	11APR88	2.930 MV/G	+ .2	
DUMMY HEAD X	ENDEVCO 2264-200	CH74	03SEP87	2.962 MV/G	08APR88	2.959 MV/G	- .1	
DUMMY HEAD Y	ENDEVCO 2264-200	BQ42	03SEP87	2.750 MV/G	11APR88	2.730 MV/G	- .7	
DUMMY HEAD Z	ENDEVCO 2264-200	CH7C	03SEP87	2.684 MV/G	03APR88	2.698 MV/G	+ .5	
DUMMY HEAD ANGULAR	ENDEVCO 7302	A150	04SEP87	8.28 UV/RAD /SEC ²	12APR88	8.01 UV/RAD /SEC ²	- 3.3	
HEAD ANGULAR	ENDEVCO 7302A	AB12	04SEP87	4.25 UV/RAD /SEC ²	12APR88	4.18 UV/RAD /SEC ²	- 1.6	
SEAT ANGULAR	ENDEVCO 7302B	PT47	22JAN87	3.719 UV/RAD /SEC ²	12APR88	3.62 UV/RAD /SEC ²	- 2.7	CALIBRATED PERIODICALLY BY ARMEL PERSONNEL. NO PRE- AND POST- CALIBRATION REQUIRED.
CHEST RV ANGULAR	ENDEVCO 7302A	AB15	04SEP87	5.90 UV/RAD /SEC ²	12APR88	6.60 UV/RAD /SEC ²	- 2.9	
*VELOCITY TACH.	GLOBE 22A672-2	4	11SEP87	4.735 V/T/S	-	-	-	

TABLE A-46: TRANSDUCER PRE- AND POST-CALIBRATION (PAGE 2 OF 7)

PROGRAM CALIBRATION LOG

PROGRAM: VIHAN
DATES: 29 SEP 87 - 23 MAR 88
FACILITY: VERTICAL DECELERATION TOWER **RUN NUMBERS:** 1360 - 1639

DATA POINT	TRANSDUCER MFG. & MODEL	SERIAL NUMBER	PRE-CAL		POST-CAL		CHANGE	NOTES
			DATE	SENS	DATE	SENS		
LEFT SEAT x FORCE	MM/DYN EA-06-062TJ-350	2	08SEP87	10.50 uv/LB	11APR88	10.39 uv/LB	-1.0	
RIGHT SEAT x FORCE	MM/DYN EA-06-062TJ-350	3	08SEP87	10.89 uv/LB	08APR88	10.87 uv/LB	-0.2	
CENTER SEAT y FORCE	MM/DYN EA-06-062TJ-350	5	08SEP87	10.06 uv/LB	11APR88	10.13 uv/LB	+0.7	
LEFT BACK z FORCE	MM/DYN EA-06-062TJ-350	003	08SEP87	11.09 uv/LB	07APR88	11.07 uv/LB	-0.2	
RIGHT BACK z FORCE	MM/DYN EA-06-062TJ-350	4	09SEP87	10.00 uv/LB	08APR88	9.97 uv/LB	-0.3	
BACK y FORCE	MM/DYN EA-06-062TJ-350	1	14SEP87	10.58 uv/LB	08APR88	10.55 uv/LB	-0.3	

TABLE A-4c: TRANSDUCER PRE- AND POST-CALIBRATION (PAGE 3 OF 7)

PROGRAM CALIBRATION LOG

PROGRAM: V. HAM DATES: 29 SEP 87 - 23 MAR 88
FACILITY: VERTICAL DECELERATION TOWER RUN NUMBERS: 1360 - 1639

DATA POINT	TRANSDUCER MFG. & MODEL	SERIAL NUMBER	PRE-CAL		POST-CAL		% CHANGE	NOTES
			DATE	SENS uv/LB	DATE	SENS uv/LB		
LEFT VERTICAL ANCHOR x FORCE	GM-3D-SW	15X	08SEP87	5.48 uv/LB	07APR88	5.44 uv/LB	-0.7	
LEFT VERTICAL ANCHOR y FORCE	GM-3D-SW	15Y	08SEP87	5.39 uv/LB	07APR88	5.39 uv/LB	0	
LEFT VERTICAL ANCHOR z FORCE	GM-3D-SW	15Z	08SEP87	6.29 uv/LB	07APR88	6.39 uv/LB	0	
RIGHT VERTICAL ANCHOR x FORCE	GM-3D-SW	21X	08SEP87	5.11 uv/LB	07APR88	5.09 uv/LB	-0.4	
RIGHT VERTICAL ANCHOR y FORCE	GM-3D-SW	21Y	08SEP87	4.89 uv/LB	07APR88	4.86 uv/LB	-0.6	
RIGHT VERTICAL ANCHOR z FORCE	GM-3D-SW	21Z	08SEP87	6.12 uv/LB	07APR88	6.13 uv/LB	+0.2	
SHOULDER x FORCE	GM-3D-SW	20Z	08SEP87	6.37 uv/LB	07APR88	6.42 uv/LB	+0.8	
SHOULDER y FORCE	GM-3D-SW	20Y	08SEP87	5.82 uv/LB	07APR88	5.85 uv/LB	+0.5	
SHOULDER z FORCE	GM-3D-SW	20X	08SEP87	5.66 uv/LB	07APR88	5.61 uv/LB	-0.9	

TABLE A-4d: TRANSDUCER PRE- AND POST-CALIBRATION (PAGE 4 OF 7)

PROGRAM CALIBRATION LOG

PROGRAM: VIHAM **DATES:** 29 SEP 87 - 23 MAR 88
FACILITY: VERTICAL DECELERATION TOWER **RUN NUMBERS:** 1360 - 1639

DATA POINT	TRANSDUCER MFC. & MODEL	SERIAL NUMBER	PRE-CAL		POST-CAL		B. CHANGE	NOTES
			DATE	SENS uv/lb	DATE	SENS uv/lb		
UPPER HEADREST x FORCE	STRAINSERT FL1U-2SG	206	05SEP86	20.13 uv/lb	-	-	-	
LOWER HEADREST x FORCE	STRAINSERT FL1U-2SG	207	20NOV85	20.00 uv/lb	-	-	-	
LEFT SEAT z FORCE	STRAINSERT FL2.5U-2SPKT	7588-1	17JUN87	8.06 uv/lb	-	-	-	
RIGHT SEAT z FORCE	STRAINSERT FL2.5U-2SPKT	7588-2	14JUL87	8.04 uv/lb	-	-	-	
CENTER SEAT z FORCE	STRAINSERT FL2.5U-2SPKT	7588-3	04SEP86	8.01 uv/lb	-	-	-	
LEFT BACK x FORCE	STRAINSERT FL1U-2SGKT	7411-1	21JAN87	19.91 uv/lb	-	-	-	
RIGHT BACK x FORCE	STRAINSERT FL1U-2SGKT	7411-2	21JAN87	19.95 uv/lb	-	-	-	
CENTER BACK x FORCE	STRAINSERT FL1U-2SGKT	5297-4	21JAN87	19.91 uv/lb	-	-	-	ALL TRANSDUCERS ON THIS SHEET ARE CALIBRATED PERIODICALLY BY PMEL AND DO NOT REQUIRE POST- CALIBRATION.
LEFT HORIZ. ANCHOR x FORCE	STRAINSERT FL1U-2SG	209	09SEP86	19.89 uv/lb	-	-	-	
RIGHT HORIZ. ANCHOR x FORCE	STRAINSERT FL1U-2SG	210	17JUN87	19.95 uv/lb	-	-	-	

TABLE A-4e: TRANSDUCER PRE- AND POST-CALIBRATION (PAGE 5 OF 7)

PROGRAM CALIBRATION LOG

PROGRAM: VIHAM DATES: 29 SEP 1987 - 23 MAR 1988
 FACILITY: VERTICAL DECELERATION TOWER RUN NUMBERS: 1360 - 1639

DATA POINT	TRANSDUCER MFG. & MODEL	SERIAL NUMBER	PRE-CAL		POST-CAL		S. CHANGE	NOTES
			DATE	SENS	DATE	SENS		
HEAD X ACCELERATION	ENTRAN EGA-125-100B	12T6T- V4-4		2.48 mv/G				
CHEST X ACCELERATION	ENTRAN EGA-125-100B	18W6W- V20-20		2.30 mv/G				
HEAD Z ACCELERATION	ENTRAN EGA-125-100B	12T6T- V11-11		2.48 mv/G				
LUMBAR Z ACCELERATION	ENTRAN EGA-125-100B	18W6W- V20-20		2.30 mv/G				
LEFT KNEE FLEXION POSITION	SRL 6886-16- 6869-30	-		18.8 mv/DEG				ALL TRANSDUCERS ON THIS PAGE WERE LOCATED ON THE LARGE ADAM. PRE- AND POST- CALIBRATIONS ARE CONTRACTOR SRL'S RESPONSIBILITY.
LEFT ELBOW FLEXION POSITION	SRL 6886-16- 6869-10	-		17.85 mv/DEG				
NECK Z FORCE	DENTON 1716	128		4.3 uv/LB				
LUMBAR Z FORCE	DENTON 1914	041						

TABLE A-4f: TRANSDUCER PRE- AND POST-CALIBRATION (PAGE 6 OF 7)

PROGRAM CALIBRATION LOG

PROGRAM: VIHAM **DATES:** 29 SEP 87 - 23 MAR 88
FACILITY: VERTICAL DECELERATION TOWER **RUN NUMBERS:** 1360 - 1639

DATA POINT	TRANSDUCER MFG. & MODEL	SERIAL NUMBER	PRE-CAL		POST-CAL		% CHANGE	NOTES
			DATE	SENS	DATE	SENS		
HEAD x ACCELERATION	ENTRAN ECA-125-100D	18464- V15-15		2.52 mv/G				
CHEST x ACCELERATION	ENTRAN ECA-125-100D	12T6T- V6-6		2.49 mv/G				
HEAD z ACCELERATION	ENTRAN ECA-125-100D	18464- V14-14		2.52 mv/G				
LIMBAR z ACCELERATION		18464- V17-17		2.43 mv/G				
LEFT KNEE FLEXION POSITION	SRL 6886-16- 6869-30	-		18.8 uv/DEG.				
LEFT ELBOW FLEXION POSITION	SRL6845-16- 6869-10	-		17.85 mv/DEG.				
LIMBAR z FORCE	DENTON 1914	040		2.7 uv/LB				
NECK z FORCE	DENTON 1716	127		4.4 uv/LB				ALL TRANSDUCERS ON THIS PAGE WERE LOCATED ON THE SMALL ADAM. PRE- AND POST- CALIBRATIONS ARE CONTRACTOR SRL'S RESPONSIBILITY.

TABLE A-4g: TRANSDUCER PRE- AND POST-CALIBRATION (PAGE 7 OF 7)

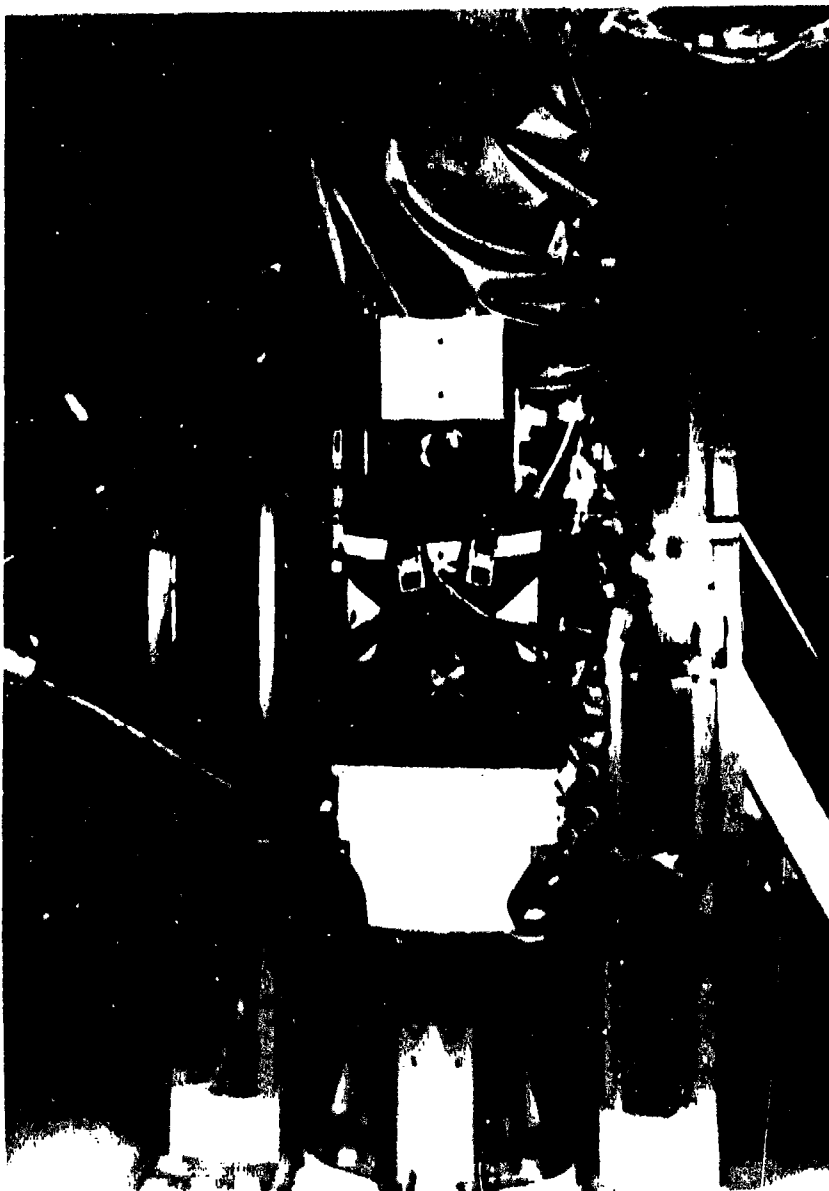


FIGURE A-1: AAMRL VERTICAL DECELERATION TOWER

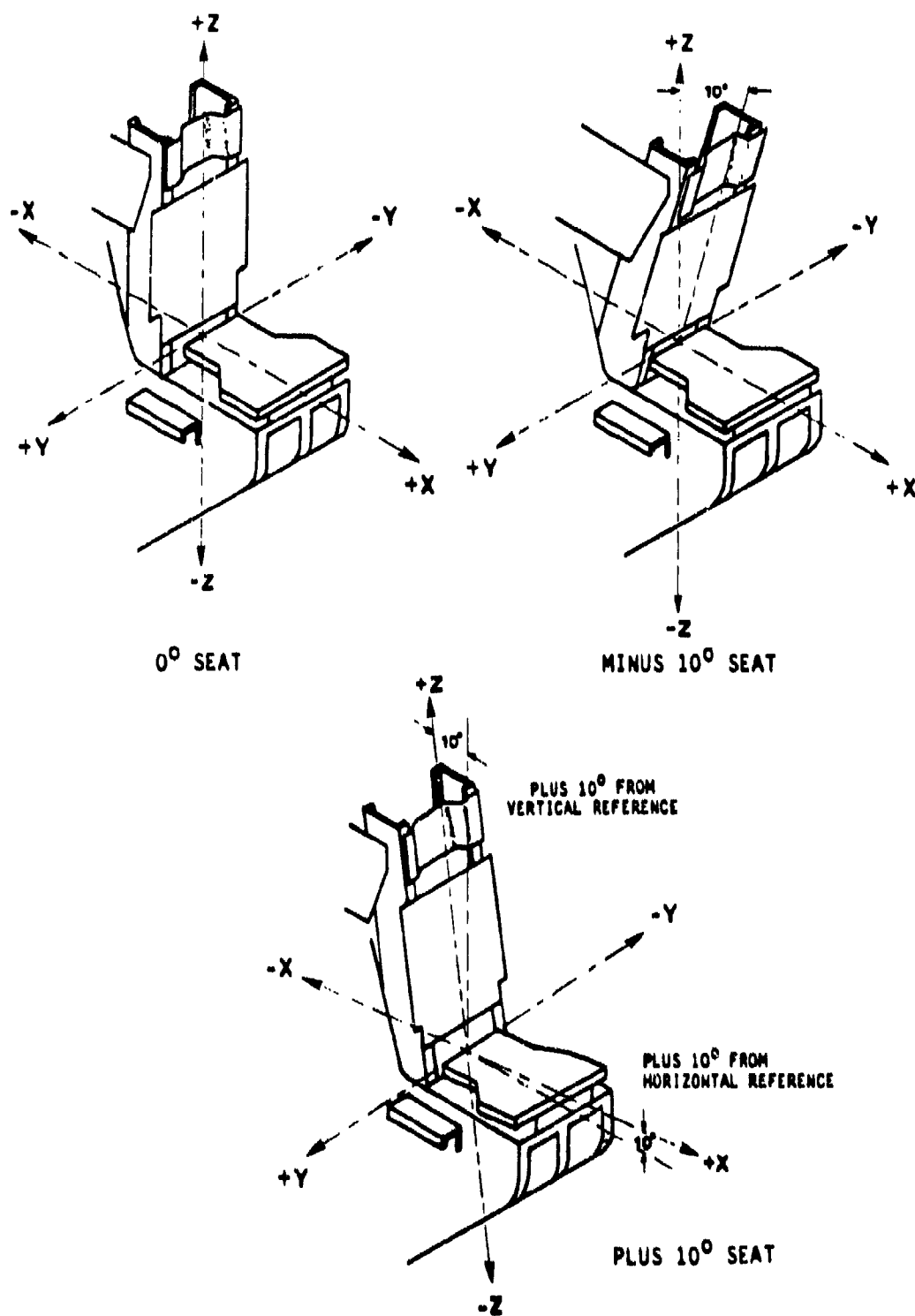


FIGURE A-2: VIP SEAT POSITIONS

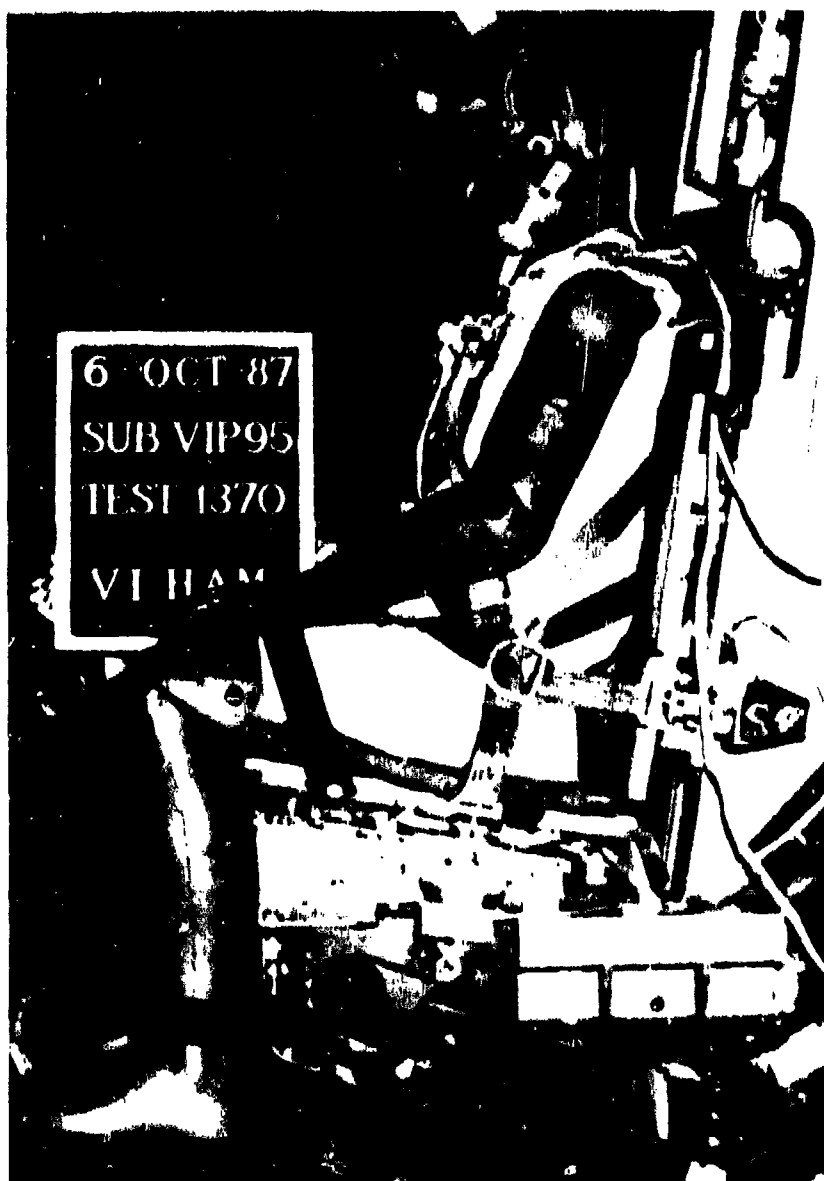


FIGURE A-3: PLUS 10 DEGREE SEAT POSITION



FIGURE A-4: 0 DEGREE SEAT POSITION



FIGURE A-5: MINUS 10 DEGREE SEAT POSITION



FIGURE A-6: X-BAND-90 DEGREE HARNESS



FIGURE A-7: PCU-15/P HARNESS

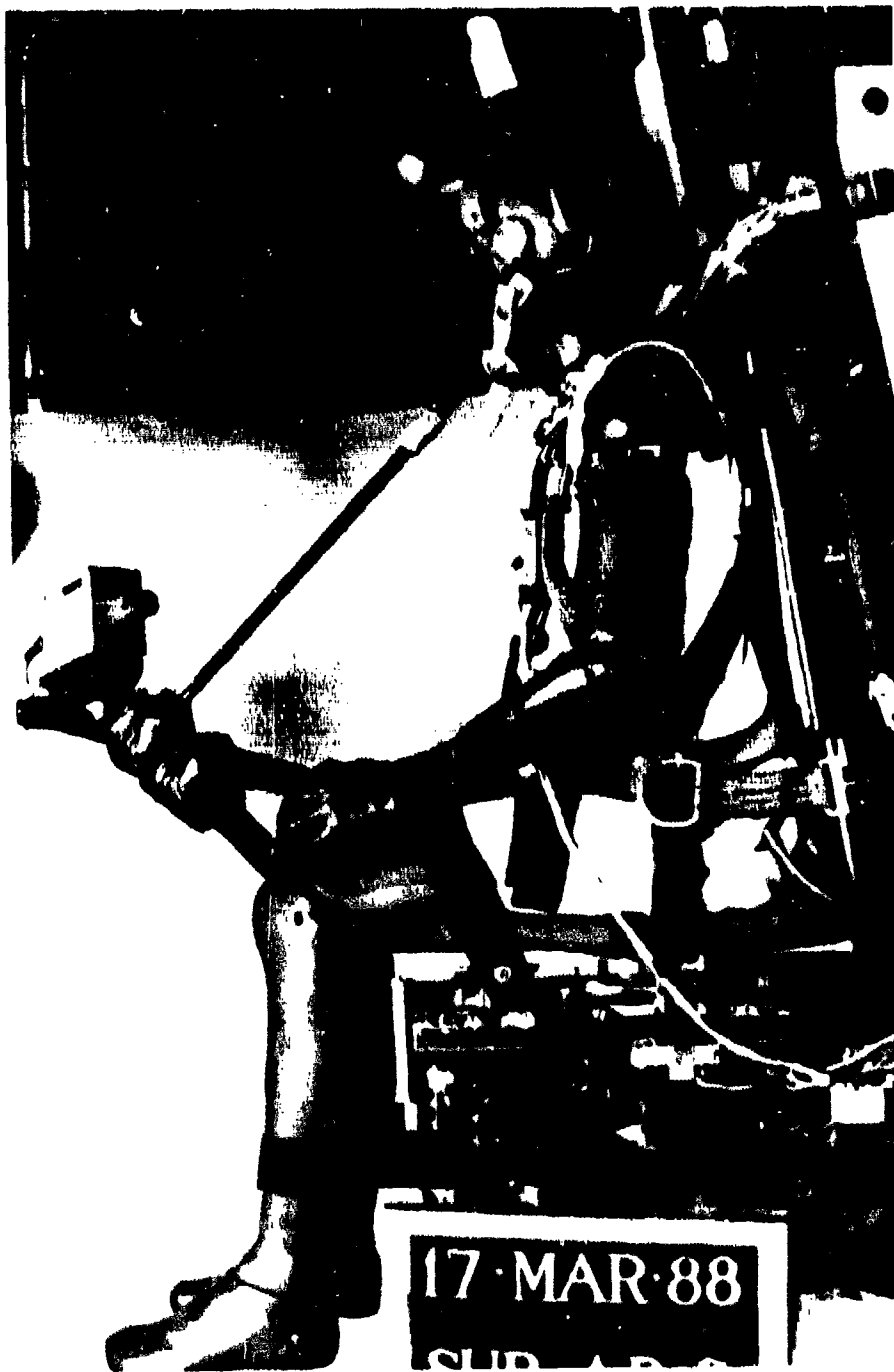


FIGURE A-8: SUBJECT LEG AND THIGH RESTRAINTS

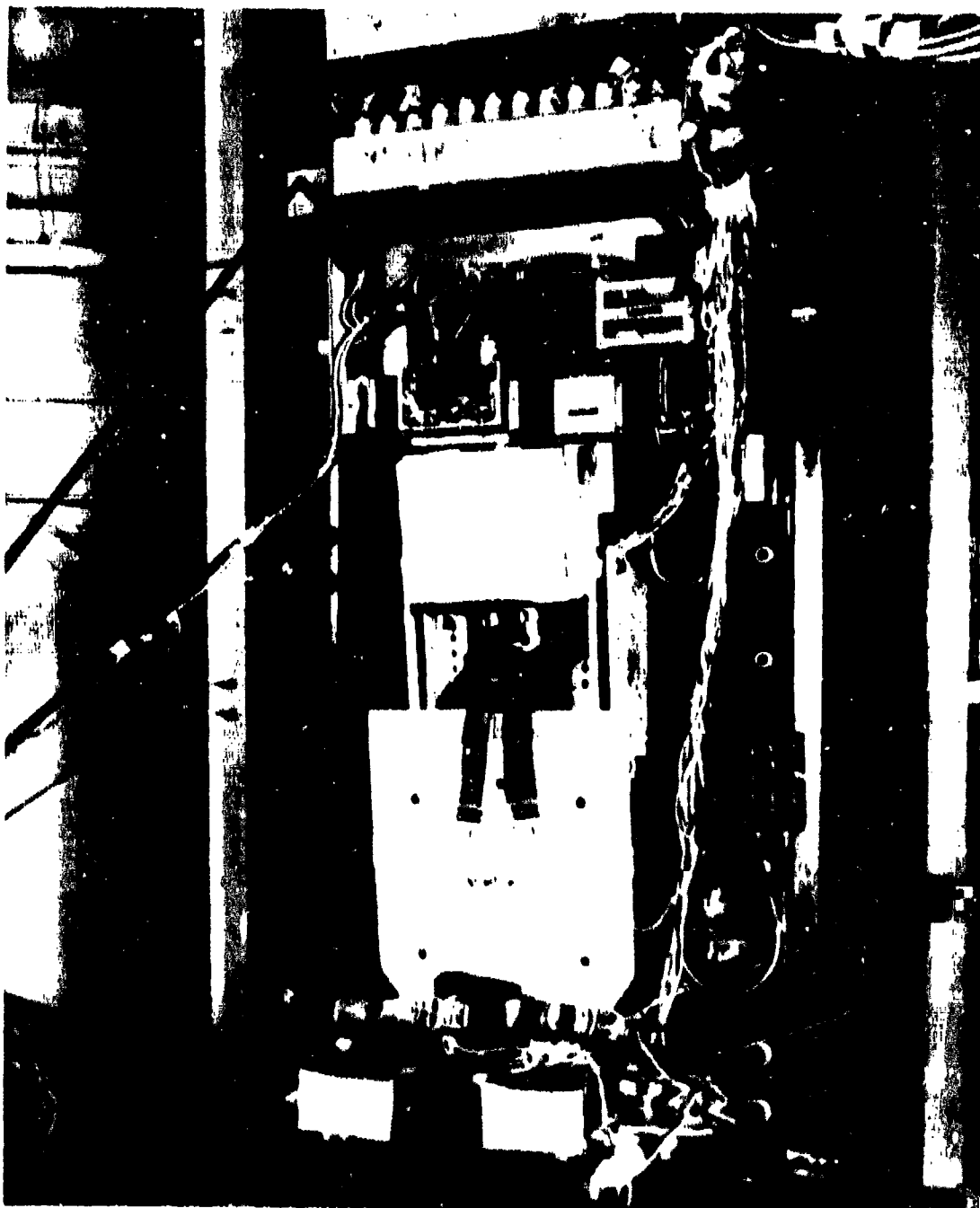
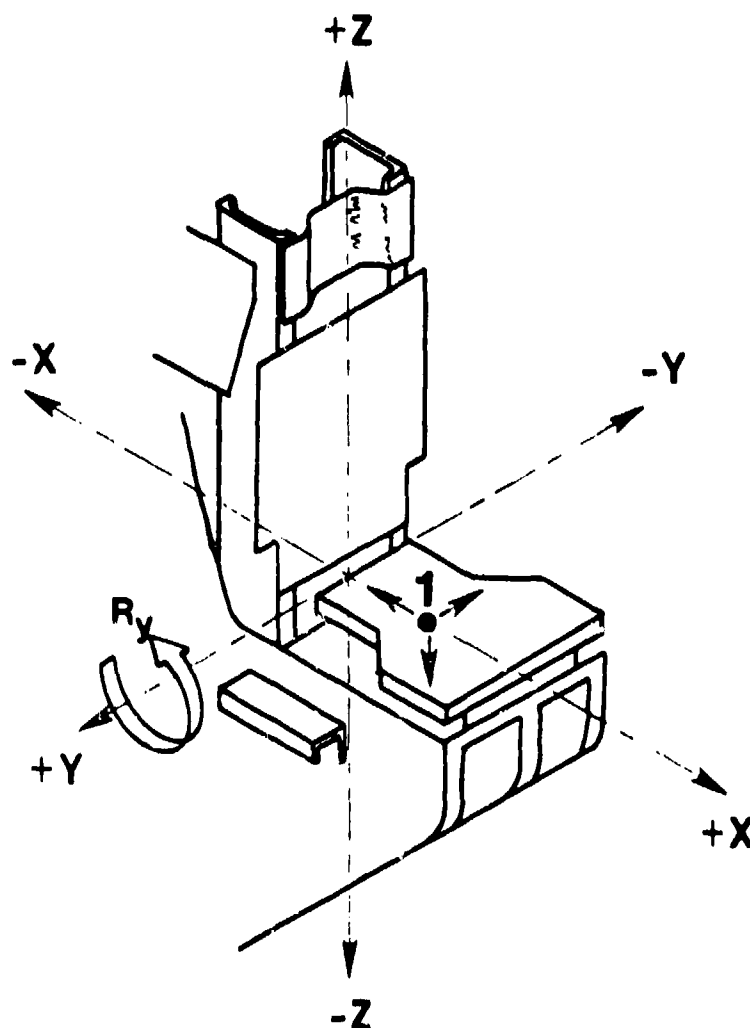


FIGURE A-9: ACES II SEAT CUSHION



FIGURE A-10: CREST CONFORTM SEAT CUSHION



1. TYPICAL FIXED LOAD CELL AND LOAD LINK MOUNTING POINT. DIRECTION OF THE ARROWS INDICATE THE DIRECTION OF FORCE APPLIED TO PRODUCE A POSITIVE OUTPUT.
2. THE LINEAR ACCELEROMETERS WERE WIRED TO PROVIDE A POSITIVE OUTPUT VOLTAGE WHEN ACCELERATIONS WERE APPLIED IN THE +x, +y AND +z DIRECTIONS AS SHOWN.
3. THE ANGULAR R_y ACCELEROMETERS WERE WIRED TO PROVIDE A POSITIVE OUTPUT VOLTAGE WHEN THE ANGULAR ACCELERATIONS WERE APPLIED IN THE +y DIRECTION ACCORDING TO THE RIGHT HAND RULE AS SHOWN.

FIGURE A-11: AAMRL/BBP COORDINATE SYSTEM

VELOCITY WHEEL



FIGURE A-12: CARRIAGE VELOCITY WHEEL

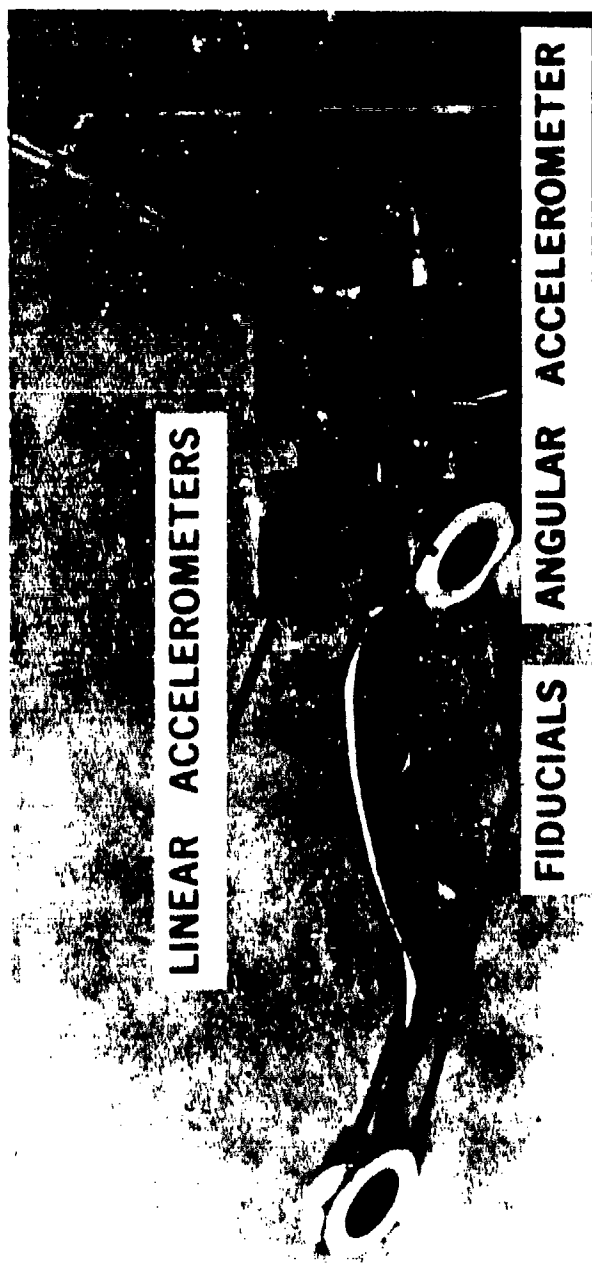
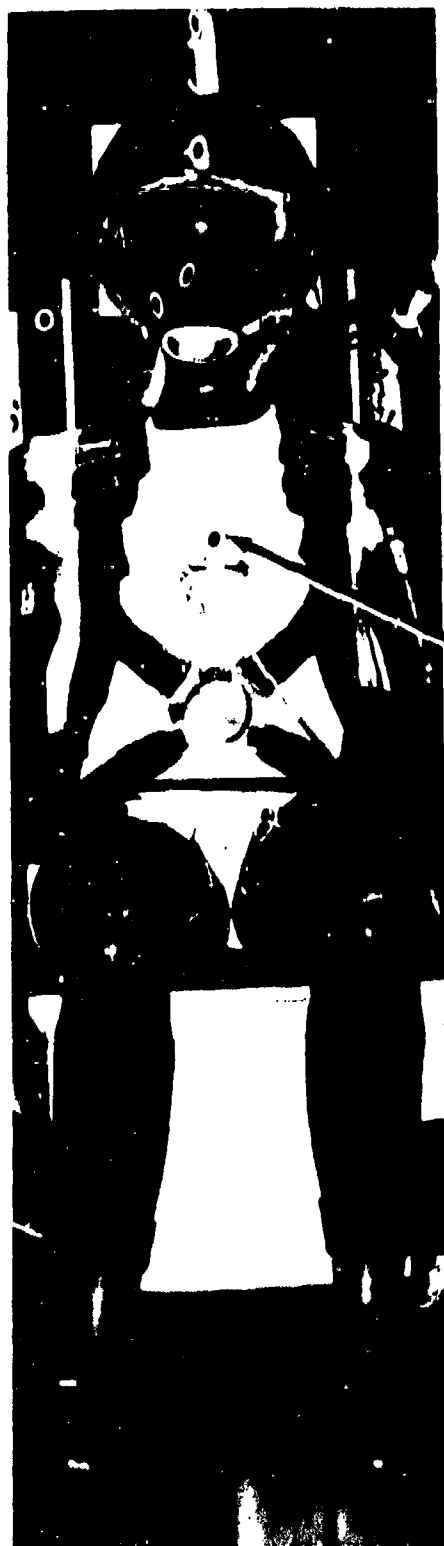
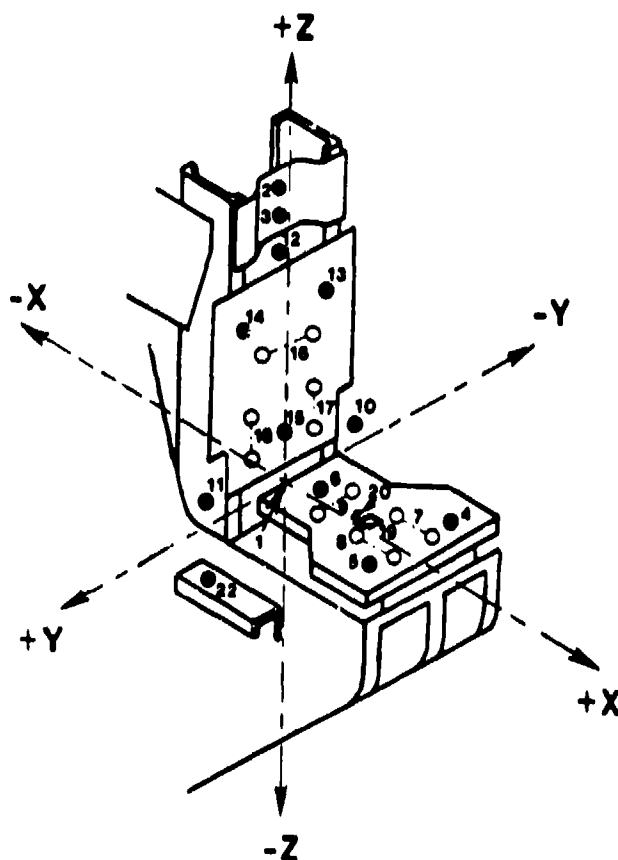


FIGURE A-13: HUMAN HEAD ACCELEROMETER PACKAGE



**CHEST
ACCELEROMETER
PACKAGE**

FIGURE A-14: CHEST ACCELEROMETER PACKAGE



<u>NO.</u>	<u>DESCRIPTION</u>	<u>NO.</u>	<u>DESCRIPTION</u>
1	SEAT REFERENCE POINT	15	CENTER BACK X FORCE
2	UPPER HEADREST X FORCE	16	CENTER BACK Y FORCE
3	LOWER HEADREST X FORCE	17	LEFT BACK Z FORCE
4	LEFT SEAT Z FORCE	18	RIGHT BACK Z FORCE
5	RIGHT SEAT Z FORCE	19	SEAT X, Y & Z ACCELERATION
6	CENTER SEAT Z FORCE	20	SEAT ANGULAR ACCELERATION
7	LEFT SEAT X FORCE		
8	RIGHT SEAT X FORCE		FOR X-BAND-90° HARNESS:
9	CENTER SEAT Y FORCE	21A	LEFT VERTICAL ANCHOR FORCE
10	LEFT HORIZONTAL ANCHOR FORCE	22A	RIGHT VERTICAL ANCHOR FORCE
11	RIGHT HORIZONTAL ANCHOR FORCE		
12	SHOULDER		FOR PCU-15/P HARNESS:
13	LEFT BACK X FORCE	21B	LEFT LAP FORCE
14	RIGHT BACK X FORCE	22B	RIGHT LAP FORCE

ITEM 21 NOT SHOWN

ITEMS 21 AND 22 HAVE NAME CHANGES ONLY FOR X-BAND-90° AND PCU-15/P HARNESS

THE HEADREST WAS ADJUSTABLE UP OR DOWN DEPENDING ON EACH SUBJECT. HEADREST LOAD CELL NUMBERS 2 AND 3 MOVE WITH THE HEADREST. THE MEASUREMENTS FOR THE HEADREST LOAD CELLS WERE TAKEN WHEN THE TOP MOUNTING HOLES IN THE HEAD REST WERE LINED UP WITH THE TOP HOLES IN THE FRAME SUPPORT.

FIGURE A-15a TRANSDUCER LOCATIONS AND DIMENSIONS (PAGE 1 OF 4)

0 DEGREE SEAT POSITION - TRANSDUCER LOCATIONS AND DESCRIPTIONS

ALL DIMENSIONS ARE REFERENCED TO THE SEAT REFERENCE POINT (SRP). THE SEAT REFERENCE POINT IS LOCATED AT THE INTERSECTION OF THE HORIZONTAL SEAT PLATE (x AXIS) CENTER LINE AND THE VERTICAL BACK PLATE (z AXIS) CENTER LINE.

NO.	CONTACT POINT DIMENSIONS IN INCHES (CM)			TRANSDUCER CENTER POINT IN INCHES (CM)		
	X	Y	Z	X	Y	Z
1	0.00 (0.00)	0.00 (0.00)	0.00 (0.00)	0.00 (0.00)	0.00 (0.00)	0.00 (0.00)
2	- 1.63 (- 4.15)	0.00 (0.00)	39.92 (101.40)	- 2.37 (- 6.02)	0.00 (0.00)	39.92 (101.40)
3	- 1.63 (- 4.15)	0.00 (0.00)	34.94 (88.75)	- 2.37 (- 6.02)	0.00 (0.00)	34.94 (88.75)
4	15.62 (39.67)	- 5.00 (-12.70)	- 1.22 (- 3.10)	15.62 (39.67)	- 5.00 (-12.70)	- 2.03 (- 5.15)
5	15.62 (39.67)	5.00 (12.70)	- 1.22 (- 3.10)	15.62 (39.67)	5.00 (12.70)	- 2.03 (- 5.15)
6	4.40 (11.17)	0.00 (0.00)	- 1.22 (- 3.10)	4.40 (11.17)	0.00 (0.00)	- 2.03 (- 5.15)
7	7.72 (19.62)	- 6.00 (-15.25)	- 1.85 (- 4.70)	9.72 (24.70)	- 6.00 (-15.25)	- 1.85 (- 4.70)
8	7.72 (19.62)	6.00 (15.25)	- 1.85 (- 4.70)	9.72 (24.70)	6.00 (15.25)	- 1.85 (- 4.70)
9	6.98 (17.72)	1.99 (5.05)	- 1.85 (- 4.70)	6.98 (17.72)	0.00 (0.00)	- 1.85 (- 4.70)
10	- 1.33 (- 3.37)	- 8.69 (-22.07)	6.28 (15.95)	- 3.87 (- 9.84)	- 8.69 (-22.07)	6.28 (15.95)
11	- 1.33 (- 3.37)	8.69 (22.07)	6.28 (15.95)	- 3.87 (- 9.84)	8.69 (22.07)	6.28 (15.95)
12	- 7.64 (-19.40)	0.00 (0.00)	28.70 (72.90)	-10.24 (-26.02)	0.00 (0.00)	28.70 (72.90)
13	- 1.63 (- 4.15)	- 3.77 (- 9.58)	16.26 (41.30)	- 2.44 (- 6.20)	- 3.77 (- 9.58)	16.26 (41.30)
14	- 1.63 (- 4.15)	3.77 (9.58)	16.26 (41.30)	- 2.44 (- 6.20)	3.77 (9.58)	16.26 (41.30)
15	- 1.63 (- 4.15)	0.00 (0.00)	5.49 (13.95)	- 2.44 (- 6.20)	0.00 (0.00)	5.49 (13.95)
16	- 2.30 (- 5.85)	- 1.95 (- 4.95)	13.90 (35.30)	- 2.30 (- 5.85)	0.00 (0.00)	13.90 (35.30)
17	- 2.30 (- 5.85)	- 3.38 (- 8.58)	7.72 (19.60)	- 2.30 (- 5.85)	- 3.38 (- 8.58)	9.72 (24.68)
18	- 2.30 (- 5.85)	3.38 (8.58)	7.72 (19.60)	- 2.30 (- 5.85)	3.38 (8.58)	9.72 (24.68)
19	-----	-----	-----	10.05 (25.52)	0.00 (0.00)	- 1.69 (- 4.30)
20	-----	-----	-----	8.59 (21.82)	0.00 (0.00)	- 1.63 (- 4.15)
21A	7.15 (18.15)	- 5.60 (-14.24)	- 1.61 (- 4.10)	7.15 (18.15)	- 5.60 (-14.24)	- 4.56 (-11.57)
22A	7.15 (18.15)	5.60 (14.24)	- 1.61 (- 4.10)	7.15 (18.15)	5.60 (14.24)	- 4.56 (-11.57)
21B	- 1.47 (- 3.73)	- 5.63 (-14.31)	- 1.61 (- 4.10)	- 1.47 (- 3.73)	- 5.63 (-14.31)	- 4.56 (-11.57)
22B	- 1.47 (- 3.73)	5.63 (14.31)	- 1.61 (- 4.10)	- 1.47 (- 3.73)	5.63 (14.31)	- 4.56 (-11.57)

SEE FIGURE A-15a FOR DESCRIPTIONS OF TRANSDUCER ITEM NUMBERS

FIGURE A-15b (PAGE 2 OF 4)

PLUS 10 DEGREE SEAT POSITION - TRANSDUCER LOCATIONS AND DESCRIPTIONS

ALL DIMENSIONS ARE REFERENCED TO THE SEAT REFERENCE POINT (SRP). THE SEAT REFERENCE POINT IS LOCATED AT THE INTERSECTION OF THE SEAT PLATE (X AXIS) CENTER LINE AND THE BACK PLATE CENTER LINE.

NO.	CONTACT POINT DIMENSIONS IN INCHES (CM)			TRANSDUCER CENTER POINT IN INCHES (CM)		
	X	Y	Z	X	Y	Z
1	0.00 (0.00)	0.00 (0.00)	0.00 (0.00)	0.00 (0.00)	0.00 (0.00)	0.00 (0.00)
2	- 1.34 (- 3.41)	0.00 (0.00)	41.27 (104.83)	- 2.08 (- 5.28)	0.00 (0.00)	41.27 (104.83)
3	- 1.34 (- 3.41)	0.00 (0.00)	36.29 (92.18)	- 2.08 (- 5.28)	0.00 (0.00)	36.29 (92.18)
4	15.17 (38.53)	- 5.00 (-12.70)	- 1.25 (- 3.18)	15.17 (38.53)	- 5.00 (-12.70)	- 2.06 (- 5.23)
5	15.17 (38.53)	5.00 (12.70)	- 1.25 (- 3.18)	15.17 (38.53)	5.00 (12.70)	- 2.06 (- 5.23)
6	3.95 (10.03)	0.00 (0.00)	- 1.25 (- 3.18)	3.95 (10.03)	0.00 (0.00)	- 2.06 (- 5.23)
7	7.28 (18.48)	- 6.00 (-15.25)	- 1.88 (- 4.78)	9.28 (23.56)	- 6.00 (-15.25)	- 1.88 (- 4.78)
8	7.28 (18.48)	6.00 (15.25)	- 1.88 (- 4.78)	9.28 (23.56)	6.00 (15.25)	- 1.88 (- 4.78)
9	6.53 (16.58)	1.99 (5.05)	- 1.88 (- 4.78)	6.53 (16.58)	0.00 (0.00)	- 1.88 (- 4.78)
10	- 1.04 (- 2.63)	- 8.69 (-22.07)	7.63 (19.38)	- 3.59 (- 9.10)	- 8.69 (-22.07)	7.63 (19.38)
11	- 1.04 (- 2.63)	8.69 (22.07)	7.63 (19.38)	- 3.59 (- 9.10)	8.69 (22.07)	7.63 (19.38)
12	- 7.35 (-18.66)	0.00 (0.00)	30.05 (76.33)	- 9.96 (-25.28)	0.00 (0.00)	30.05 (76.33)
13	- 1.34 (- 3.41)	- 3.77 (- 9.58)	17.61 (44.73)	- 2.15 (- 5.46)	- 3.77 (- 9.58)	17.61 (44.73)
14	- 1.34 (- 3.41)	3.77 (9.58)	17.61 (44.73)	- 2.15 (- 5.46)	3.77 (9.58)	17.61 (44.73)
15	- 1.34 (- 3.41)	0.00 (0.00)	6.84 (17.38)	- 2.15 (- 5.46)	0.00 (0.00)	6.84 (17.38)
16	- 2.01 (- 5.11)	- 1.95 (- 4.95)	15.25 (38.73)	- 2.01 (- 5.11)	0.00 (0.00)	15.25 (38.73)
17	- 2.01 (- 5.11)	- 3.38 (- 8.58)	9.07 (23.03)	- 2.01 (- 5.11)	- 3.38 (- 8.58)	11.07 (28.11)
18	- 2.01 (- 5.11)	3.38 (8.58)	9.07 (23.03)	- 2.01 (- 5.11)	3.38 (8.58)	11.07 (28.11)
19				9.60 (24.38)	0.00 (0.00)	- 1.72 (- 4.38)
20				8.14 (20.68)	0.00 (0.00)	- 1.67 (- 4.23)
21A	7.20 (18.29)	- 5.60 (-14.24)	- 1.50 (- 3.81)	7.20 (18.29)	- 5.60 (-14.24)	- 4.40 (-11.28)
22A	7.20 (18.29)	5.60 (14.24)	- 1.50 (- 3.81)	7.20 (18.29)	5.60 (14.24)	- 4.40 (-11.28)
21B						
22B						

SEE FIGURE A-15a FOR DESCRIPTIONS OF TRANSDUCER ITEM NUMBERS

FIGURE A-15c (PAGE 3 OF 4)

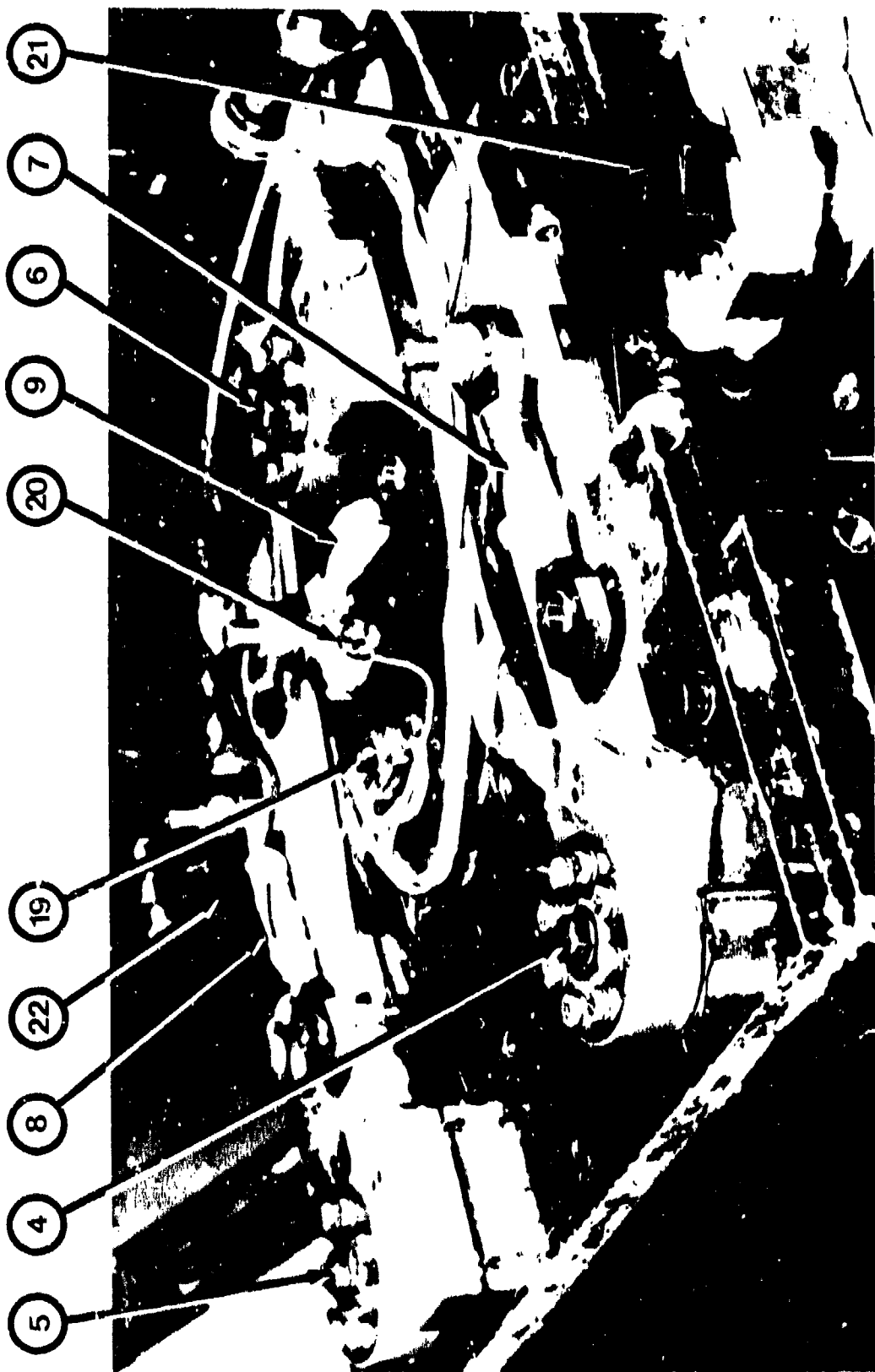
MINUS 10 DEGREE SEAT POSITION - TRANSDUCER LOCATIONS AND DESCRIPTIONS

ALL DIMENSIONS ARE REFERENCED TO THE SEAT REFERENCE POINT (SRP). THE SEAT REFERENCE POINT IS LOCATED AT THE INTERSECTION OF THE HORIZONTAL SEAT PLATE (x AXIS) CENTER LINE AND THE BACK PLATE (z AXIS) CENTER LINE.

NO.	CONTACT POINT DIMENSIONS IN INCHES (CM)			TRANSDUCER CENTER POINT IN INCHES (CM)		
	X	Y	Z	X	Y	Z
1	0.00 (0.00)	0.00 (0.00)	0.00 (0.00)	0.00 (0.00)	0.00 (0.00)	0.00 (0.00)
2	5.31 (13.48)	0.00 (0.00)	39.53 (100.40)	4.58 (11.54)	0.00 (0.00)	39.66 (100.73)
3	4.44 (11.28)	0.00 (0.00)	34.62 (87.94)	3.72 (9.44)	0.00 (0.00)	34.75 (88.27)
4	15.64 (39.73)	- 5.00 (-12.70)	- 1.22 (- 3.10)	15.64 (39.73)	- 5.00 (-12.70)	- 2.03 (- 5.15)
5	15.64 (39.73)	5.00 (12.70)	- 1.22 (- 3.10)	15.64 (39.73)	5.00 (12.70)	- 2.03 (- 5.15)
6	4.42 (11.23)	0.00 (0.00)	- 1.22 (- 3.10)	4.42 (11.23)	0.00 (0.00)	- 2.03 (- 5.15)
7	7.75 (19.68)	- 6.00 (-15.25)	- 1.85 (- 4.70)	9.75 (24.76)	- 6.00 (-15.25)	- 1.85 (- 4.70)
8	7.75 (19.68)	6.00 (15.25)	- 1.85 (- 4.70)	9.75 (24.76)	6.00 (15.25)	- 1.85 (- 4.70)
9	7.00 (17.78)	1.99 (5.05)	- 1.85 (- 4.70)	7.00 (17.78)	0.00 (0.00)	- 1.85 (- 4.70)
10	- 0.23 (- 0.59)	- 8.69 (-22.07)	6.34 (16.11)	- 2.74 (- 6.96)	- 8.69 (-22.07)	6.79 (17.24)
11	- 0.23 (- 0.59)	8.69 (22.07)	6.34 (16.11)	- 2.74 (- 6.96)	8.69 (22.07)	6.79 (17.24)
12	- 2.55 (- 6.49)	0.00 (0.00)	29.52 (74.98)	- 5.12 (-13.01)	0.00 (0.00)	29.97 (76.13)
13	- 1.20 (- 3.04)	- 3.77 (- 9.58)	16.22 (41.21)	0.40 (1.02)	- 3.77 (- 9.58)	16.37 (41.57)
14	- 1.20 (- 3.04)	3.77 (9.58)	16.22 (41.21)	0.40 (1.02)	3.77 (9.58)	16.37 (41.57)
15	- 0.67 (- 1.71)	0.00 (0.00)	5.62 (14.28)	- 1.47 (- 3.73)	0.00 (0.00)	5.76 (14.64)
16	- 0.13 (- 0.33)	- 1.95 (- 4.95)	14.02 (35.60)	0.13 (0.33)	0.00 (0.00)	14.02 (35.60)
17	- 0.94 (- 2.40)	- 3.38 (- 8.58)	7.93 (20.14)	- 0.60 (- 1.52)	- 3.38 (- 8.58)	9.90 (25.14)
18	- 0.94 (- 2.40)	3.38 (8.58)	7.93 (20.14)	- 0.60 (- 1.52)	3.38 (8.58)	9.90 (25.14)
19	-----	-----	-----	-0.07 (25.58)	0.00 (0.00)	- 1.69 (- 4.30)
20	-----	-----	-----	8.61 (21.88)	0.00 (0.00)	- 1.63 (- 4.15)
21A	7.17 (18.21)	- 5.60 (-14.24)	- 1.61 (- 4.10)	7.17 (18.21)	- 5.60 (-14.24)	- 4.55 (-11.57)
22A	7.17 (18.21)	5.60 (14.24)	- 1.61 (- 4.10)	7.17 (18.21)	5.60 (14.24)	- 4.55 (-11.57)
21B	- 1.44 (- 3.67)	- 5.63 (-14.31)	- 1.61 (- 4.10)	- 1.44 (- 3.67)	- 5.63 (-14.31)	- 4.56 (-11.57)
22B	- 1.44 (- 3.67)	5.63 (14.31)	- 1.61 (- 4.10)	- 1.44 (- 3.67)	5.63 (14.31)	- 4.56 (-11.57)

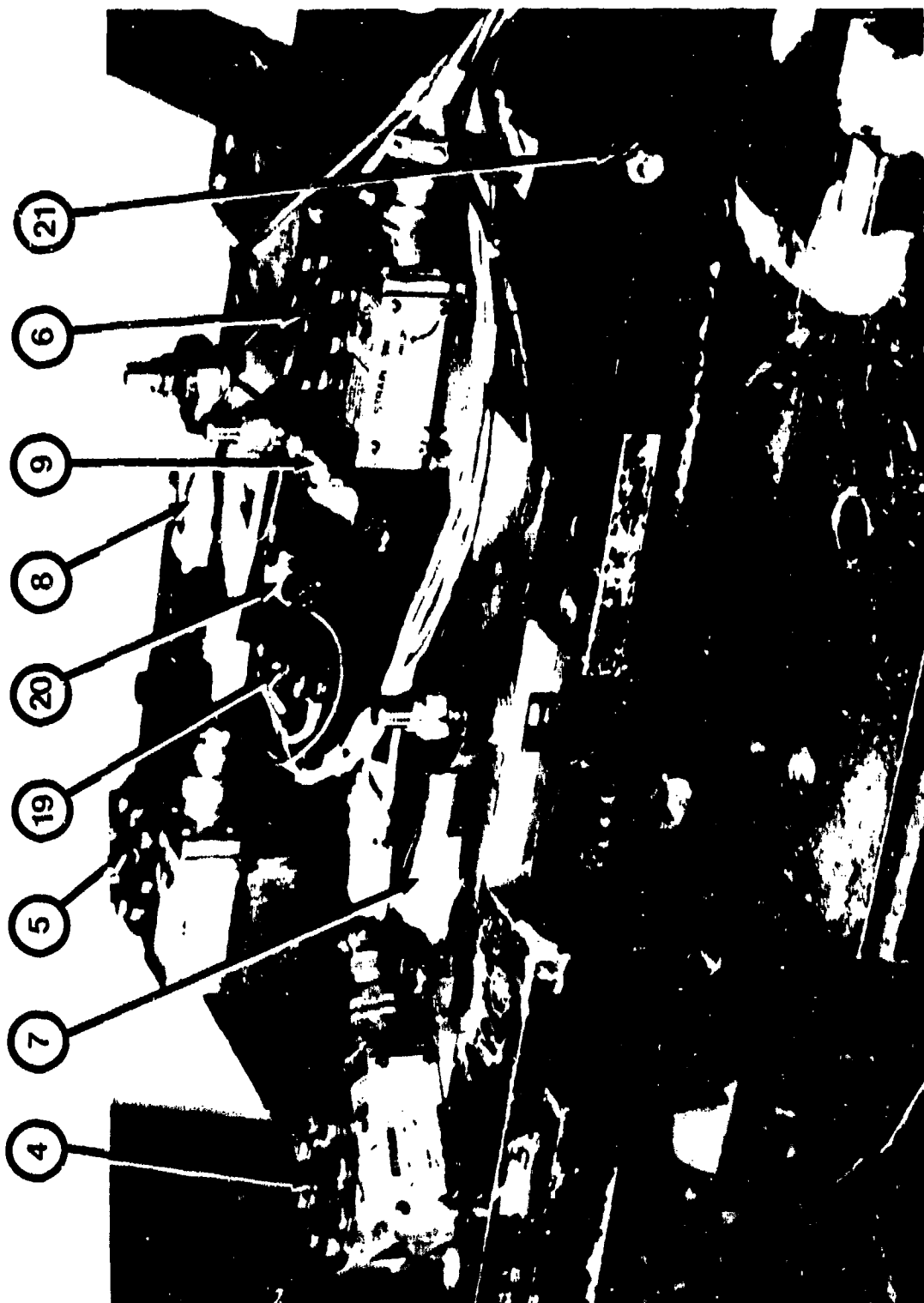
SEE FIGURE A-15a FOR DESCRIPTIONS OF TRANSDUCER ITEM NUMBERS

FIGURE A-15d (PAGE 4 OF 4)



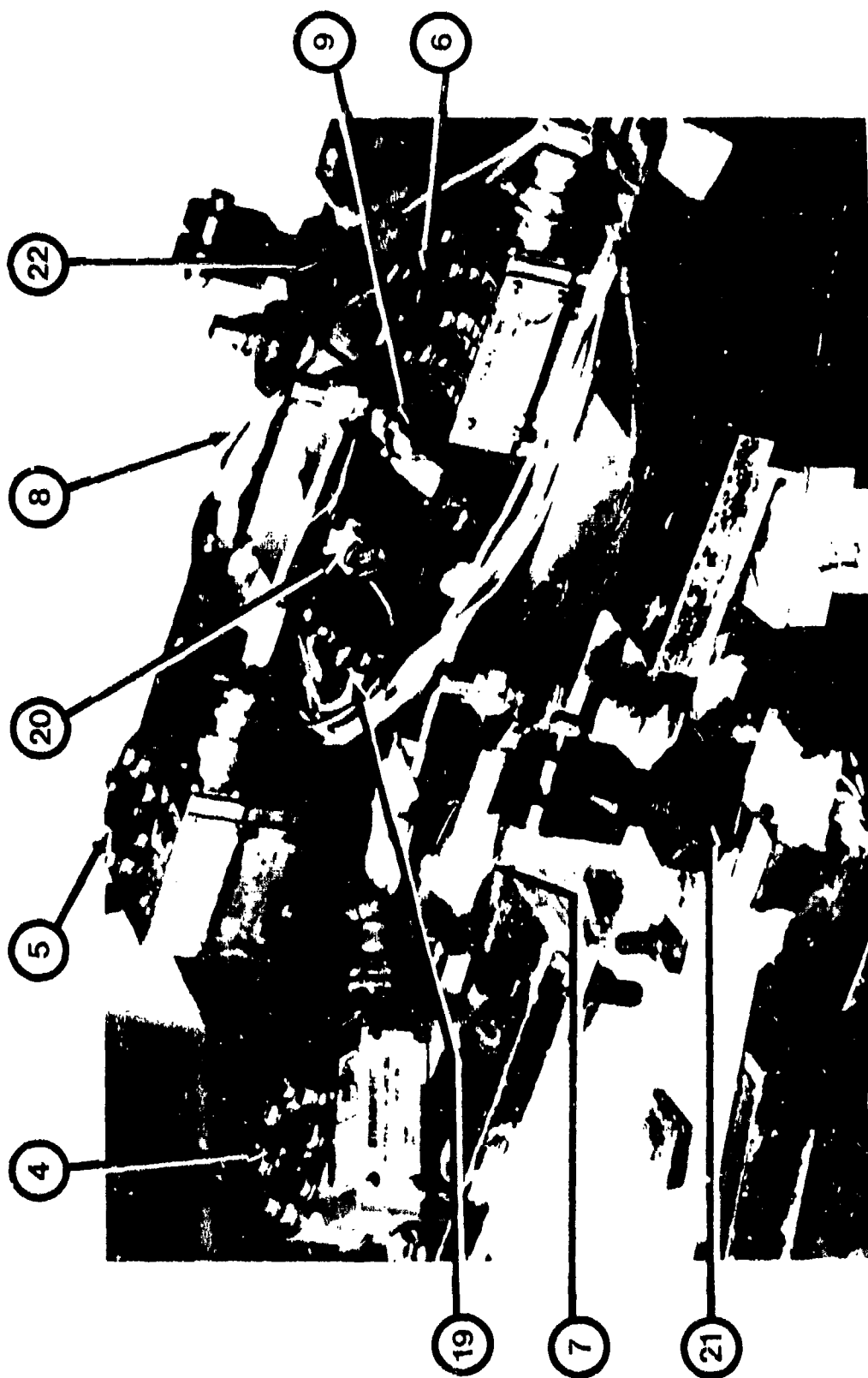
NOTE: REFER TO FIGURE A-15a FOR A DESCRIPTION OF THE TRANSDUCER ITEM NUMBERS.

FIGURE A-17: SEAT PAN INSTRUMENTATION
(θ AND MINUS 1θ DEGREE SEAT POSITION WITH X-BAND-90 DEGREE HARNESS)



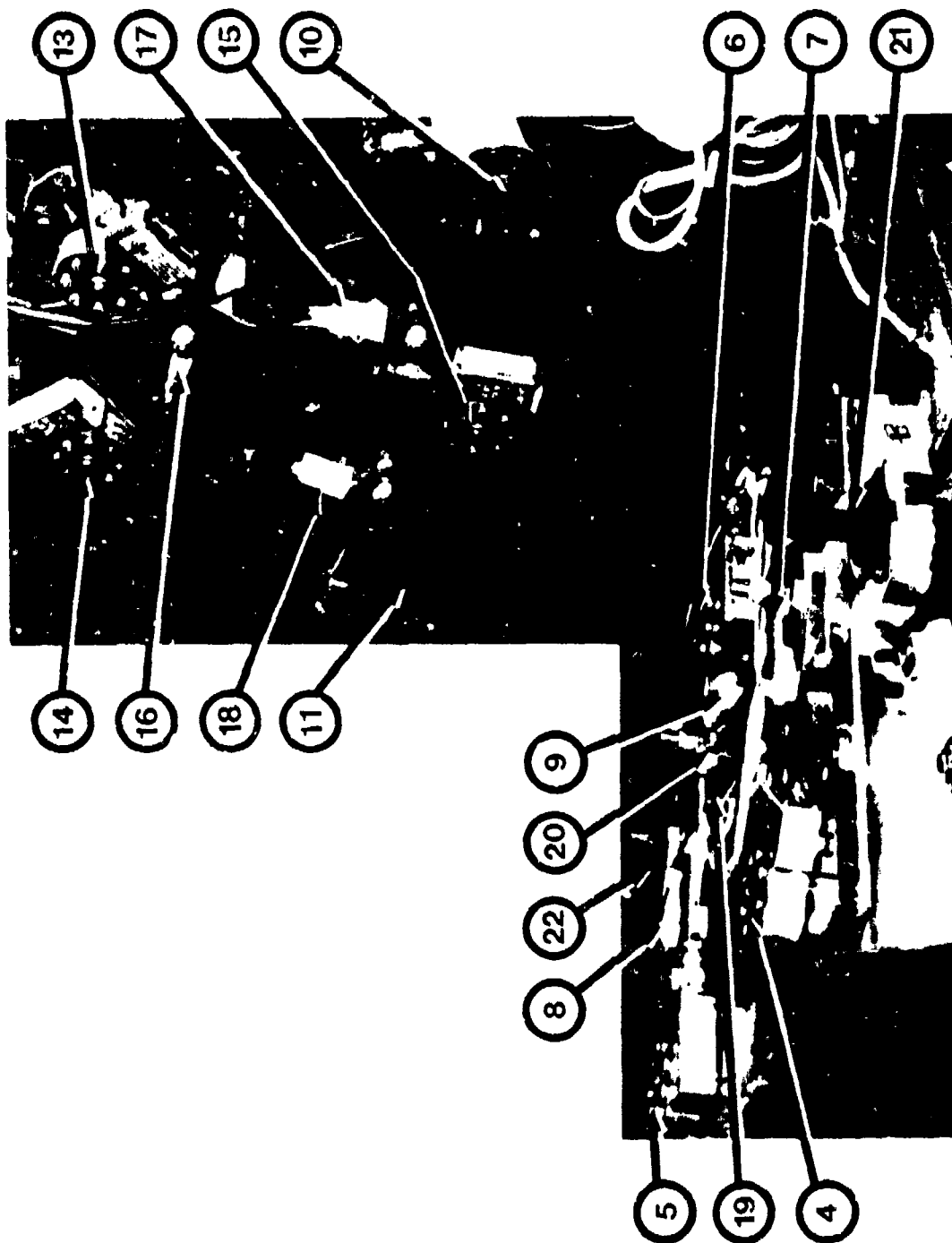
NOTE: REFER TO FIGURE A-15a FOR A DESCRIPTION OF THE TRANSDUCER ITEM NUMBERS.

FIGURE A-18: SEAT PAN INSTRUMENTATION
(0 AND MINUS 10 DEGREE SEAT POSITION WITH PCU-15/P HARNESS)



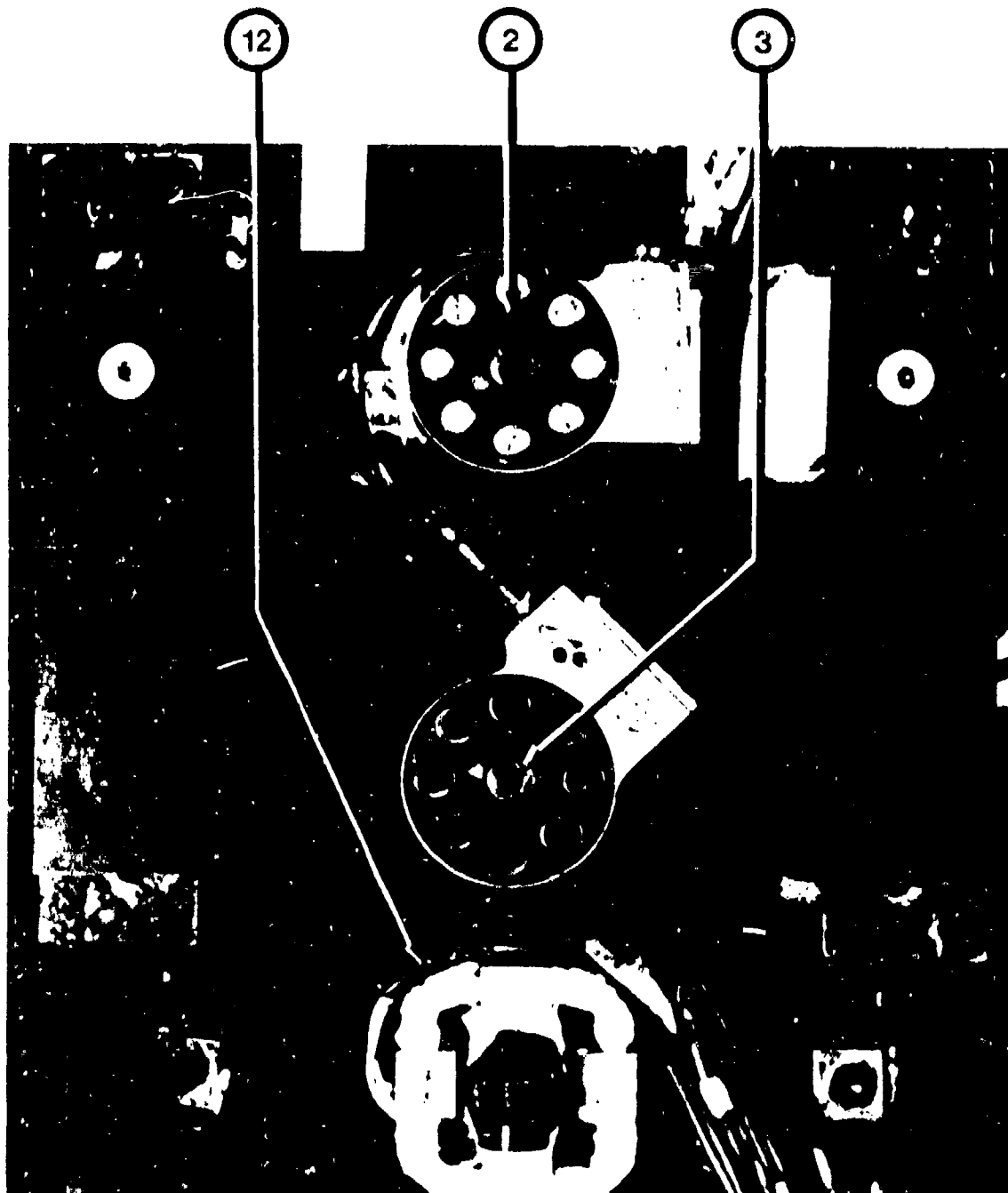
NOTE: REFER TO FIGURE A-15a FOR A DESCRIPTION OF THE TRANSDUCER ITEM NUMBERS.

FIGURE A-19: SEAT PAN INSTRUMENTATION
(PLUS 10 DEGREE SEAT POSITION WITH X-BAND-90 DEGREE HARNESS)



NOTE: REFER TO FIGURE A-15a FOR A DESCRIPTION OF THE TRANSDUCER ITEM NUMBERS.

FIGURE A-20: SEAT PAN AND SEAT BACK INSTRUMENTATION
(PLUS 10 DEGREE SEAT POSITION WITH X-BAND-90 DEGREE HARNESS)



NOTE: REFER TO FIGURE A-15a
FOR A DESCRIPTION OF THE TRANSDUCER ITEM NUMBERS.

FIGURE A-21: HEADREST AND SHOULDER LOAD CELL INSTRUMENTATION

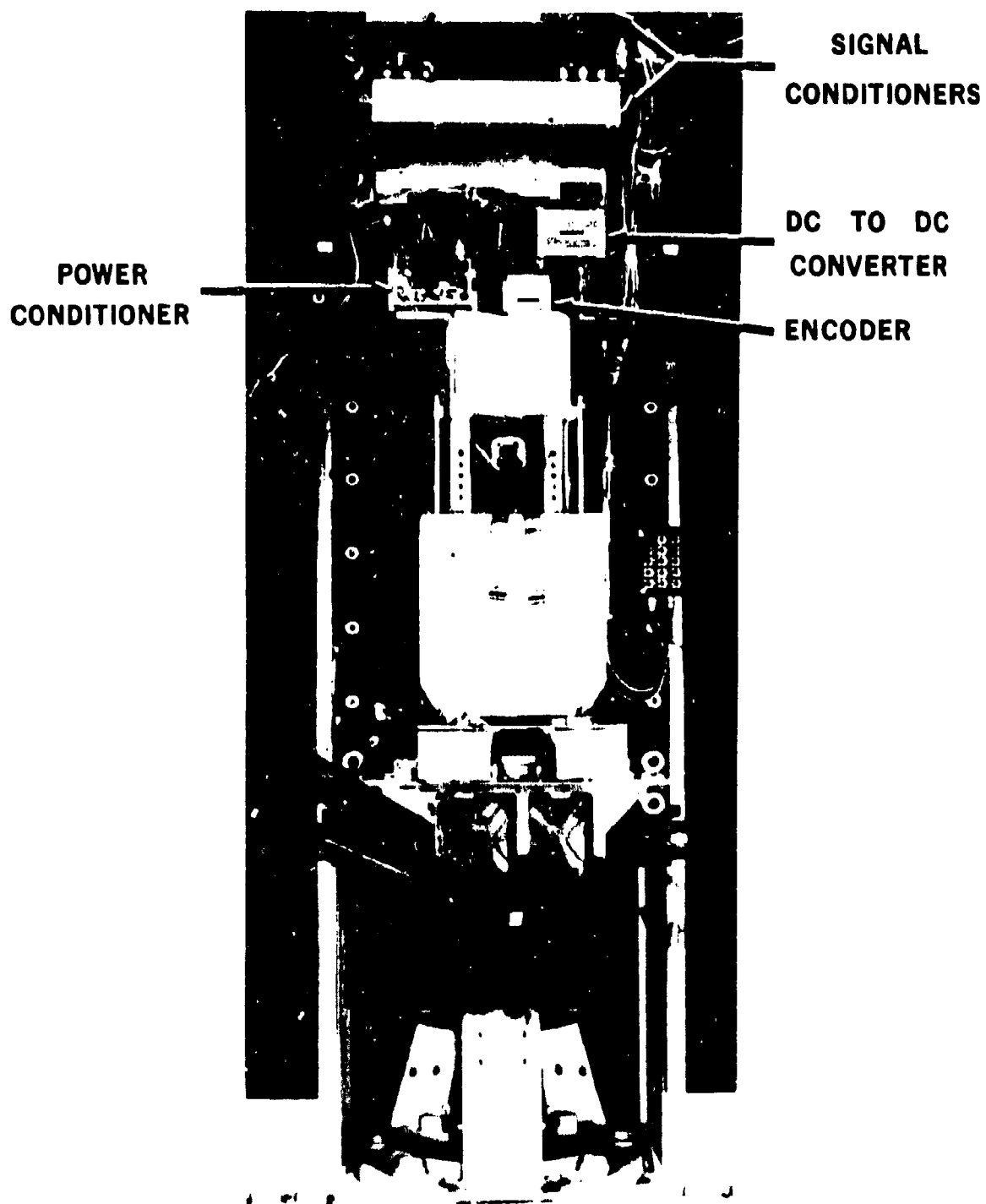


FIGURE A-22: ADACS INSTALLATION

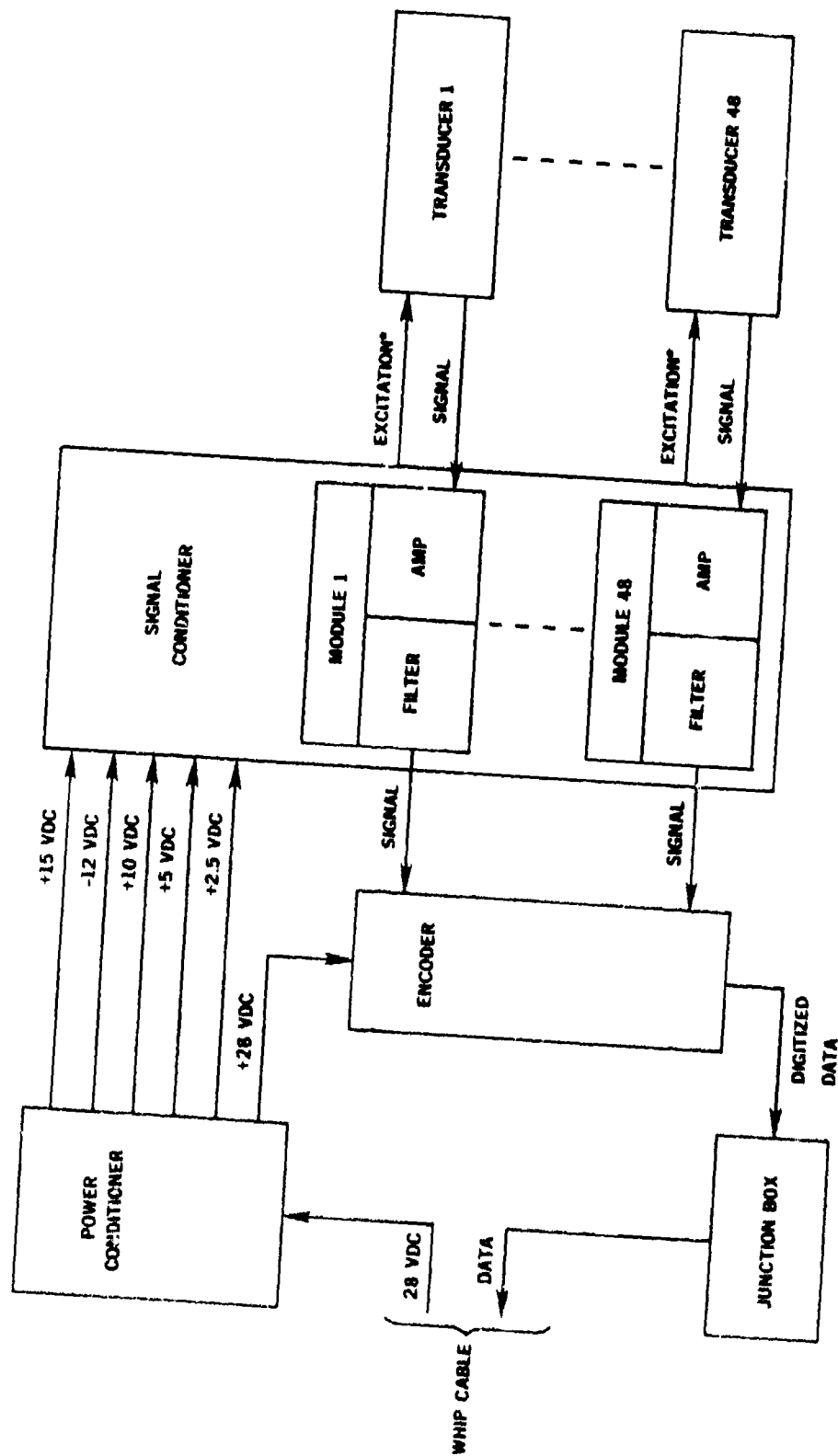


FIGURE A-23: AUTOMATIC DATA ACQUISITION AND CONTROL SYSTEM

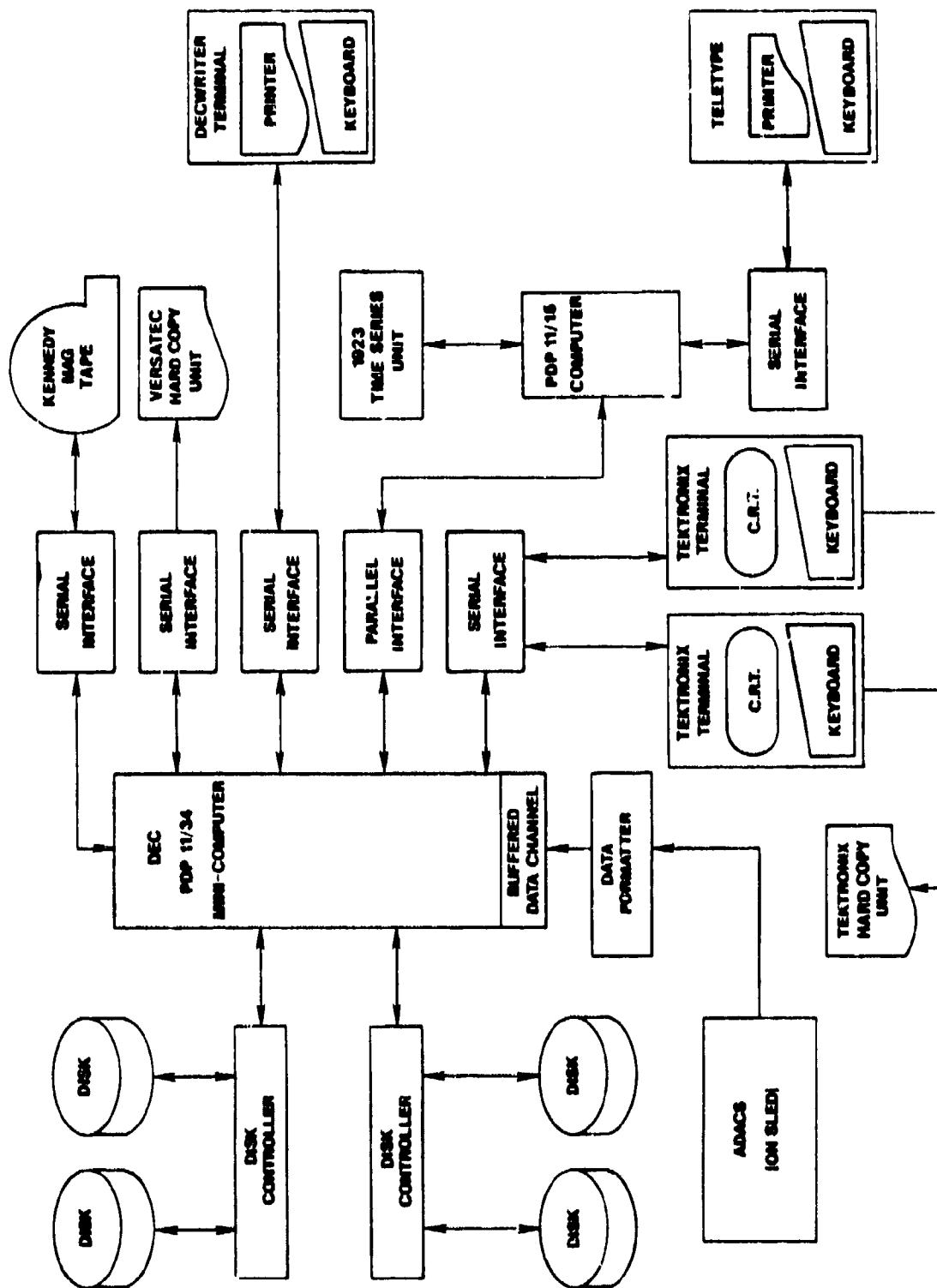


FIGURE A-24: DATA ACQUISITION AND STORAGE SYSTEM BLOCK DIAGRAM

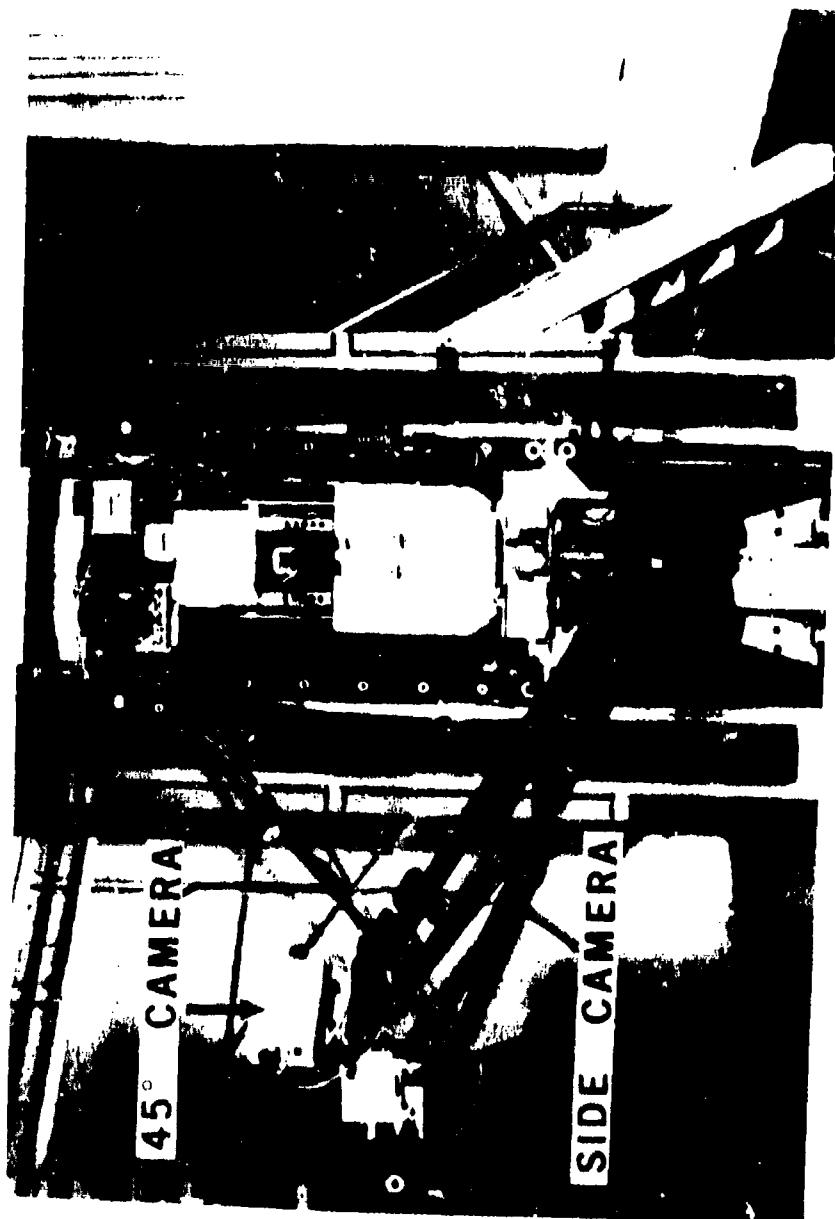
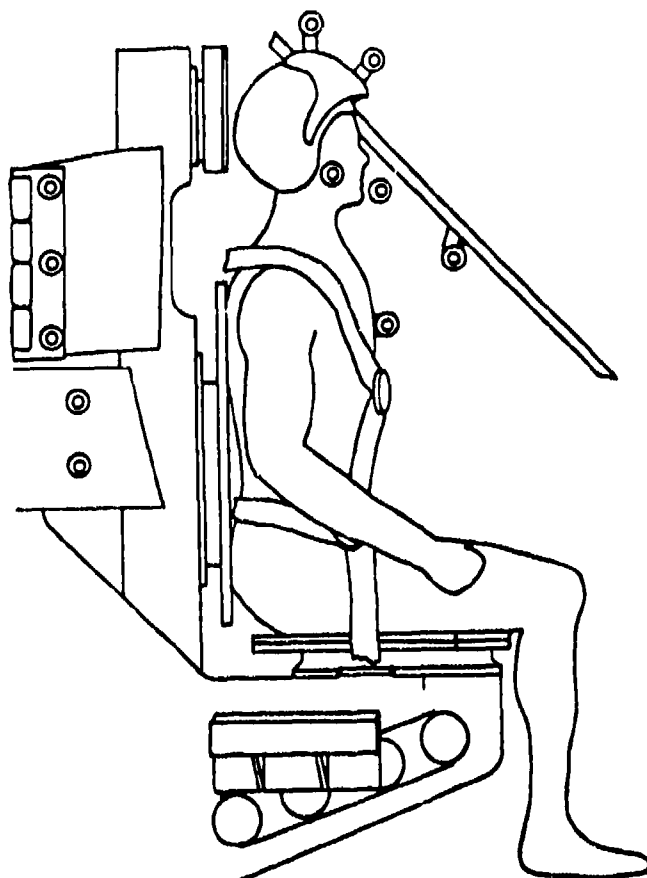


FIGURE A-25: ONBOARD CAMERA LOCATIONS



ALL DIMENSIONS ARE REFERENCED TO THE SEAT REFERENCE POINT (SRP).
THE SEAT REFERENCE POINT IS LOCATED AT THE INTERSECTION OF THE
SEAT PLATE (X AXIS) CENTER LINE AND THE BACK PLATE CENTER LINE.

0 DEGREE SEAT POSITION

	DIMENSIONS IN FEET		
	<u>X</u>	<u>Y</u>	<u>Z</u>
1. UPPER HELMET	-	-	-
2. FRONTAL HELMET	-	-	-
3. CHEEK	-	-	-
4. MOUTH PACK	-	-	-
5. CHEST PACK	-	-	-
6. UPPER NUMBER PLATE	-1.1154	+0.7272	+2.7791
7. MIDDLE NUMBER PLATE	-1.1154	+0.7485	+2.1908
8. LOWER NUMBER PLATE	-1.1006	+0.7689	+1.6252
9. MIDDLE BACK FRAME	-0.9366	+0.6403	+1.3723
10. LOWER BACK FRAME	-0.9569	+0.6288	+0.8165
11. CAMERA STRUT	+1.2578	+2.8317	+2.3242

FIGURE A-26a: FIDUCIAL TARGET LOCATIONS (PAGE 1 OF 2)

FIDUCIAL TARGET LOCATIONS 6 THROUGH 11 VARY WITH RESPECT TO THE SEAT BACK ANGLE. THE FOLLOWING DIMENSIONS ARE FOR THE PLUS AND MINUS 10 DEGREE SEAT POSITIONS:

PLUS 10 DEGREE SEAT POSITION

DESCRIPTION		DIMENSIONS IN FEET		
		<u>X</u>	<u>Y</u>	<u>Z</u>
1.	UPPER HELMET	-	-	-
2.	FRONTAL HELMET	-	-	-
3.	CHEEK	-	-	-
4.	MOUTH PACK	-	-	-
5.	CHEST PACK	-	-	-
6.	UPPER NUMBER PLATE	-0.6442	+0.7272	+3.0063
7.	MIDDLE NUMBER PLATE	-0.7464	+0.7485	+2.4270
8.	LOWER NUMBER PLATE	-0.8301	+0.7689	+1.8674
9.	MIDDLE BACK FRAME	-0.7125	+0.6403	+1.5898
10.	LOWER BACK FRAME	-0.8290	+0.6288	+1.0460
11.	CAMERA STRUT	+1.6139	+2.8317	+2.1462

MINUS 10 DEGREE SEAT POSITION

DESCRIPTION		DIMENSIONS IN FEET		
		<u>X</u>	<u>Y</u>	<u>Z</u>
1.	UPPER HELMET	-	-	-
2.	FRONTAL HELMET	-	-	-
3.	CHEEK	-	-	-
4.	MOUTH PACK	-	-	-
5.	CHEST PACK	-	-	-
6.	UPPER NUMBER PLATE	-1.0643	+0.7272	+2.8104
7.	MIDDLE NUMBER PLATE	-1.0643	+0.7485	+2.2221
8.	LOWER NUMBER PLATE	-1.0495	+0.7689	+1.6565
9.	MIDDLE BACK FRAME	-0.8855	+0.6403	+1.4035
10.	LOWER BACK FRAME	-0.9058	+0.6288	+0.8478
11.	CAMERA STRUT	+1.3088	+2.8317	+2.3555

FIGURE A-26b: FIDUCIAL TARGET LOCATIONS (PAGE 2 OF 2)

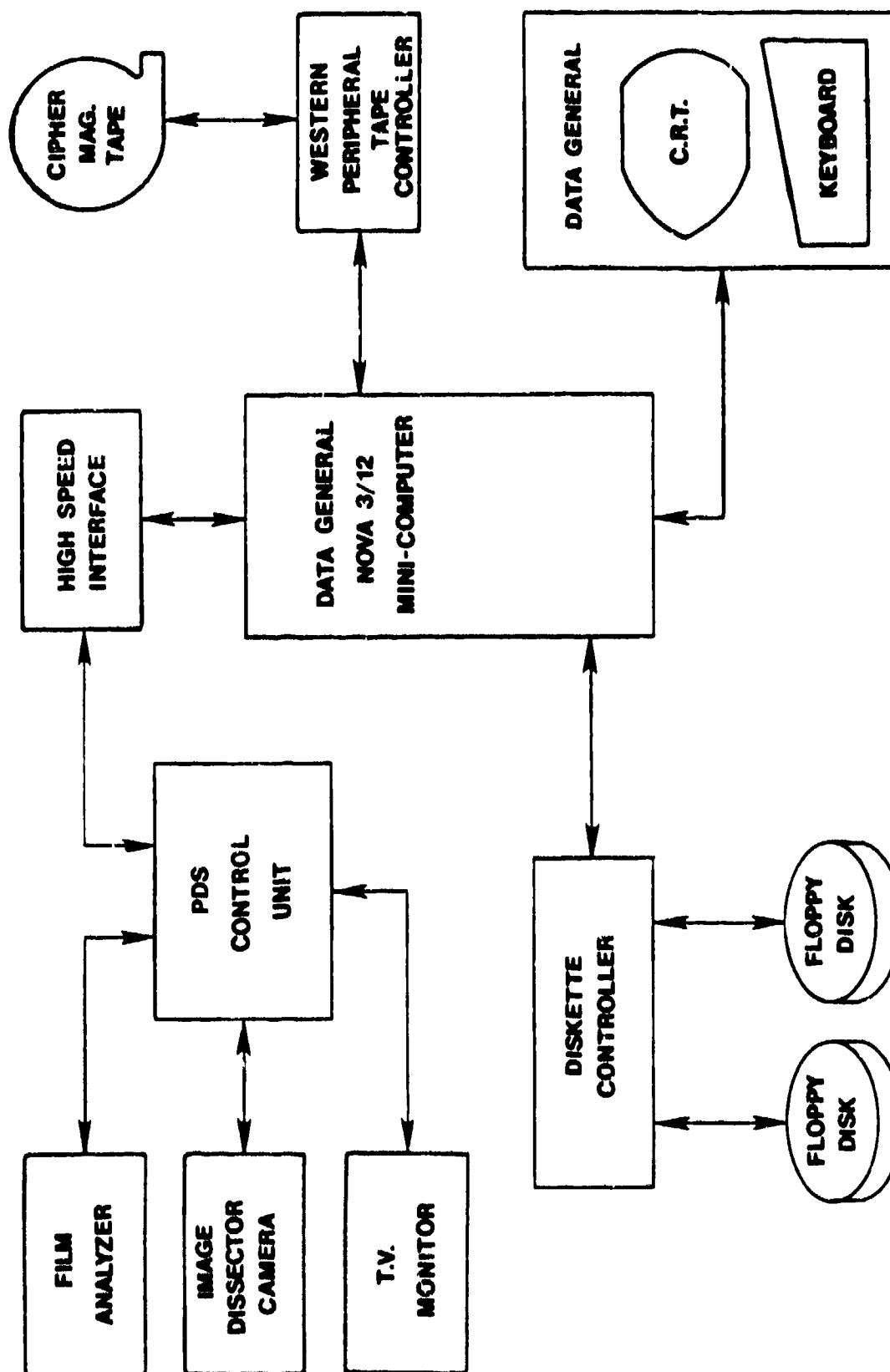


FIGURE A-27: AUTOMATIC FILM READER

APPENDIX B

ANTHROPOMETRY OF TEST SUBJECTS

SUBJECT ID	WT (LB)	HT (IN)	SIT HT (IN)	MID-SHOULDER SIT HT (IN)	BUTTOCK TO KNEE (IN)	AGE (YR)
M-21	120	66.1	34.2	23.6	23.1	28
T-5	123	64.8	32.9	22.4	23.1	32
K-3	139	68.1	34.8	23.8	24.4	25
Z-2	148	68.4	36.9	25.5	23.0	26
B-9	150	68.1	34.9	25.8	23.2	21
H-8	150	70.4	37.3	25.1	23.6	31
M-25	150	70.0	36.8	24.8	23.4	25
S-3	162	69.6	36.6	25.6	23.8	38
B-1	163	70.5	37.0	25.7	24.0	28
D-5	179	72.0	36.2	25.0	25.4	25
K-5	180	68.8	35.0	24.2	24.3	24
P-5	186	68.5	36.1	24.6	23.2	26
S-11	189	71.3	36.7	25.1	24.1	23
*R-11	191	73.5	36.0	----	----	24
M-19	194	74.2	38.5	26.1	25.6	28
MEAN	161.6	69.6	36.0	24.8	23.9	26.9
S.D.	24.2	2.5	1.4	1.0	0.8	4.2

*R-11 was used in Cells A and C only

APPENDIX C

NUMERICAL LISTING OF TESTS

NUMERICAL LISTING OF TESTS

TEST	CELL	SUBJ	TEST	CELL	SUBJ
1390	X	B1	1451	C	ADAM-L
1391	X	P5	1452	C	ADAM-L
1392	X	B9	1453	C	ADAM-L
1393	X	R11	1455	C	D5
1394	X	S11	1456	C	K5
1395	X	T5	1457	C	M25
1399	Y	K3	1458	C	H8
1400	Y	H8	1459	C	B1
1401	Y	S3	1460	C	S3
1404	Y	M21	1461	C	Z2
1405	Y	M19	1462	C	T5
1406	Y	D5	1464	C	M21
1408	A	S11	1465	A	CG-5
1409	A	R11	1466	A	CG-95
1410	A	T5	1467	C	ADAM-L
1412	A	P5	1474	D	CG-5
1413	A	K3	1475	D	CG-5
1414	A	M19	1476	D	CG-95
1415	A	D5	1480	B	M25
1416	A	B9	1481	B	S11
1417	X	M25	1482	B	H8
1418	A	M21	1483	B	P5
1419	A	ADAM-L	1484	B	K3
1420	A	ADAM-S	1486	B	B1
1422	A	B1	1487	B	B2
1423	X	Z2	1488	B	K5
1424	X	K5	1489	B	D5
1426	A	H8	1490	B	M19
1427	A	S3	1492	B	B9
1428	C	P5	1493	B	M21
1429	C	S11	1494	B	ADAM-L
1430	C	K3	1495	B	ADAM-S
1431	C	R11	1496	B	CG-5
1432	C	M19	1497	B	CG-5
1433	C	ADAM-S	1498	B	ADAM-L
1434	C	ADAM-S	1499	B	ADAM-L
1435	C	ADAM-S	1500	B	ADAM-S
1436	C	ADAM-S	1501	E	ADAM-S
1437	C	ADAM-S	1502	E	ADAM-L
1438	C	ADAM-L	1504	E	M19
1439	C	ADAM-L	1505	E	K5
1440	C	CG-5	1506	E	S11
1441	C	CG-5	1507	E	B9
1442	C	CG-5	1509	E	S3
1443	C	CG-5	1510	E	M25
1444	C	CG-5	1511	E	D5
1445	C	CG-95	1512	E	P5
1446	C	CG-95	1513	E	H8
1447	C	CG-95	1514	E	K3
1448	C	CG-95	1515	E	ADAM-L
1449	C	CG-95	1516	E	ADAM-L
1450	C	ADAM-L	1517	E	CG-95

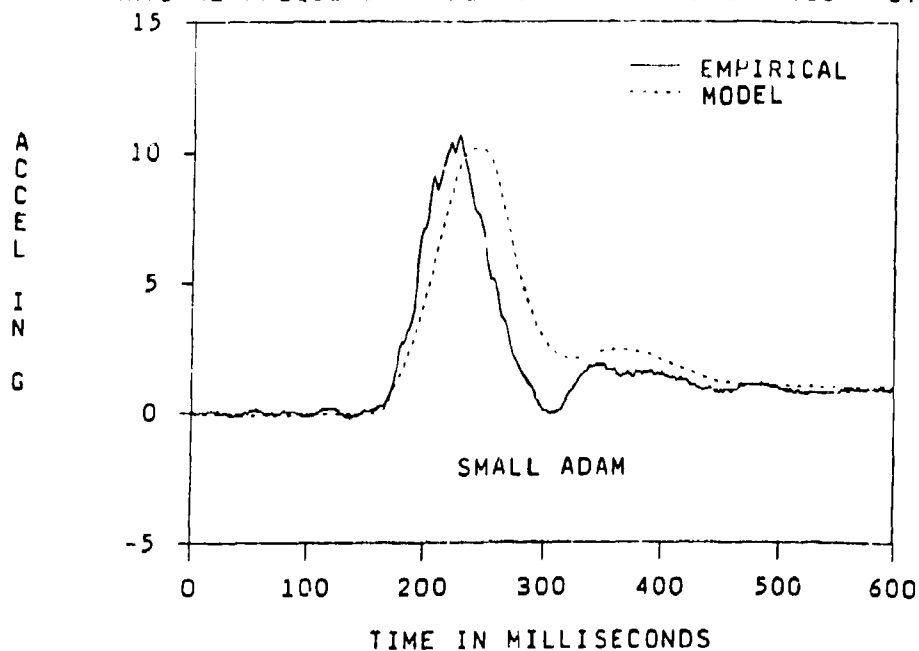
NUMERICAL LISTING OF TESTS

TEST	CELL	SUBJ	TEST	CELL	SUBJ
1518	F	CG-95	1584	E	ADAM-L
1519	E	CG-5	1585	F	ADAM-L
1520	F	CG-5	1586	C	CG-95
1521	E	B1	1587	C	B9
1522	E	M21	1588	A	K5
1523	E	T5	1589	A	M25
1524	E	Z2	1590	C	ADAM-S
1526	F	P5	1592	M	CG-5
1527	F	S11	1593	N	CG-5
1528	F	S3	1594	O	CG-5
1529	F	B9	1595	H	CG-95
1530	F	K3	1597	I	CG-95
1531	F	M25	1598	J	CG-95
1533	F	M21	1599	C	ADAM-L
1534	F	B1	1600	F	ADAM-L
1535	F	K5	1601	H	ADAM-S
1536	F	M19	1602	I	ADAM-S
1537	F	Z2	1603	J	ADAM-S
1538	F	ADAM-L	1604	H	ADAM-S
1539	F	ADAM-L	1605	I	ADAM-L
1541	F	D5	1606	H	ADAM-S
1542	F	H8	1607	H	ADAM-S
1543	F	T5	1608	H	ADAM-S
1544	E	ADAM-L	1609	H	CG-95
1545	F	ADAM-L	1610	H	CG-95
1546	E	ADAM-S	1611	H	CG-95
1547	F	ADAM-S	1612	H	CG-5
1550	D	ADAM-S	1613	H	CG-5
1551	D	ADAM-L	1614	H	CG-5
1553	D	M21	1615	I	CG-5
1554	D	Z2	1616	J	CG-5
1557	D	P5	1617	C	CG-5
1558	D	K5	1618	I	ADAM-L
1559	D	K3	1621	L	B1
1560	D	T5	1622	L	K3
1561	D	S11	1623	L	S3
1563	D	B1	1624	L	H8
1564	D	S3	1625	L	B9
1565	D	H8	1627	L	K5
1567	D	D5	1628	L	D5
1568	D	B9	1629	L	S11
1569	D	M19	1630	L	M19
1571	A	Z2	1631	L	T5
1572	B	ADAM-S	1632	L	CG-5
1573	B	ADAM-L	1633	L	CG-95
1575	B	T5	1634	L	ADAM-L
1576	B	S3	1635	L	ADAM-L
1578	G	CG-95	1636	L	ADAM-L
1579	G	CG-5	1637	H	ADAM-L
1580	G	ADAM-S	1638	H	ADAM-L
1581	G	ADAM-L	1639	H	ADAM-L
1583	E	ADAM-L			

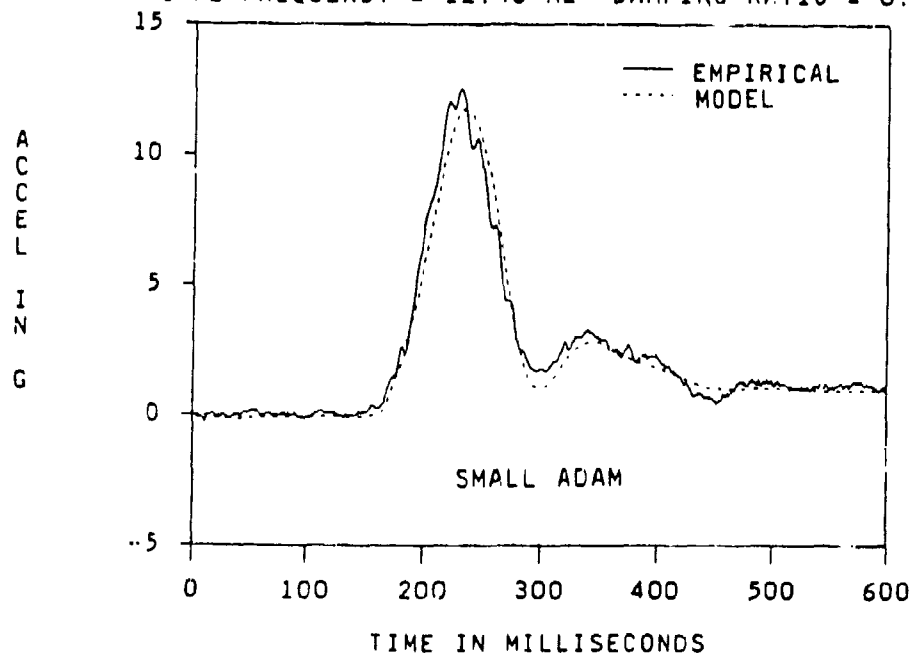
APPENDIX D

TRANSFER FUNCTION ANALYSIS PLOTS

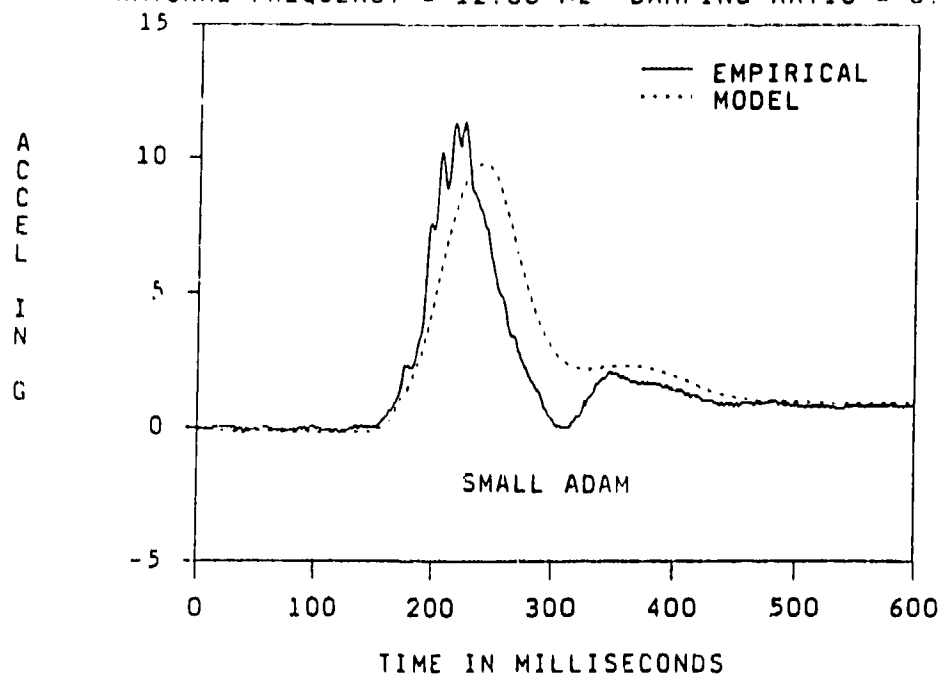
VIHAM STUDY TEST 1435 HEAD Z ACCEL
 NATURAL FREQUENCY = 12.28 HZ DAMPING RATIO = 0.6197



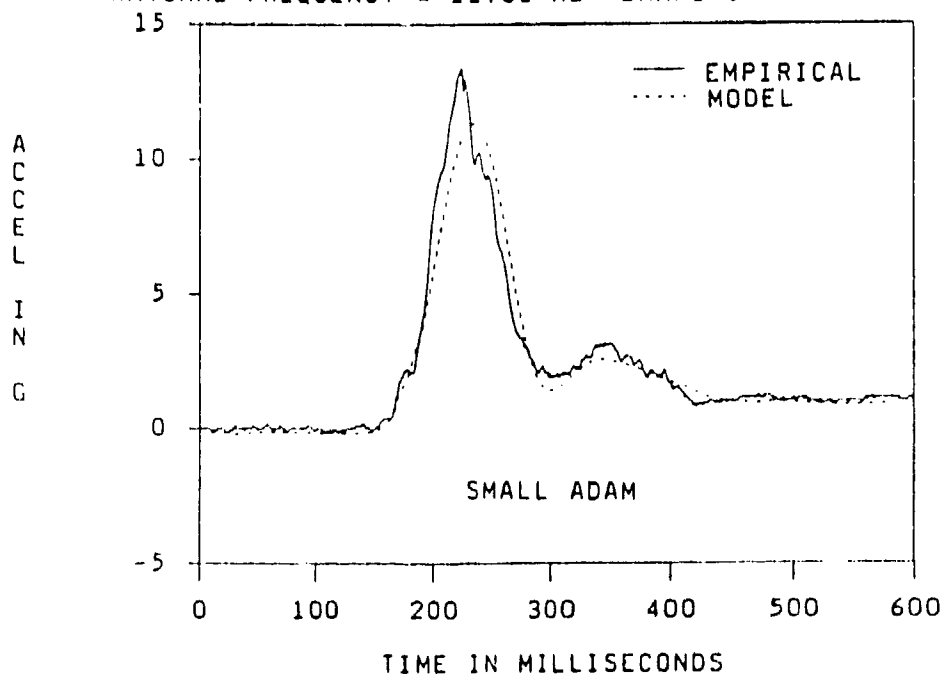
VIHAM STUDY TEST 1435 CHEST Z ACCEL
 NATURAL FREQUENCY = 12.46 HZ DAMPING RATIO = 0.2834



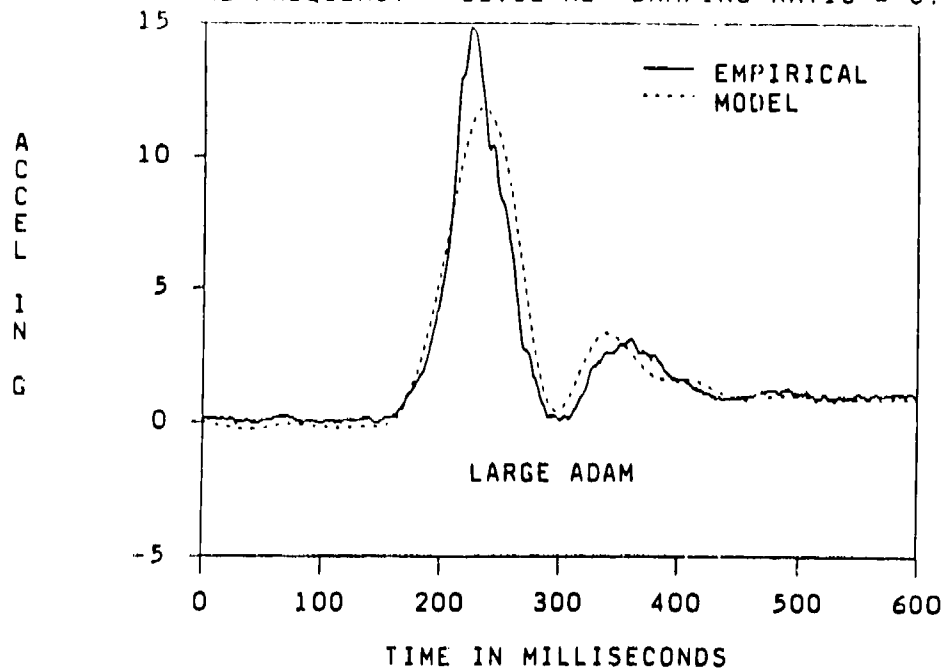
VIHAM STUDY TEST 1436 HEAD Z ACCEL
NATURAL FREQUENCY = 12.88 HZ DAMPING RATIO = 0.7398



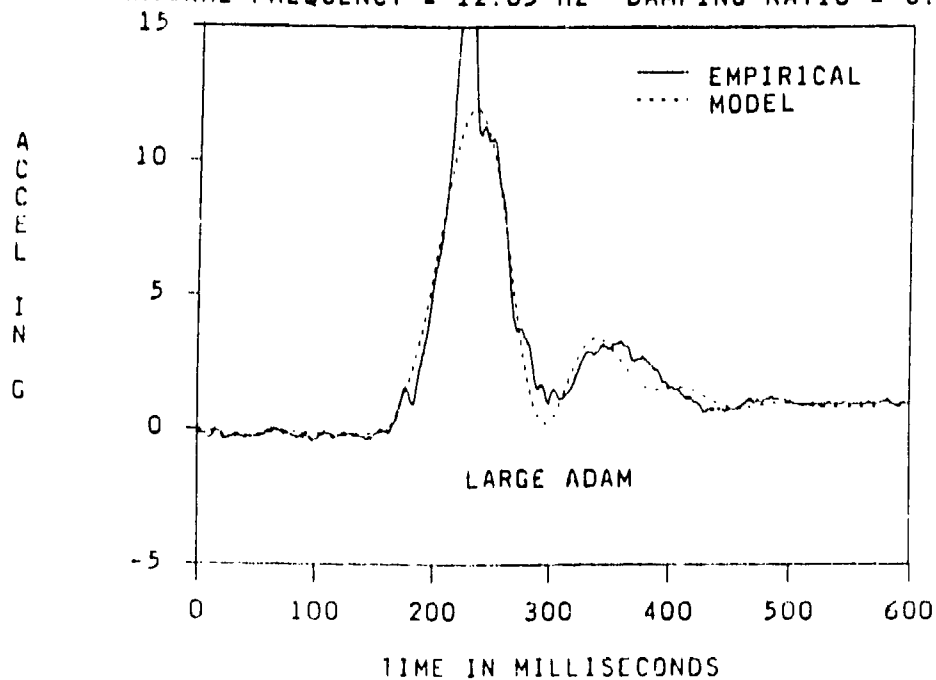
VIHAM STUDY TEST 1436 CHEST Z ACCEL
NATURAL FREQUENCY = 12.81 HZ DAMPING RATIO = 0.3521



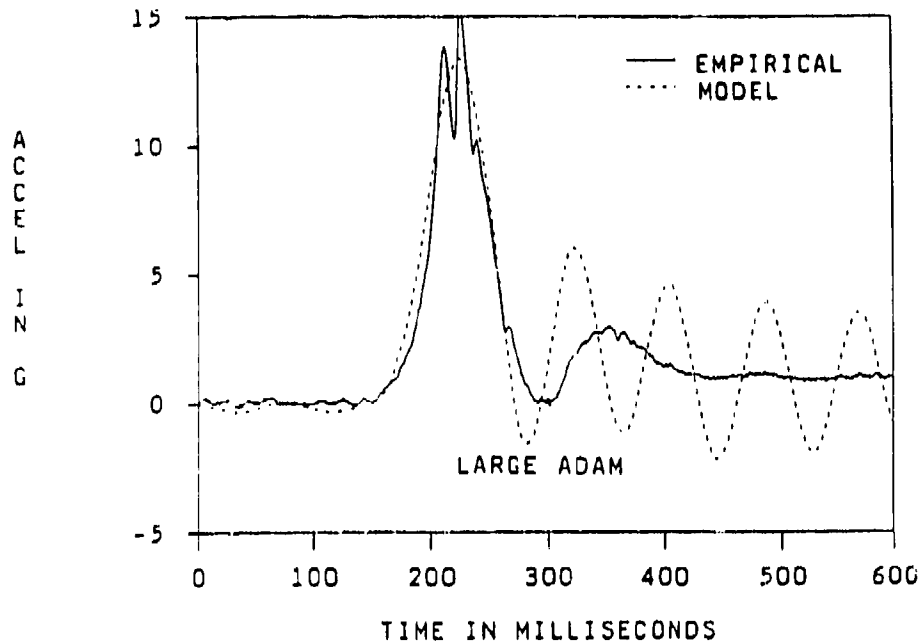
VIHAM STUDY TEST 1451 HEAD Z ACCEL
 NATURAL FREQUENCY = 12.12 HZ DAMPING RATIO = 0.2061



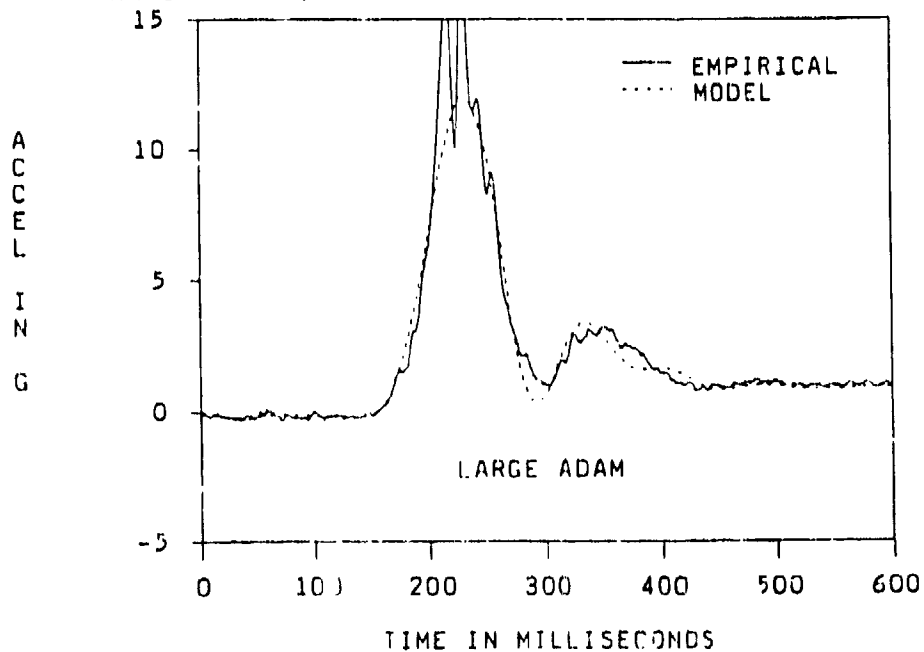
VIHAM STUDY TEST 1451 CHEST Z ACCEL
 NATURAL FREQUENCY = 12.05 HZ DAMPING RATIO = 0.1896



VIHAM STUDY TEST 1452 HEAD Z ACCEL
 NATURAL FREQUENCY = 12.18 HZ DAMPING RATIO = 0.2210



VIHAM STUDY TEST 1452 CHEST Z ACCEL
 NATURAL FREQUENCY = 12.09 HZ DAMPING RATIO = 0.1994



APPENDIX E

SAMPLE TEST DATA

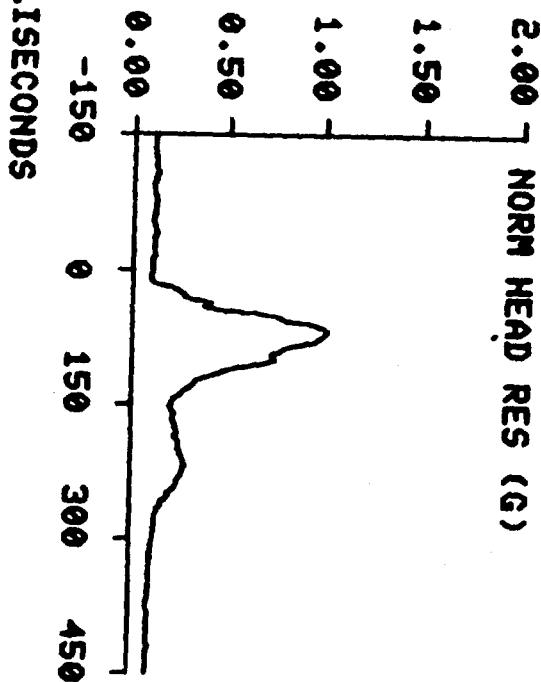
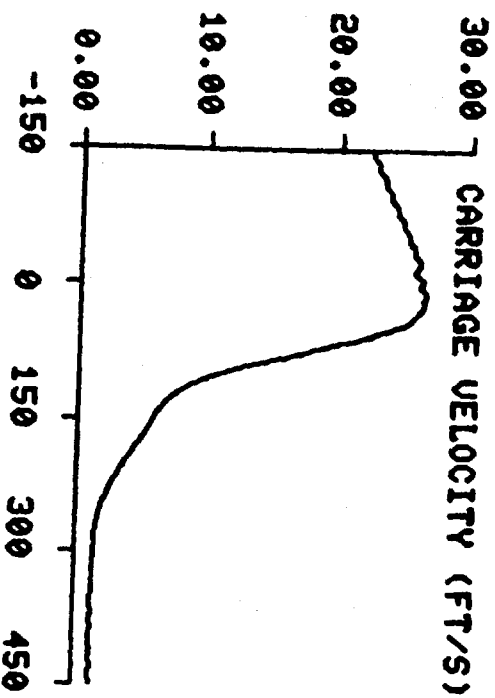
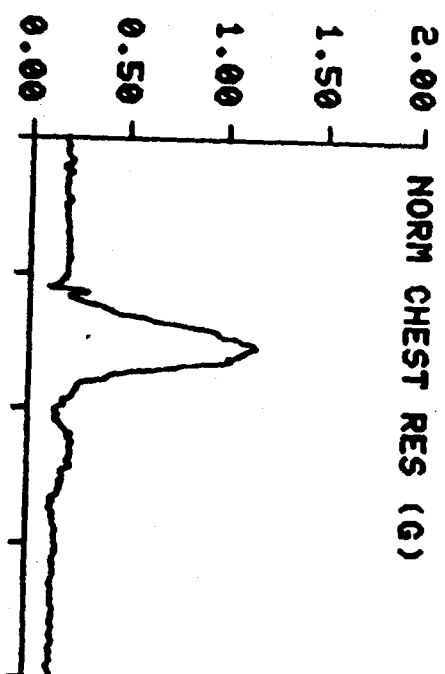
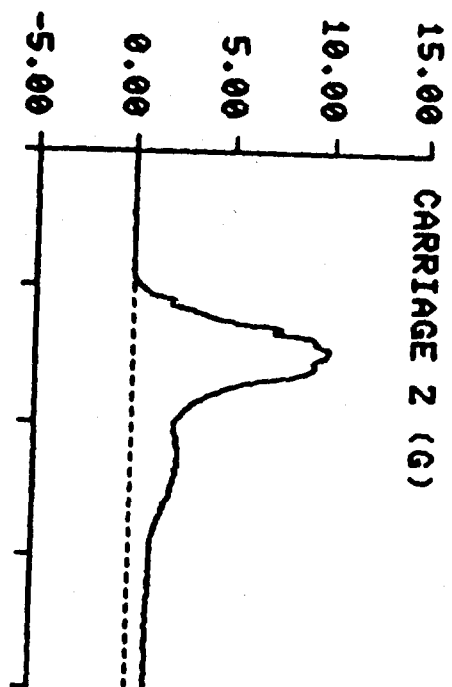
VIHAM STUDY TEST: 1430 SUBJ: K-3 WT: 138.0 NOM G: 10.0 CELL: C

DATA ID	IMMEDIATE PREIMPACT	MAXIMUM VALUE	MINIMUM VALUE	TIME OF MAXIMUM	TIME OF MINIMUM
REFERENCE MARK TIME (MS)				-152.	
2.5V EXT PWR (VOLTS)	2.50	2.51	2.49	64.	62.
10V EXT PWR (VOLTS)	10.00	10.00	10.00	12.	62.
CARRIAGE ACCELERATION (G)					
Z AXIS	0.03	9.93	0.46	66.	0.
SEAT ACCELERATION (G)					
X AXIS	-0.03	2.00	-1.30	11.	52.
Y AXIS	-0.09	1.61	-1.74	50.	70.
Z AXIS	-0.11	10.77	0.04	68.	0.
RESULTANT	0.20	10.81	-0.39	68.	0.
RY (RAD/S**2)	-3.70	20.66	-32.83	28.	22.
CARRIAGE VELOCITY (FT/S)	26.06	26.68	1.20	8.	358.
CHEST ACCELERATION (G)					
X AXIS	0.03	5.08	0.00	64.	2.
Y AXIS	-1.30	-0.33	-2.49	31.	58.
Z AXIS	-1.49	10.61	-1.34	79.	0.
RESULTANT	1.95	11.47	-0.95	81.	15.
RY (RAD/S**2)	-3.60	211.38	-178.17	23.	53.
HEAD ACCELERATION (G)					
X AXIS	-0.41	-0.50	-4.36	0.	112.
Y AXIS	-0.45	-0.18	-0.92	184.	63.
Z AXIS	-0.83	9.94	-0.81	68.	0.
RESULTANT	1.03	10.12	-0.89	68.	376.
RY (RAD/S**2)	-1.36	111.72	-235.20	139.	113.
HEADREST FORCES (LB)					
UPPER	0.69	3.11	-12.33	22.	52.
LOWER	-0.72	12.90	-1.96	76.	16.
SUM	-0.03	8.58	-8.10	22.	29.
SHOULDER STRAP FORCES (LB)					
X AXIS	47.90	143.69	32.44	92.	417.
Y AXIS	2.21	9.08	-1.12	58.	36.
Z AXIS	13.80	100.06	12.19	85.	405.
RESULTANT	49.90	172.08	34.72	92.	420.
HARNESB ANCHOR FORCES (LB)					
LEFT HORIZ X AXIS	46.56	59.80	23.37	74.	437.
RIGHT HORIZ X AXIS	58.87	80.17	31.32	82.	413.
LEFT VERTICAL X AXIS	-12.36	-0.88	-16.77	92.	11.
LEFT VERTICAL Y AXIS	72.57	73.68	26.74	0.	61.
LEFT VERTICAL Z AXIS	136.10	138.12	12.62	1.	68.
LEFT VERTICAL RES	154.74	156.75	30.40	1.	68.
RIGHT VERTICAL X AXIS	-36.70	-12.00	-38.76	91.	9.
RIGHT VERTICAL Y AXIS	67.09	68.35	23.00	0.	72.
RIGHT VERTICAL Z AXIS	132.67	134.55	16.72	0.	73.
RIGHT VERTICAL RES	153.12	155.22	31.35	0.	73.
BACKREST FORCES (LB)					
LEFT X AXIS	46.93	70.34	21.39	54.	413.
RIGHT X AXIS	46.68	83.68	21.23	23.	449.
CENTER X AXIS	6.75	92.38	4.72	119.	0.
X AXIS SUM	100.35	186.59	52.37	110.	449.
Y AXIS	7.53	14.22	1.29	56.	63.
LEFT Z AXIS	-34.94	117.35	-32.87	74.	1.
RIGHT Z AXIS	-29.67	114.36	-27.38	55.	0.
Z AXIS SUM	-64.61	214.55	-60.25	73.	1.
Z SUM MINUS TARE	-39.55	31.06	-67.62	135.	12.
RESULTANT	119.61	270.78	54.11	55.	449.
RESULTANT MINUS TARE	108.14	187.78	54.47	56.	449.
SEAT FORCES (LB)					
LEFT X AXIS	-3.44	43.84	-27.21	87.	61.
RIGHT X AXIS	-0.80	31.12	-32.81	230.	90.
X AXIS SUM	-4.24	51.32	-17.74	258.	63.
Y AXIS	-12.56	7.02	-77.02	129.	69.
LEFT Z AXIS	16.01	461.15	16.25	82.	0.
RIGHT Z AXIS	9.98	481.83	12.50	73.	0.
CENTER Z AXIS	205.63	1087.83	176.84	62.	447.
Z AXIS SUM	231.63	2022.82	236.63	74.	447.
Z SUM MINUS TARE	252.24	1861.05	236.49	75.	410.
RESULTANT	232.01	1190.23	238.17	74.	401.
RESULTANT MINUS TARE	252.59	1861.97	237.88	75.	410.

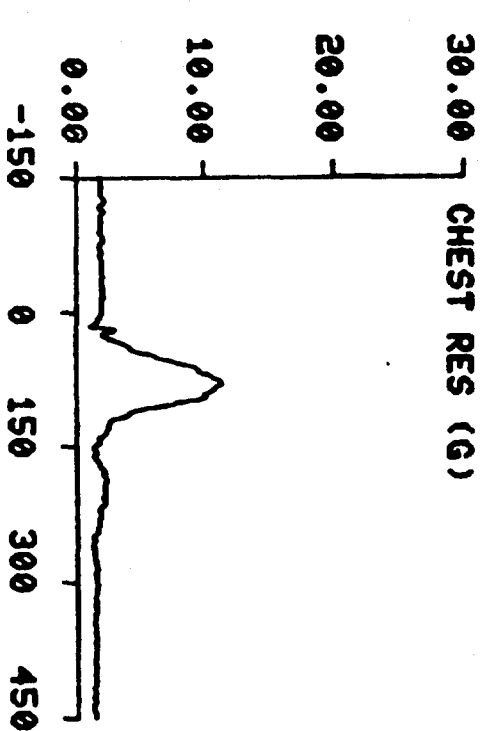
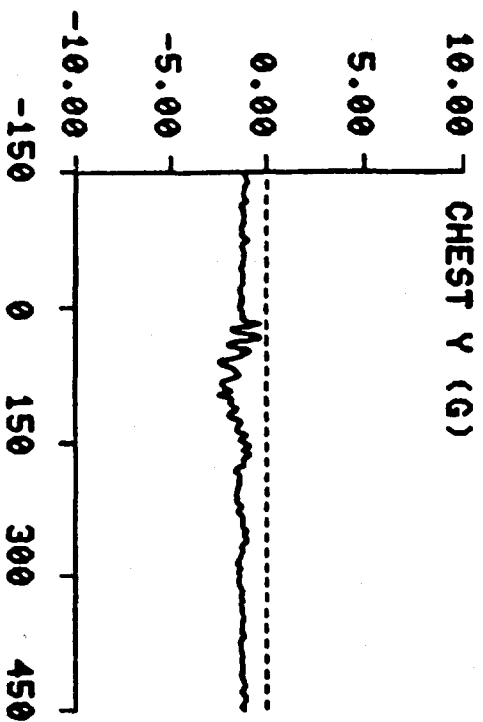
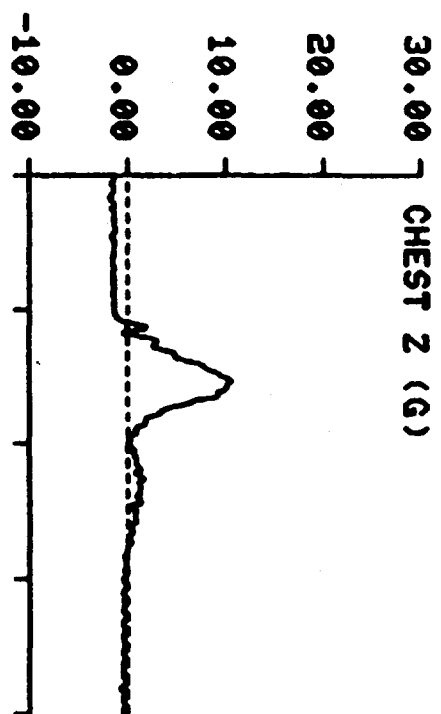
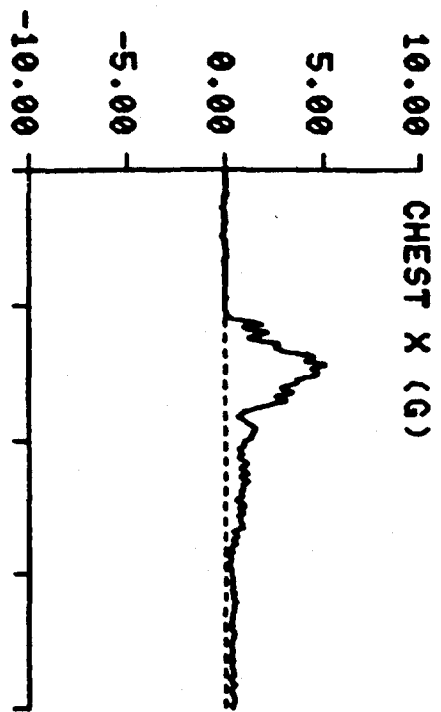
VIHAM STUDY TEST: 1430 SUBJ: K-3 WT: 138.0 NOM G: 10.0 CELL: C

DATA ID	IMMEDIATE PREIMPACT	MAXIMUM VALUE	MINIMUM VALUE	TIME OF MAXIMUM	TIME OF MINIMUM
REFERENCE MARK TIME (MS)				-152.	
2.5V EXT PWR (VOLTS)	2.50	2.51	2.49	64.	62.
10V EXT PWR (VOLTS)	10.00	10.00	10.00	12.	62.
CARRIAGE ACCELERATION (G)					
Z AXIS	0.03	9.93	0.46	66.	0.
SEAT ACCELERATION (G)					
X AXIS	-0.03	2.00	-1.30	11.	52.
Y AXIS	-0.09	1.61	-1.74	50.	70.
Z AXIS	-0.11	10.77	0.04	68.	0.
RESULTANT	0.20	10.81	0.39	68.	0.
RY (RAD/S**2)	-5.70	20.66	-32.83	28.	22.
CARRIAGE VELOCITY (FT/S)	26.06	26.68	1.20	8.	358.
CHEST ACCELERATION (G)					
X AXIS	0.03	5.08	0.00	64.	2.
Y AXIS	-1.30	-0.33	-2.49	31.	58.
Z AXIS	-1.45	10.61	-1.34	79.	0.
RESULTANT	1.95	11.47	0.95	81.	15.
RY (RAD/S**2)	-3.60	211.38	-178.17	23.	53.
HEAD ACCELERATION (G)					
X AXIS	-0.41	-0.50	-4.36	0.	112.
Y AXIS	-0.45	-0.18	-0.92	184.	63.
Z AXIS	-0.83	9.94	-0.81	68.	0.
RESULTANT	1.03	10.12	0.89	68.	376.
RY (RAD/S**2)	-1.36	111.72	-235.20	139.	113.
HEADREST FORCES (LB)					
UPPER	0.69	3.11	-12.33	22.	52.
LOWER	-0.72	12.90	-1.96	76.	16.
SUM	-0.03	8.58	-8.10	22.	29.
SHOULDER STRAP FORCES (LB)					
X AXIS	47.90	143.69	32.44	92.	417.
Y AXIS	2.21	9.08	-1.12	58.	36.
Z AXIS	13.80	100.06	12.19	85.	405.
RESULTANT	49.90	172.08	34.72	92.	420.
HARNESS ANCHOR FORCES (LB)					
LEFT HORIZ X AXIS	46.56	59.80	23.37	74.	437.
RIGHT HORIZ X AXIS	58.87	80.17	31.32	82.	413.
LEFT VERTICAL X AXIS	-12.36	-0.88	-16.77	92.	11.
LEFT VERTICAL Y AXIS	72.57	73.68	26.74	0.	61.
LEFT VERTICAL Z AXIS	136.10	138.12	12.63	1.	68.
LEFT VERTICAL RES	154.74	156.75	30.40	1.	68.
RIGHT VERTICAL X AXIS	-36.70	-12.00	-38.76	91.	9.
RIGHT VERTICAL Y AXIS	67.03	68.35	23.00	0.	72.
RIGHT VERTICAL Z AXIS	132.67	134.55	16.72	0.	73.
RIGHT VERTICAL RES	153.12	155.22	31.35	0.	73.
BACKREST FORCES (LB)					
LEFT X AXIS	46.93	70.34	21.39	24.	413.
RIGHT X AXIS	46.68	83.88	21.25	23.	449.
CENTER X AXIS	6.75	92.58	4.72	119.	3.
X AXIS SUM	100.35	186.59	52.37	110.	449.
Y AXIS	7.53	14.22	1.29	56.	63.
LEFT Z AXIS	-34.94	117.35	-32.87	74.	1.
RIGHT Z AXIS	-29.67	114.36	-27.38	55.	0.
Z AXIS SUM	-64.61	214.55	-60.25	73.	1.
Z SUM MINUS TARE	-39.55	31.06	-67.62	135.	12.
RESULTANT	119.61	270.78	54.11	56.	449.
RESULTANT MINUS TARE	108.14	187.78	54.47	56.	449.
SEAT FORCES (LB)					
LEFT X AXIS	-3.44	43.84	-27.21	87.	61.
RIGHT X AXIS	-0.80	31.12	-32.81	230.	90.
X AXIS SUM	-4.24	51.32	-17.74	258.	63.
Y AXIS	-12.56	7.02	-77.02	129.	69.
LEFT Z AXIS	16.01	661.15	16.25	82.	0.
RIGHT Z AXIS	9.98	481.83	12.50	72.	0.
CENTER Z AXIS	203.63	1087.83	176.84	62.	447.
Z AXIS SUM	231.63	2022.82	236.63	74.	447.
Z SUM MINUS TARE	252.24	1861.05	236.49	75.	410.
RESULTANT	232.01	1180.23	238.17	74.	401.
RESULTANT MINUS TARE	252.59	1861.97	237.88	75.	410.

VIHAM STUDY TEST: 1430 SUBJ: K-3 CELL: C

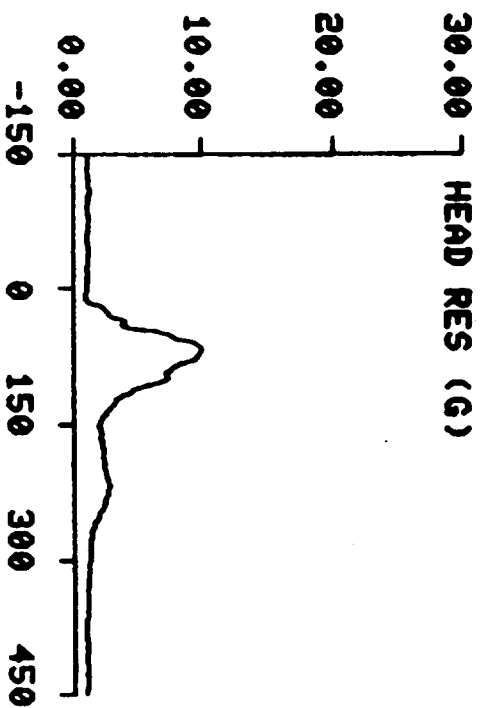
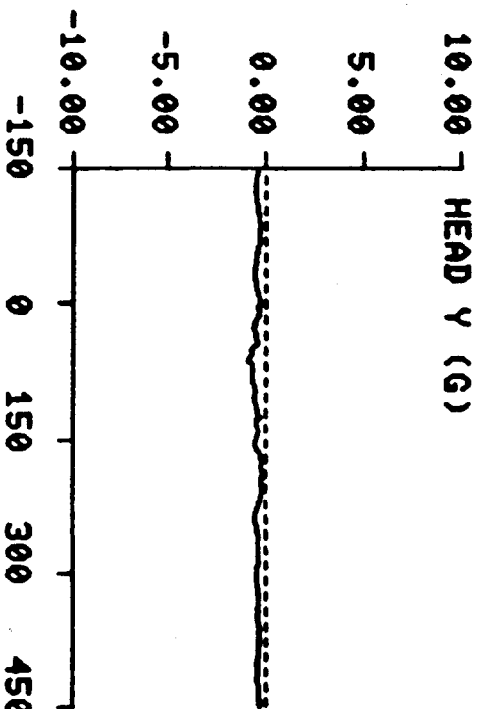
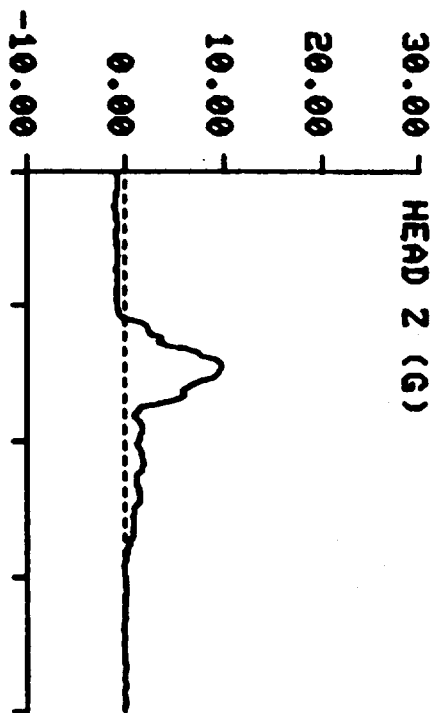
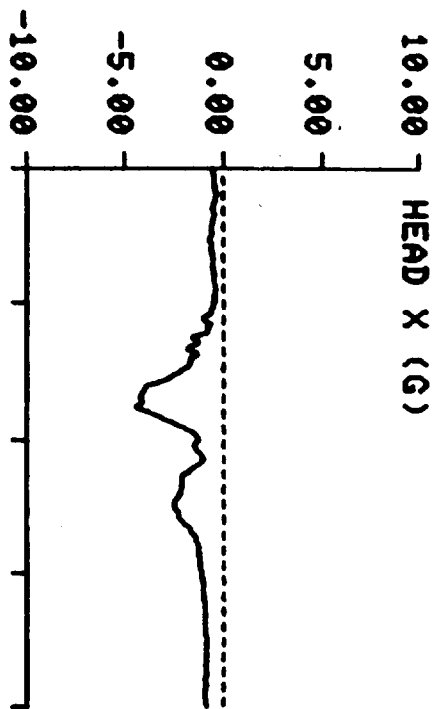


VIHAM STUDY TEST: 1430 SUBJ: K-3 CELL: C



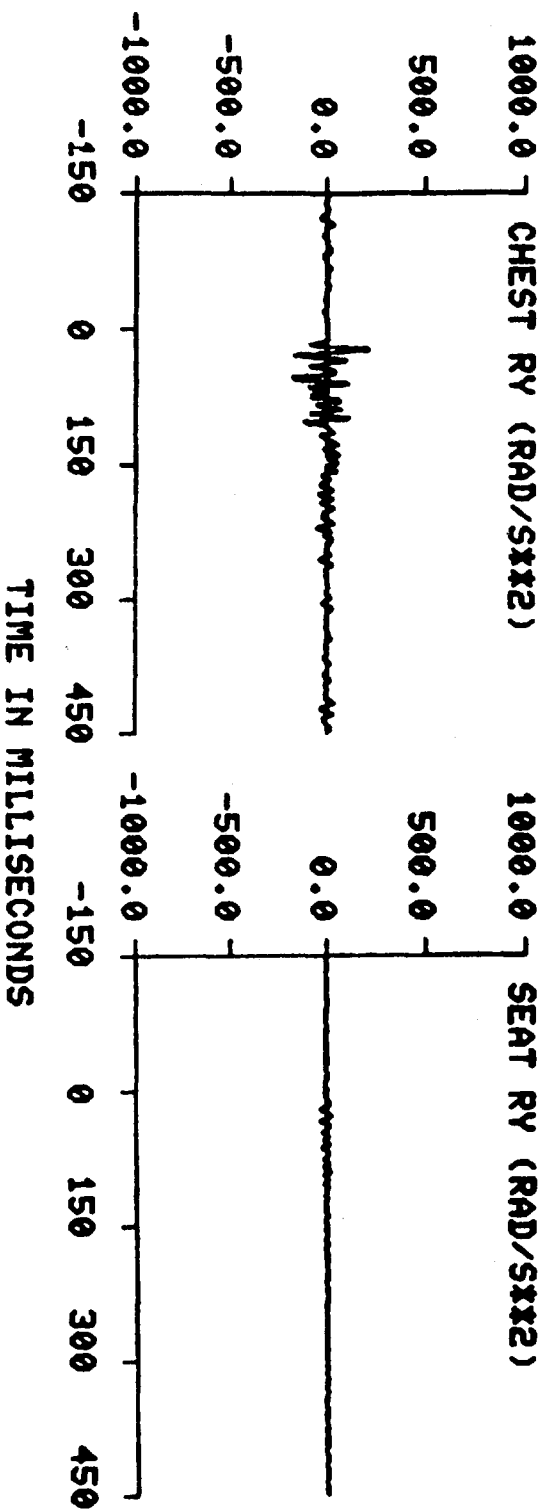
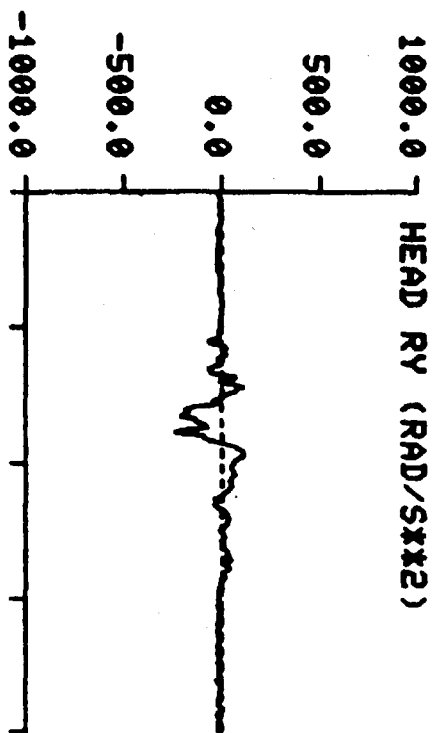
TIME IN MILLISECONDS

VIHAM STUDY TEST: 1430 SUBJ: K-3 CELL: C

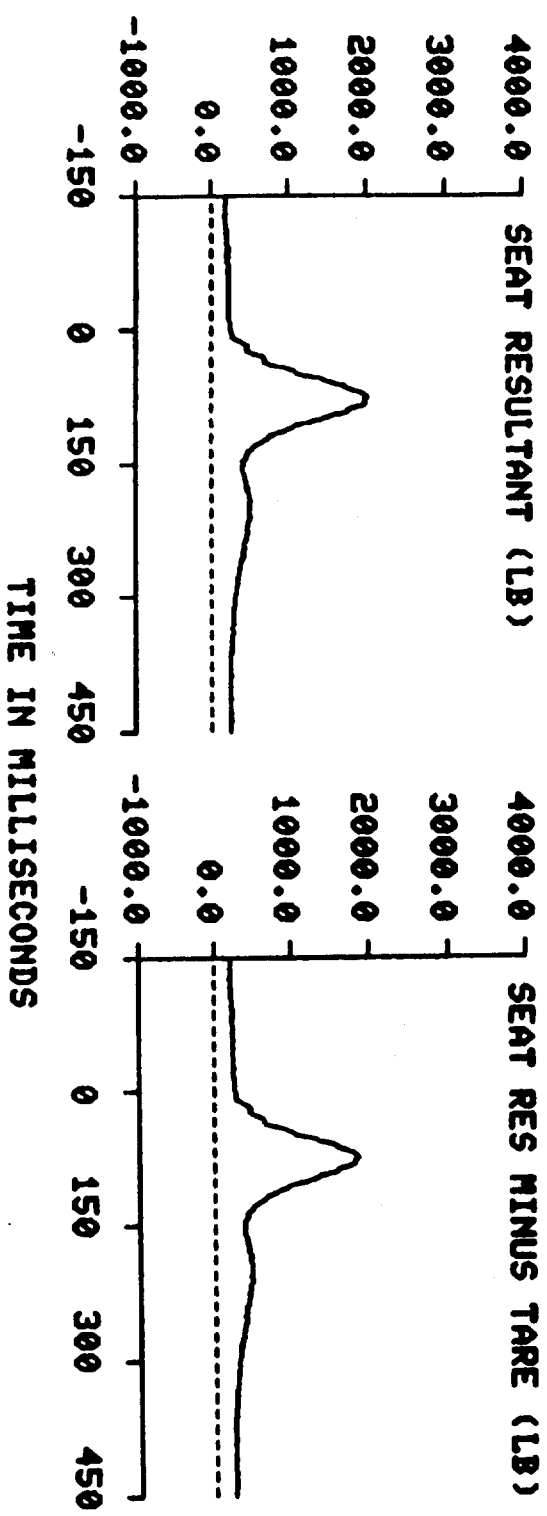
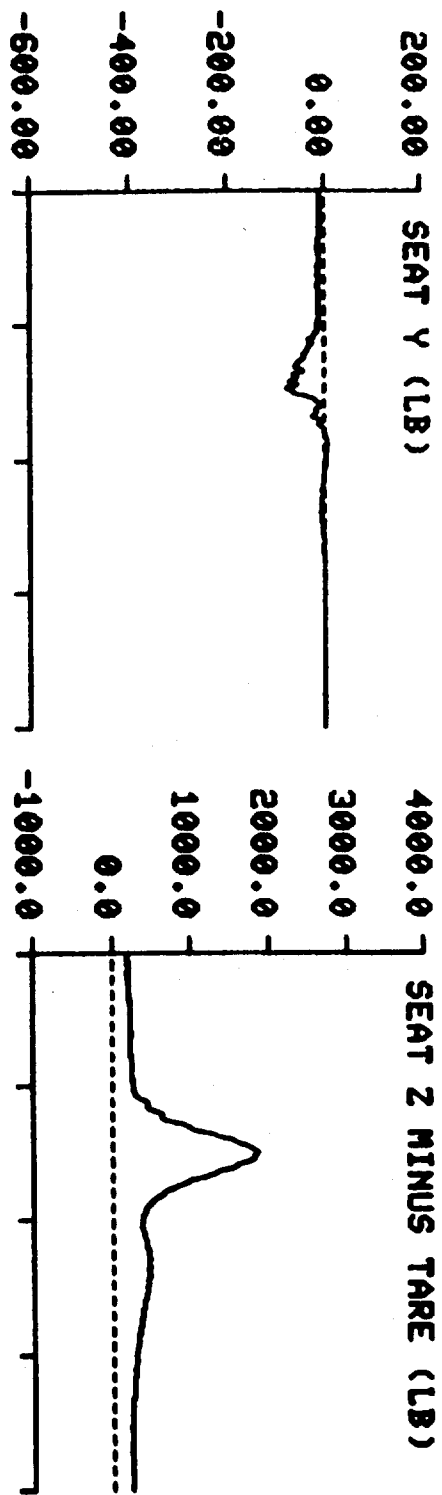


TIME IN MILLISECONDS

VIHAM STUDY TEST: 1430 SUBJ: K-3 CELL: C



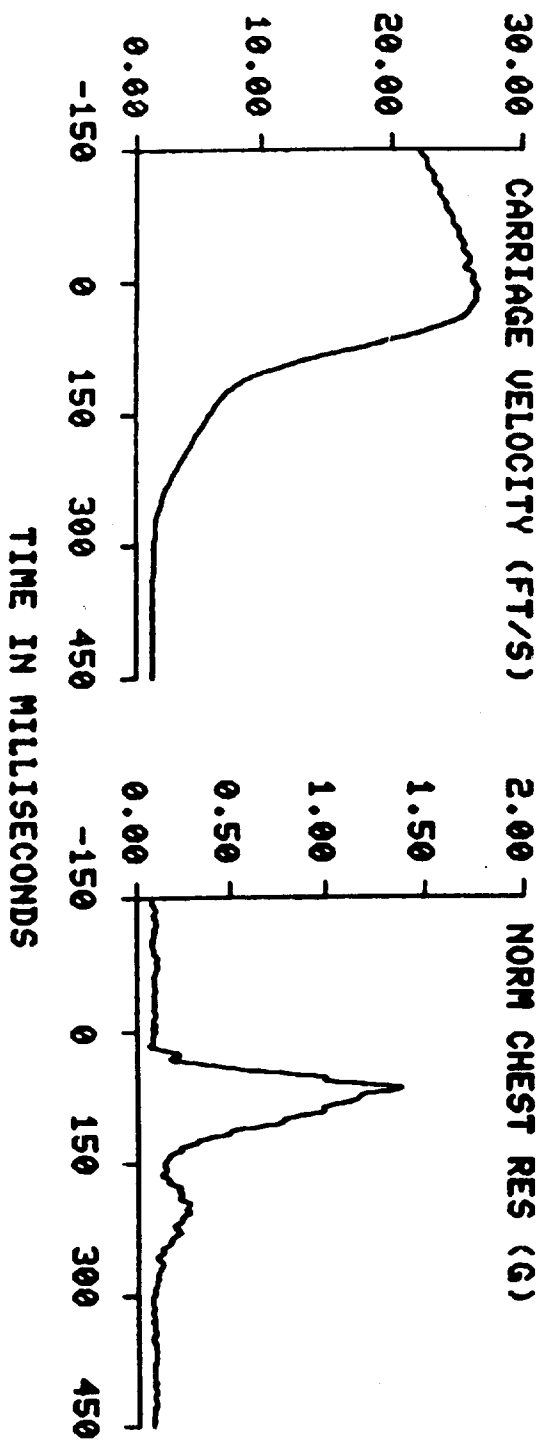
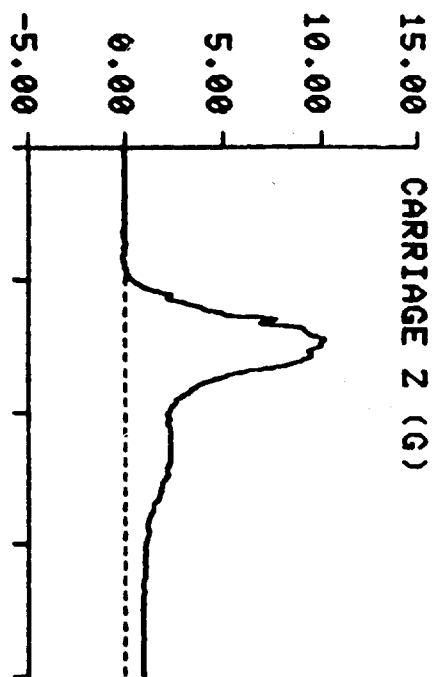
VIHAM STUDY TEST: 1430 SUBJ: K-3 CELL: C



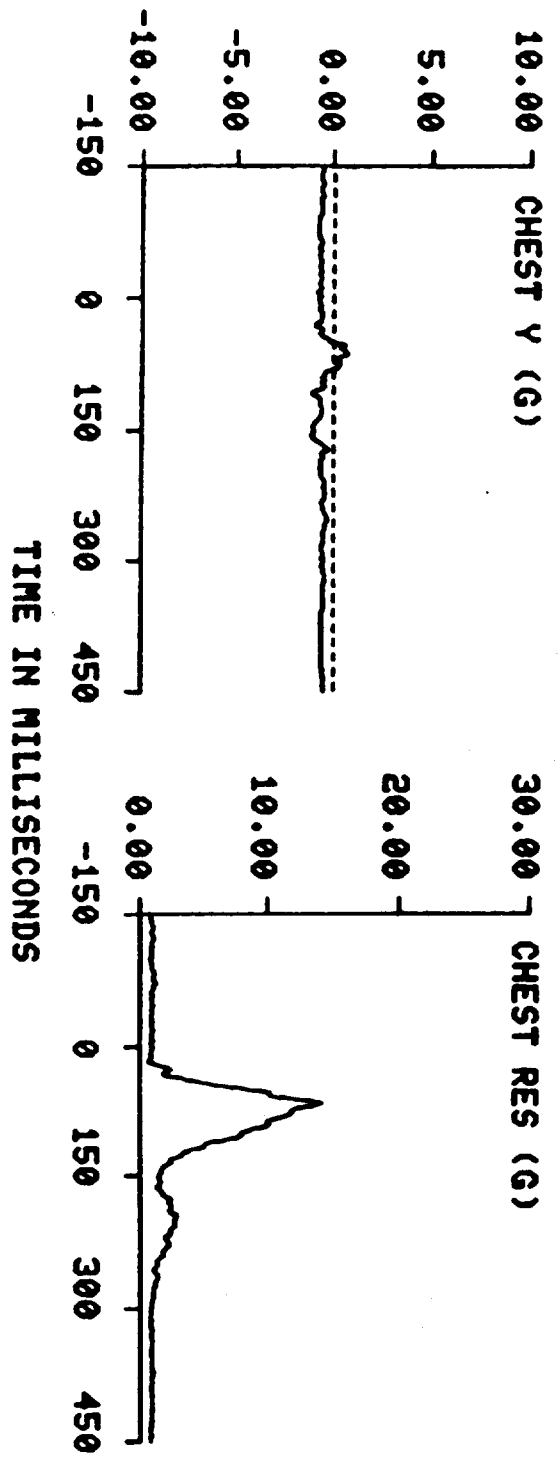
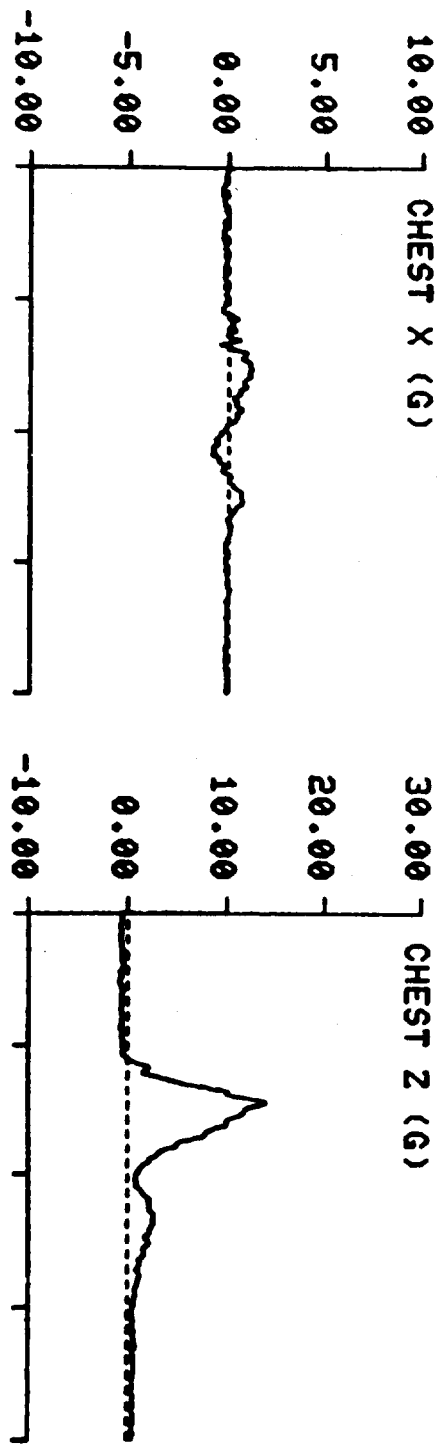
VIHAM STUDY TEST: 1437 SUBJ: ADAM-S WT: 143.0 NOM G: 10.0 CELL: C

DATA ID	IMMEDIATE PREIMPACT	MAXIMUM VALUE	MINIMUM VALUE	TIME OF MAXIMUM	TIME OF MINIMUM
REFERENCE MARK TIME (MS)				-153.	
2.5V EXT PWR (VOLTS)	2.50	2.50	2.50	0.	63.
10V EXT PWR (VOLTS)	10.00	10.00	10.00	54.	63.
CARRIAGE ACCELERATION (G)					
Z AXIS	0.00	10.20	0.43	66.	0.
SEAT ACCELERATION (G)					
X AXIS	-0.04	1.97	-1.60	11.	52.
Y AXIS	-0.11	2.03	-1.41	51.	29.
Z AXIS	-0.01	11.26	0.10	67.	2.
RESULTANT	0.20	11.27	0.44	67.	0.
RY (RAD/S**2)	5.29	47.34	-32.90	29.	23.
CARRIAGE VELOCITY (FT/S)	25.97	26.62	1.14	8.	382.
CHEST ACCELERATION (G)					
X AXIS	-0.13	1.18	-0.79	76.	168.
Y AXIS	-0.70	0.71	-1.17	61.	156.
Z AXIS	-0.56	14.09	-0.57	66.	0.
RESULTANT	0.91	14.11	0.63	66.	16.
RY (RAD/S**2)	5.07	396.46	-239.32	66.	74.
ADAM CHEST X ACCEL (G)	0.53	1.32	-0.49	230.	169.
ADAM HEAD ACCELERATION (G)					
X AXIS	0.12	1.11	-4.05	249.	116.
Z AXIS	-0.01	11.27	0.07	72.	0.
ADAM LUMBAR Z ACCEL (G)	0.05	12.73	0.14	48.	0.
ADAM LUMBAR Z FORCE (LB)	-50.15	598.09	-49.80	57.	0.
ADAM NECK Z FORCE (LB)	-14.43	123.59	-14.86	64.	4.
ADAM LF KNEE (DEGREES)	74.53	75.78	73.39	125.	71.
ADAM LF ELBOW (DEGREES)	60.83	70.27	60.33	143.	29.
SHOULDER STRAP FORCES (LB)					
X AXIS	11.17	68.90	5.47	60.	228.
Y AXIS	5.20	15.61	2.19	58.	147.
Z AXIS	7.88	86.88	8.90	64.	0.
RESULTANT	14.65	107.55	13.57	60.	298.
HARNESS ANCHOR FORCES (LB)					
LEFT HORIZ X AXIS	19.01	30.13	3.74	160.	63.
RIGHT HORIZ X AXIS	24.55	25.65	1.85	4.	70.
LEFT VERTICAL X AXIS	-2.48	5.33	-6.01	36.	11.
LEFT VERTICAL Y AXIS	35.81	36.01	0.08	1.	51.
LEFT VERTICAL Z AXIS	50.31	50.08	-24.83	1.	67.
LEFT VERTICAL RES	61.80	61.70	7.80	1.	119.
RIGHT VERTICAL X AXIS	-13.84	1.97	-15.06	51.	9.
RIGHT VERTICAL Y AXIS	27.74	26.78	-4.52	4.	70.
RIGHT VERTICAL Z AXIS	53.57	49.08	-19.99	0.	68.
RIGHT VERTICAL RES	61.90	57.32	1.08	6.	116.
BACKREST FORCES (LB)					
LEFT X AXIS	14.55	41.39	-5.05	241.	31.
RIGHT X AXIS	16.19	50.16	-2.45	91.	21.
CENTER X AXIS	-4.13	58.24	-17.07	44.	63.
X AXIS SUM	26.61	100.89	-7.00	86.	158.
Y AXIS	1.69	28.58	-34.88	26.	33.
LEFT Z AXIS	-14.55	121.19	-12.22	73.	0.
RIGHT Z AXIS	-11.42	135.82	-10.89	58.	14.
Z AXIS SUM	-25.97	217.32	-21.87	71.	0.
Z SUM MINUS TARE	-3.25	52.50	-48.04	46.	28.
RESULTANT	37.25	231.48	10.27	69.	307.
RESULTANT MINUS TARE	27.00	103.68	2.10	68.	183.
SEAT FORCES (LB)					
LEFT X AXIS	0.38	38.86	-77.18	108.	55.
RIGHT X AXIS	-0.03	42.52	-55.67	139.	80.
X AXIS SUM	0.35	66.24	-72.34	136.	55.
Y AXIS	-3.64	23.51	-108.73	114.	48.
LEFT Z AXIS	9.87	445.85	11.78	61.	1.
RIGHT Z AXIS	4.41	277.94	4.41	54.	3.
CENTER Z AXIS	57.41	1239.83	60.53	69.	0.
Z AXIS SUM	71.69	1917.03	79.83	68.	1.
Z SUM MINUS TARE	90.37	1731.37	93.32	69.	9.
RESULTANT	71.82	1919.09	80.34	68.	1.
RESULTANT MINUS TARE	90.12	1733.52	94.34	69.	9.

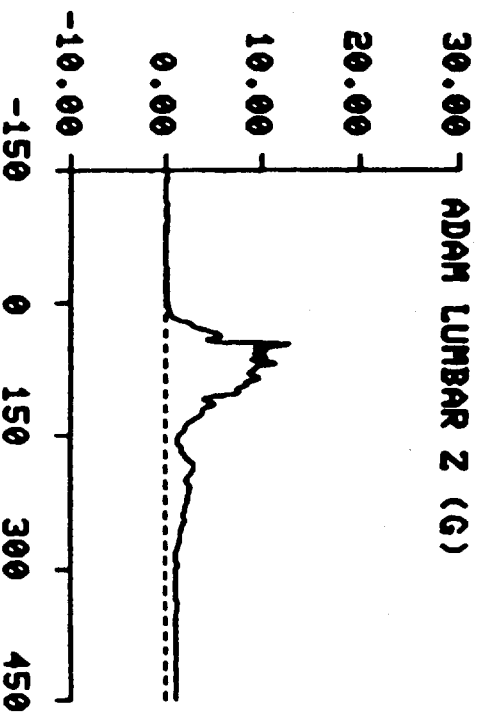
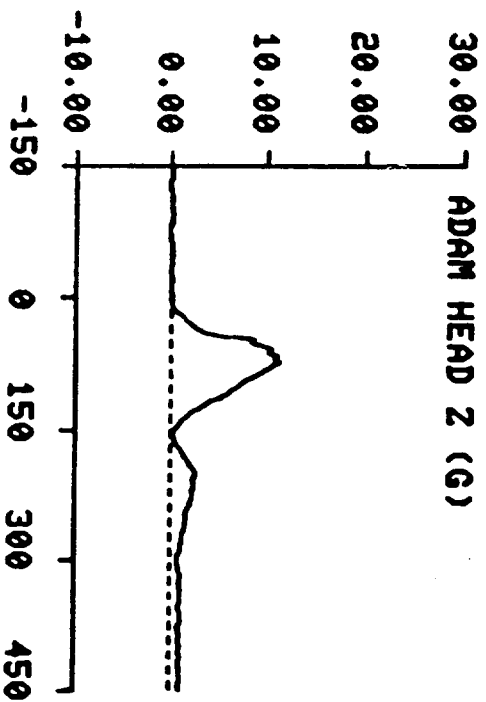
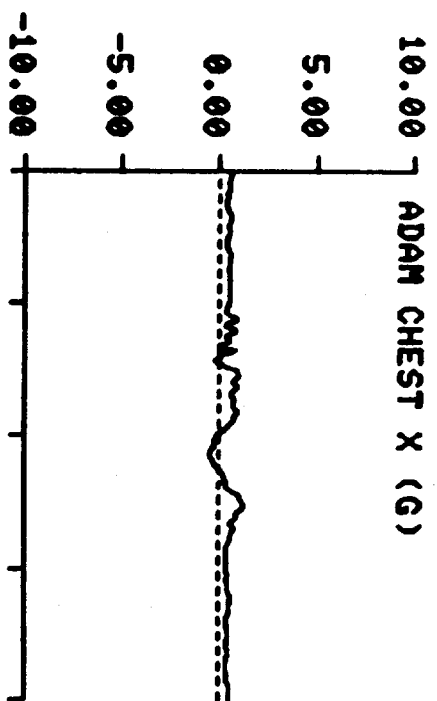
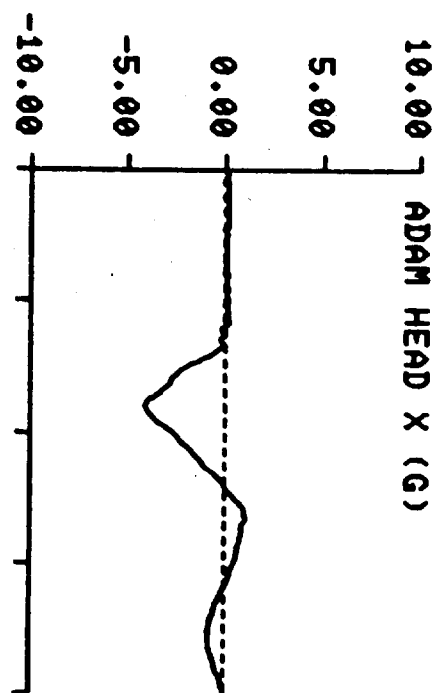
VIHAM STUDY TEST: 1437 SUBJ: ADAM-S CELL: C



VIHAM STUDY TEST: 1437 SUBJ: ADAM-S CELL: C

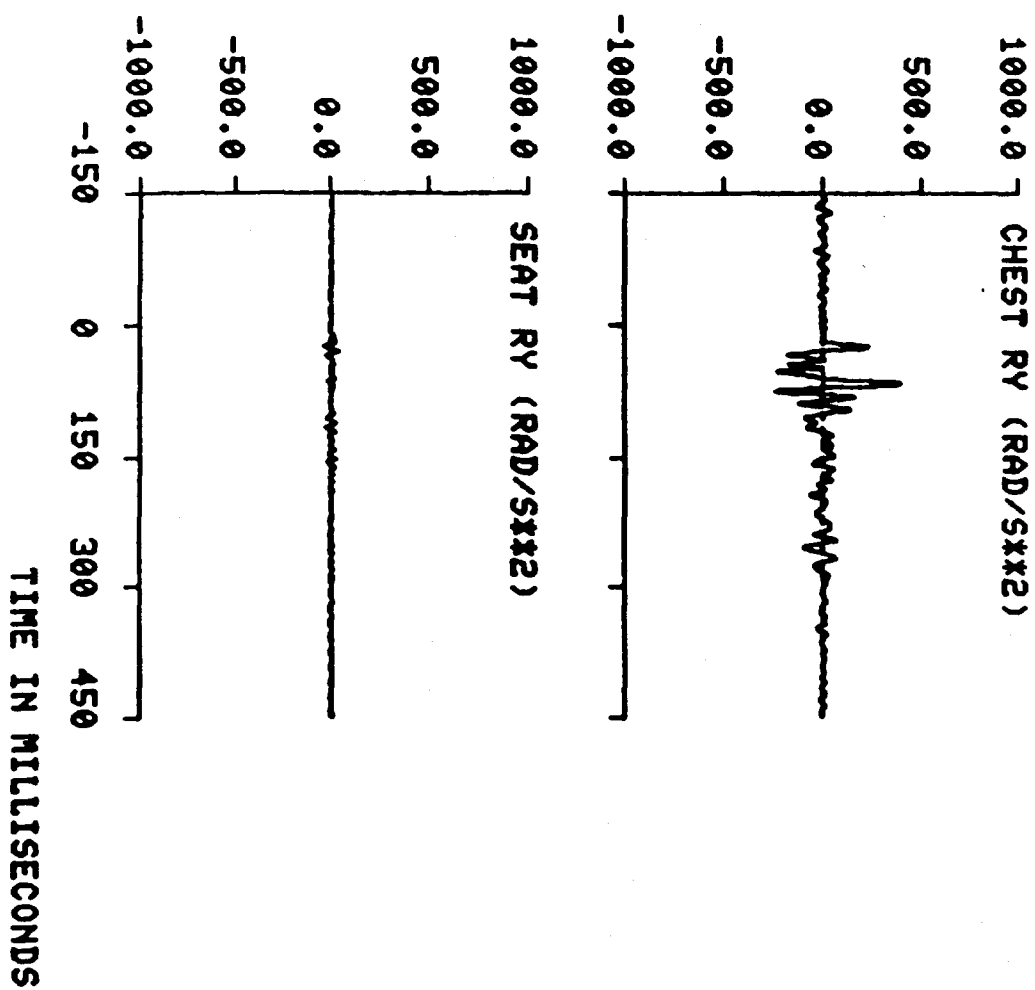


VIHAN STUDY TEST: 1437 SUBJ: ADAM-S CELL: C

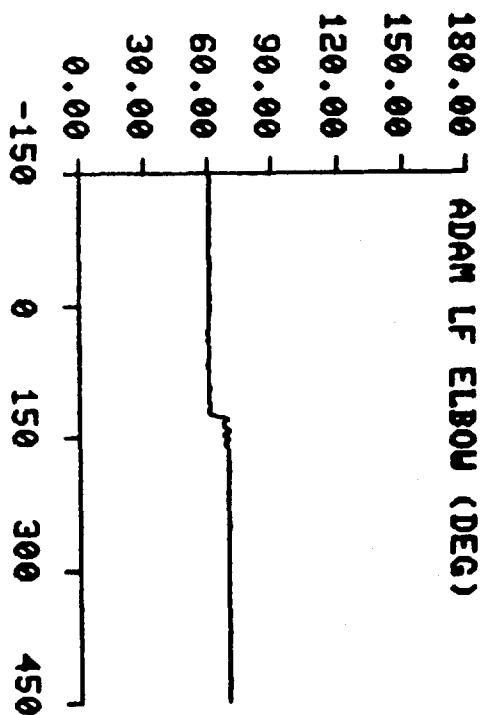
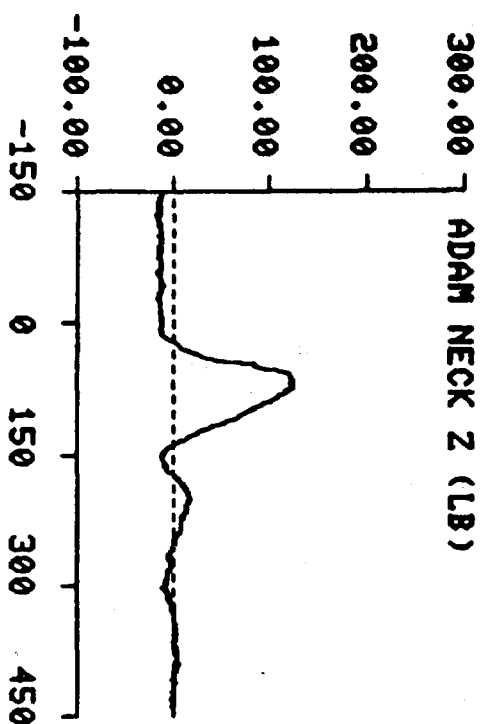
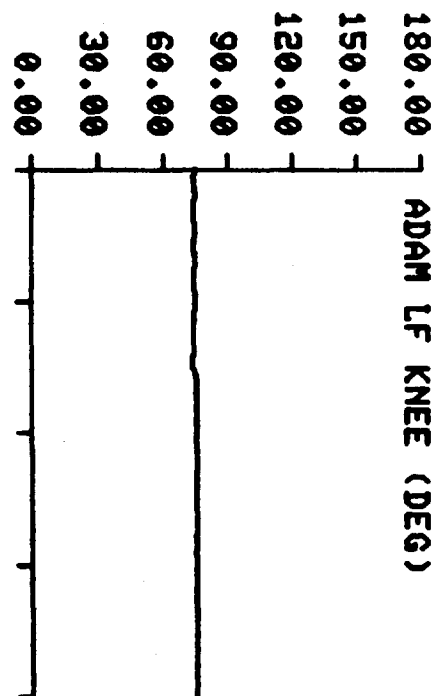
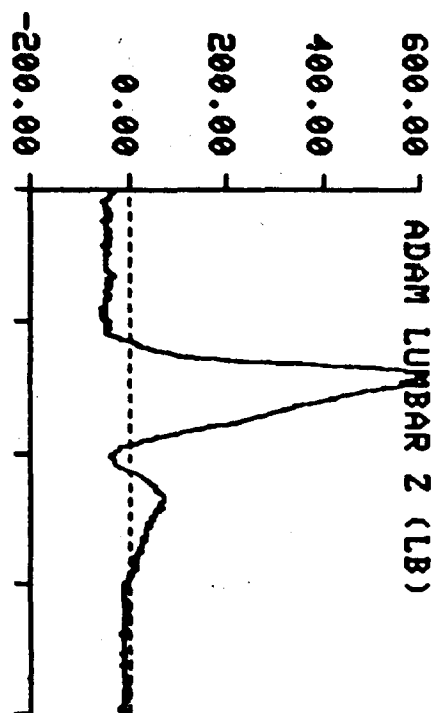


TIME IN MILLISECONDS

VIHAM STUDY TEST: 1437 SUBJ: ADAM-S CELL: C

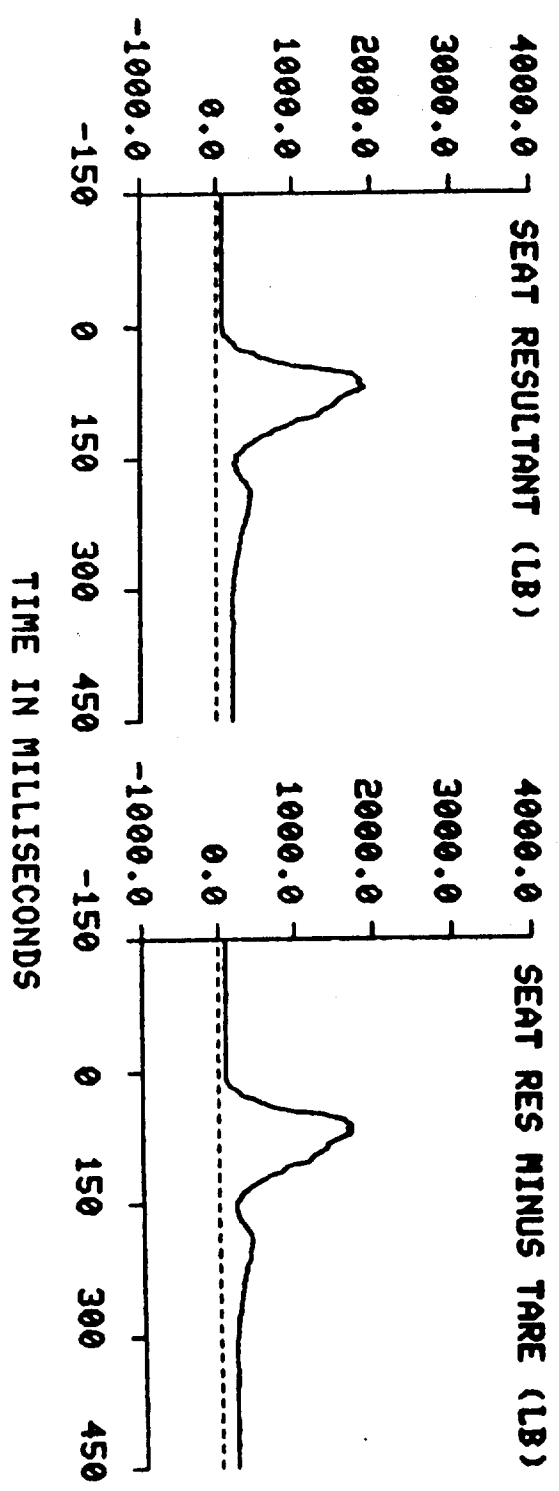
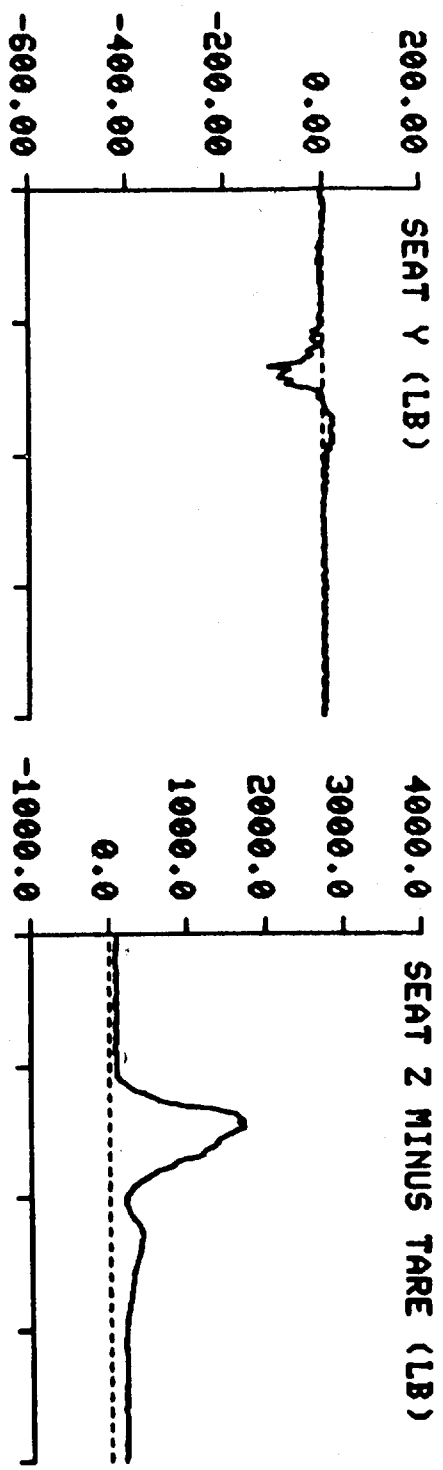


VIHAM STUDY TEST: 1437 SUBJ: ADAM-S CELL: C



TIME IN MILLISECONDS

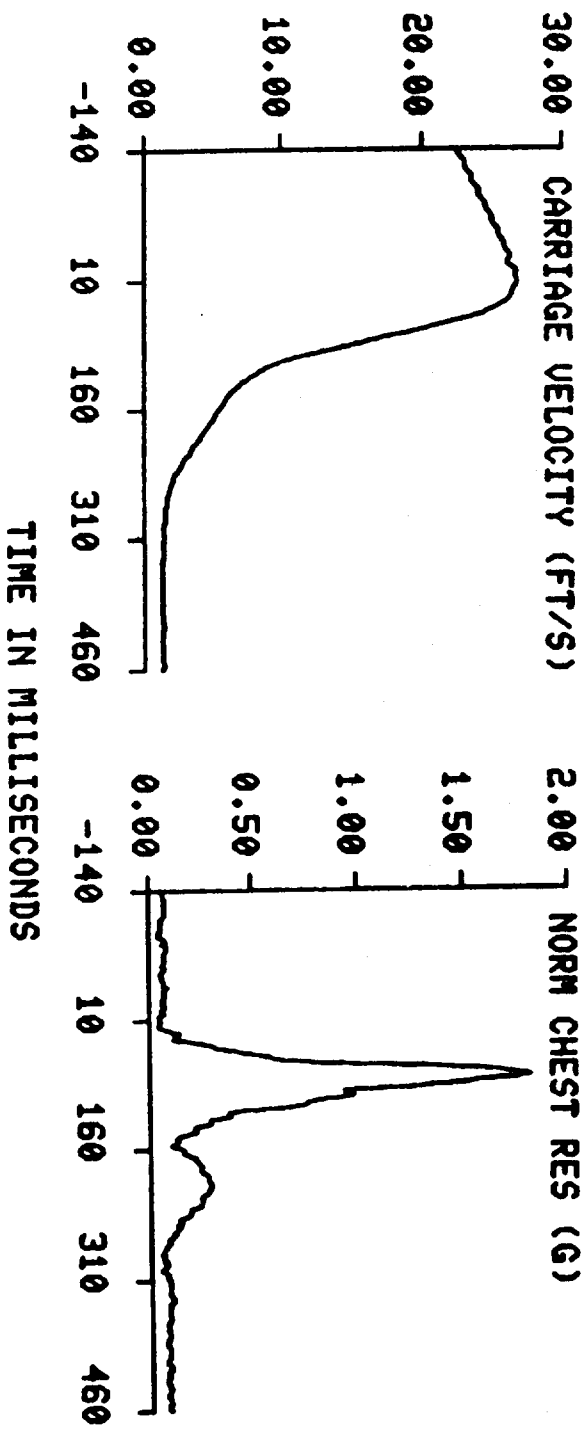
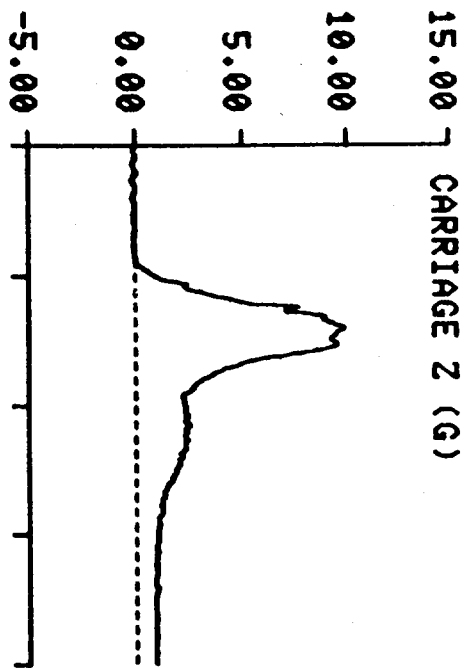
VIHAM STUDY TEST: 1437 SUBJ: ADAM-S CELL: C



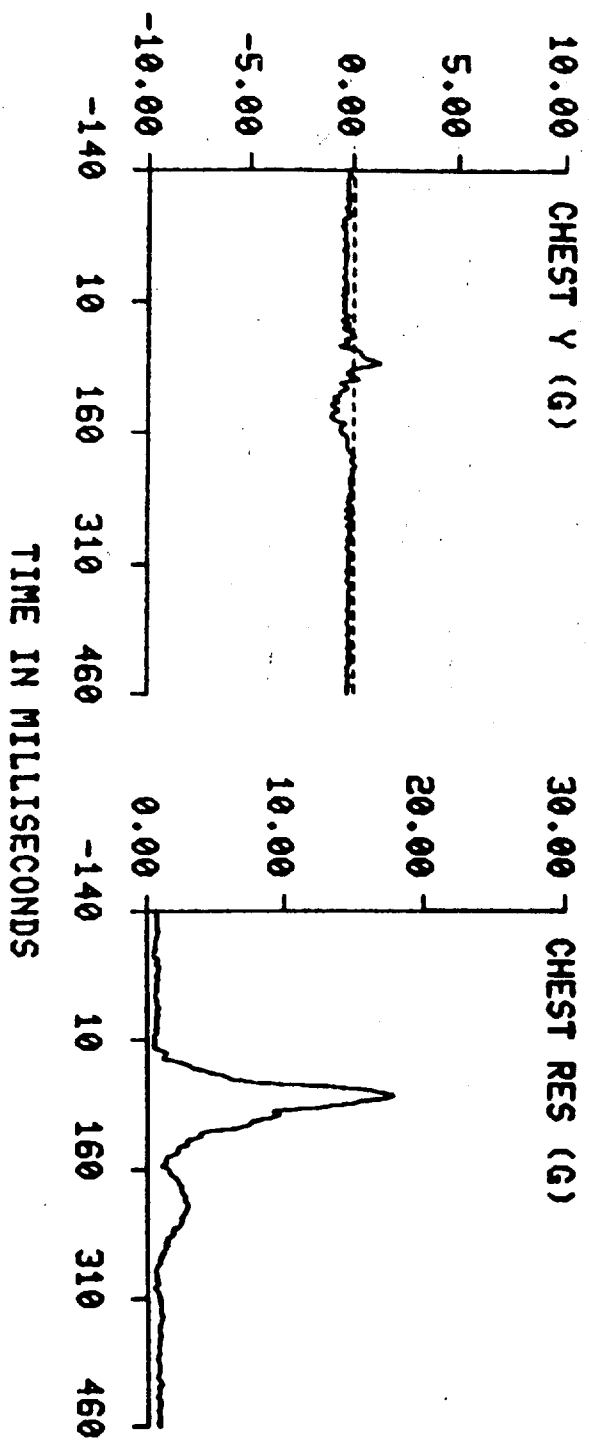
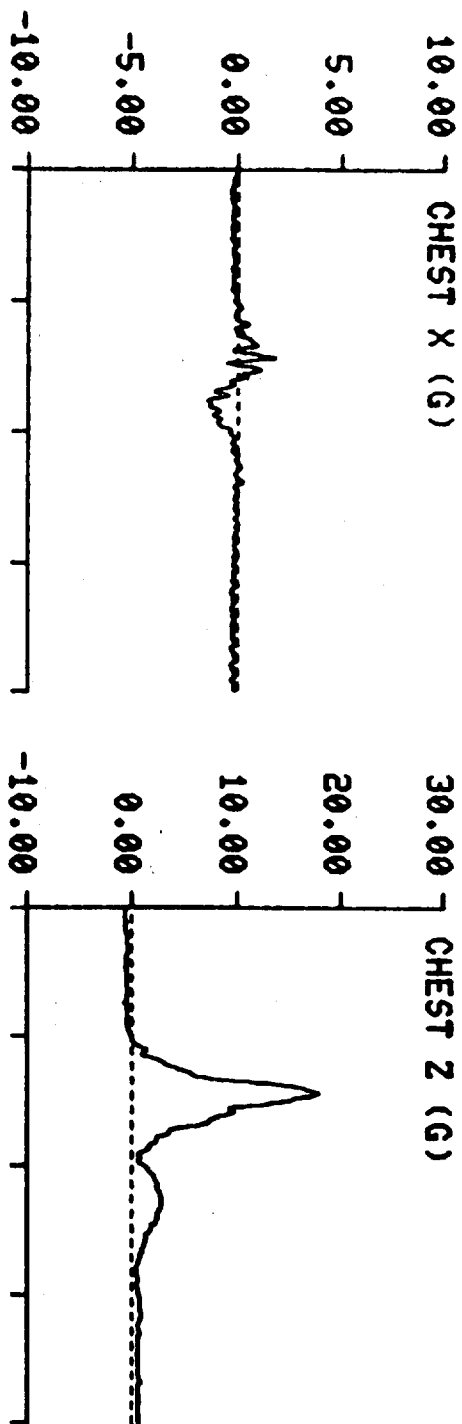
VIHAM STUDY TEST: 1467 SUBJ: ADAM-L WT: 212.0 NOM G: 10.0 CELL: C

DATA ID	IMMEDIATE PREIMPACT	MAXIMUM VALUE	MINIMUM VALUE	TIME OF MAXIMUM	TIME OF MINIMUM
REFERENCE MARK TIME (MS)				-148.	
2.5V EXT PWR (VOLTS)	2.50	2.50	2.50	279.	18.
10V EXT PWR (VOLTS)	10.00	10.00	10.00	179.	6.
CARRIAGE ACCELERATION (G)					
Z AXIS	-0.01	9.83	0.42	68.	0.
SEAT ACCELERATION (G)					
X AXIS	-0.02	1.33	-1.74	58.	53.
Y AXIS	-0.14	1.88	-1.28	24.	140.
Z AXIS	-0.09	11.64	-0.65	69.	24.
RESULTANT	0.20	11.66	0.35	69.	4.
RY (RAD/S**2)	-5.36	35.20	-51.72	30.	24.
CARRIAGE VELOCITY (FT/S)	26.14	26.75	1.20	1.	424.
CHEST ACCELERATION (G)					
X AXIS	-0.20	1.78	-1.44	73.	123.
Y AXIS	-0.42	1.26	-1.11	78.	128.
Z AXIS	-0.48	17.88	-0.42	76.	0.
RESULTANT	0.67	17.92	0.39	76.	7.
RY (RAD/S**2)	-0.22	1216.20	-613.95	77.	96.
ADAM CHEST X ACCEL (G)	0.05	0.25	-1.84	68.	122.
ADAM HEAD ACCELERATION (G)					
X AXIS	0.18	0.64	-5.32	223.	126.
Z AXIS	-0.01	15.36	-0.06	73.	141.
ADAM LUMBAR Z ACCEL (G)	-0.16	14.02	-0.09	71.	0.
ADAM LUMBAR Z FORCE (LB)	-80.68	1285.64	-79.20	72.	0.
ADAM NECK Z FORCE (LB)	-13.51	190.77	-17.41	73.	1.
ADAM LF KNEE (DEGREES)	79.86	80.21	77.55	21.	87.
ADAM LF ELBOW (DEGREES)	63.98	65.55	63.03	131.	77.
SHOULDER STRAP FORCES (LB)					
X AXIS	13.05	169.94	5.99	126.	262.
Y AXIS	0.89	9.62	-1.65	80.	26.
Z AXIS	1.83	94.17	1.91	98.	0.
RESULTANT	13.23	188.00	7.95	127.	263.
HARNESS ANCHOR FORCES (LB)					
LEFT HORIZ X AXIS	28.39	53.95	11.23	142.	72.
RIGHT HORIZ X AXIS	50.79	70.55	22.95	142.	209.
LEFT VERTICAL X AXIS	1.21	6.58	-3.63	53.	127.
LEFT VERTICAL Y AXIS	42.26	47.14	-0.96	143.	80.
LEFT VERTICAL Z AXIS	67.39	73.64	-21.69	150.	69.
LEFT VERTICAL RES	79.56	87.20	6.54	151.	109.
RIGHT VERTICAL X AXIS	-19.20	-0.44	-24.77	55.	139.
RIGHT VERTICAL Y AXIS	35.74	35.33	-6.20	0.	69.
RIGHT VERTICAL Z AXIS	75.42	71.04	-25.45	0.	68.
RIGHT VERTICAL RES	85.64	81.51	5.99	0.	35.
BACKREST FORCES (LB)					
LEFT X AXIS	7.69	9.04	-2.26	26.	144.
RIGHT X AXIS	22.88	29.44	-3.13	10.	43.
CENTER X AXIS	53.47	97.40	-13.05	58.	130.
X AXIS SUM	84.04	98.28	-14.68	58.	130.
Y AXIS	5.94	41.69	-27.64	57.	91.
LEFT Z AXIS	-12.80	103.79	-22.89	56.	361.
RIGHT Z AXIS	-10.37	125.72	-11.04	67.	5.
Z AXIS SUM	-23.17	177.37	-18.12	70.	0.
Z SUM MINUS TARE	1.27	62.26	-64.47	197.	69.
RESULTANT	87.39	197.75	15.79	57.	131.
RESULTANT MINUS TARE	84.28	106.64	5.40	58.	144.
SEAT FORCES (LB)					
LEFT X AXIS	-13.87	30.62	-27.40	108.	14.
RIGHT X AXIS	-3.53	51.53	-14.68	140.	66.
X AXIS SUM	-17.40	68.07	-29.18	135.	70.
Y AXIS	-0.91	1.66	-110.81	116.	71.
LEFT Z AXIS	12.12	519.64	8.06	74.	0.
RIGHT Z AXIS	12.71	605.54	11.87	76.	0.
CENTER Z AXIS	92.40	2327.66	100.08	72.	3.
Z AXIS SUM	117.23	3424.90	126.24	73.	3.
Z SUM MINUS TARE	137.33	3259.32	137.79	73.	0.
RESULTANT	118.53	3426.79	127.54	72.	3.
RESULTANT MINUS TARE	138.44	3261.31	139.08	73.	0.

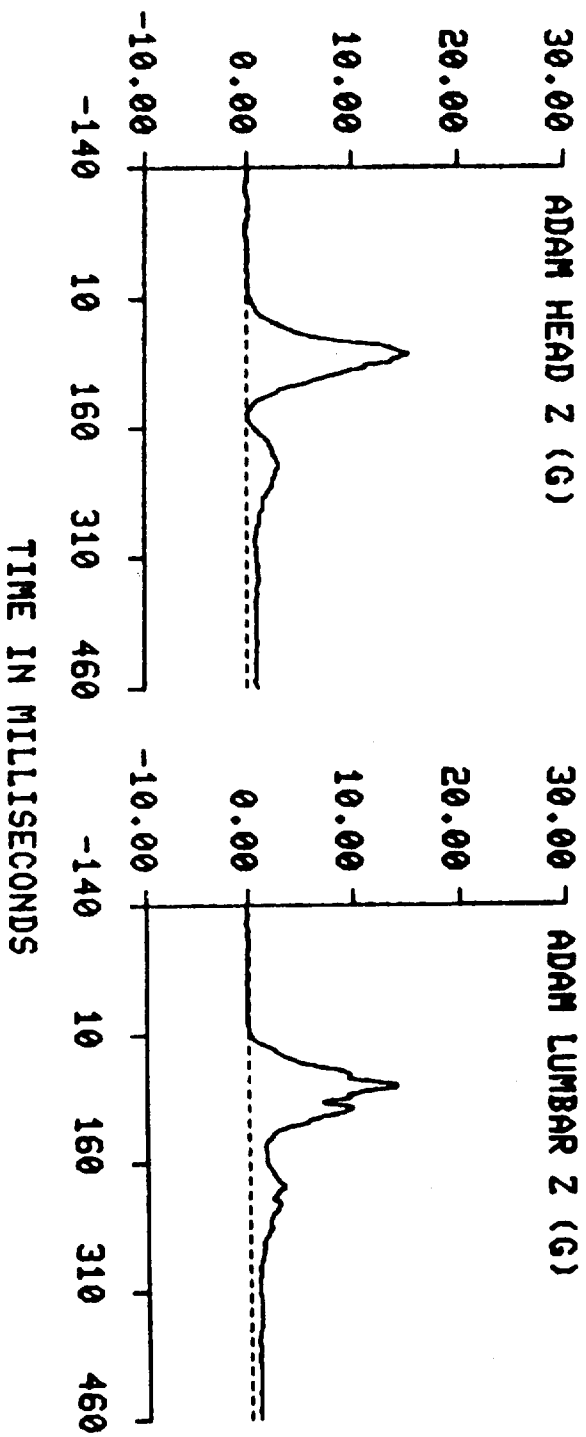
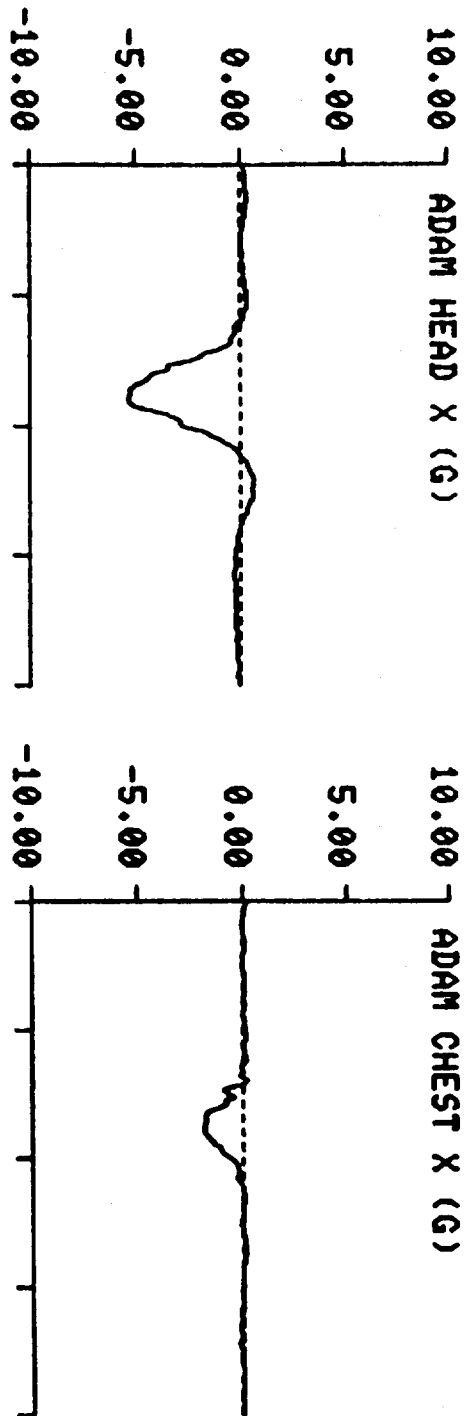
VIHAM STUDY TEST: 1467 SUBJ: ADAM-L CELL: C



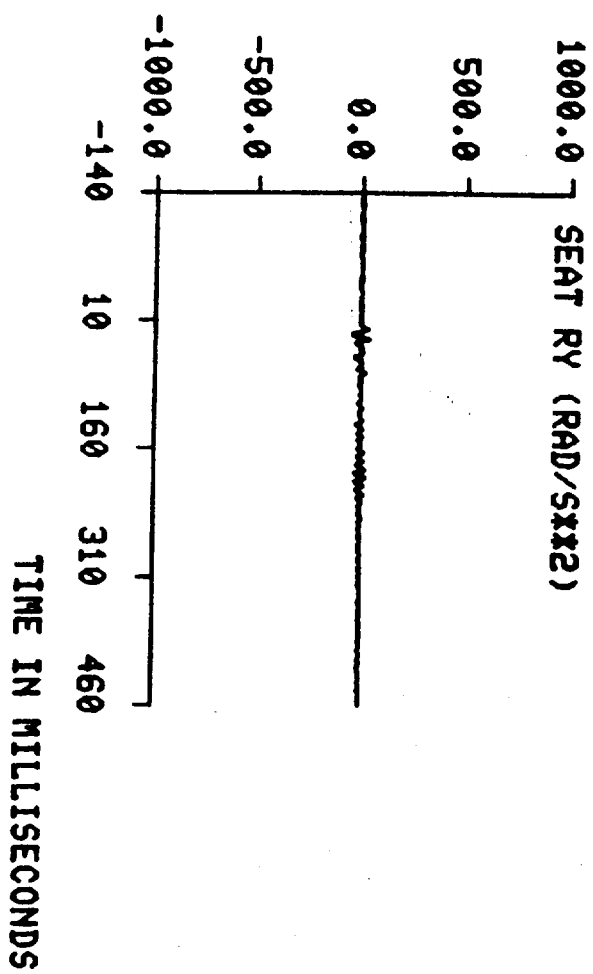
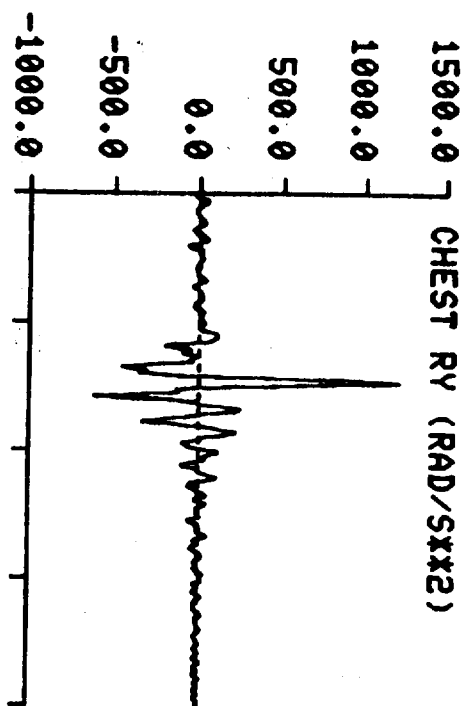
VIHAM STUDY TEST: 1467 SUBJ: ADAM-L CELL: C



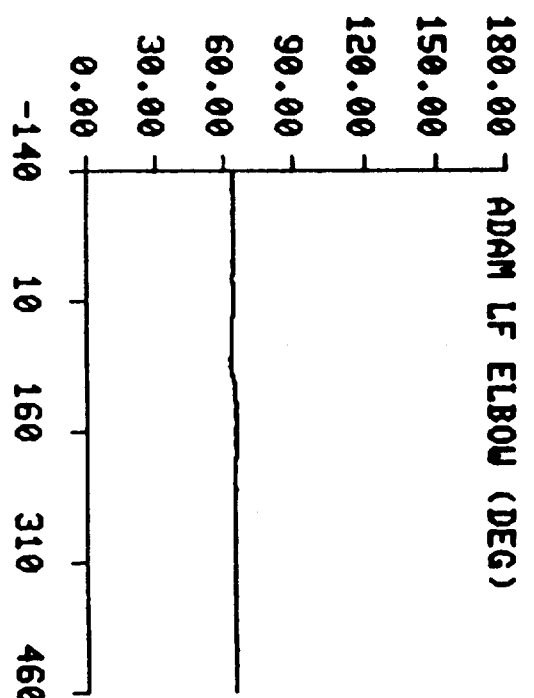
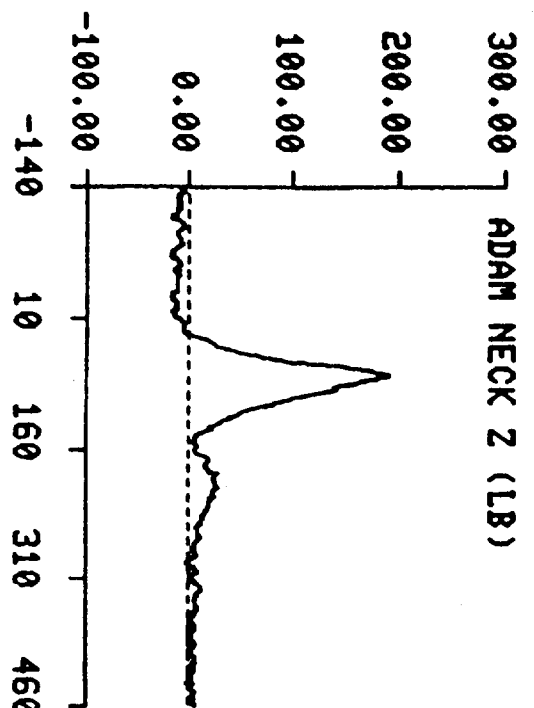
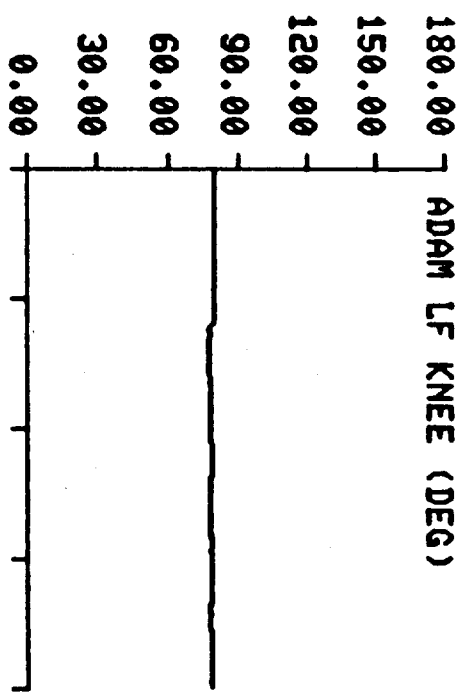
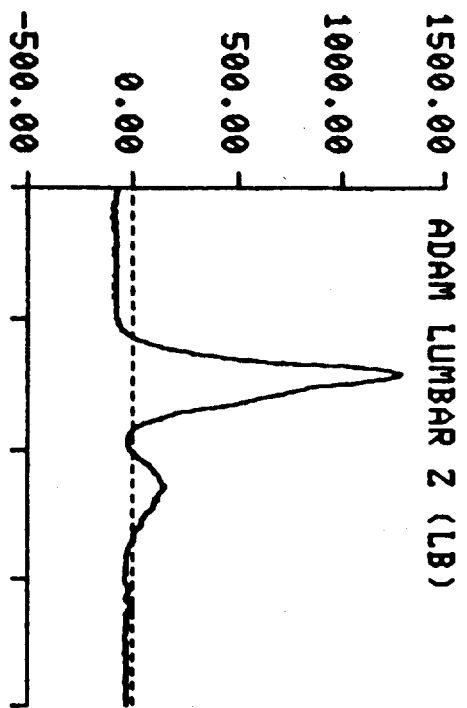
VIHAM STUDY TEST: 1467 SUBJ: ADAM-L CELL: C



VIHAM STUDY TEST: 1467 SUBJ: ADAM-L CELL: C

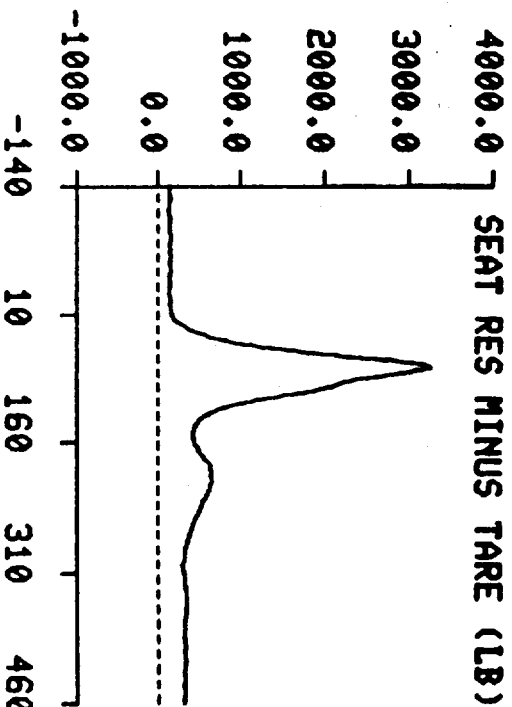
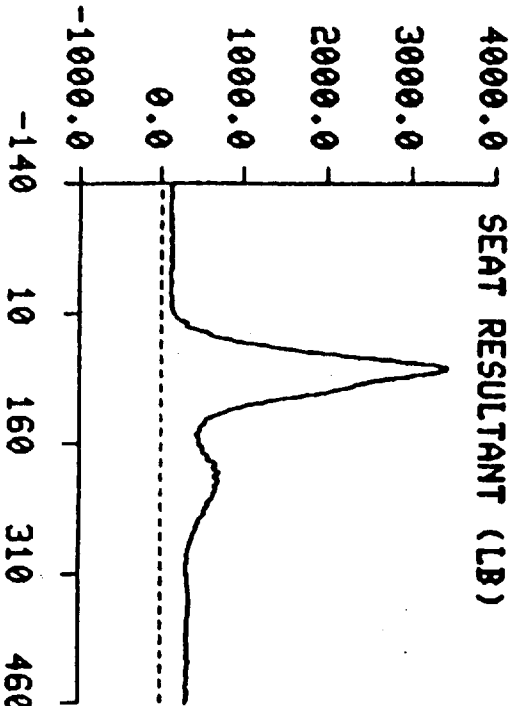
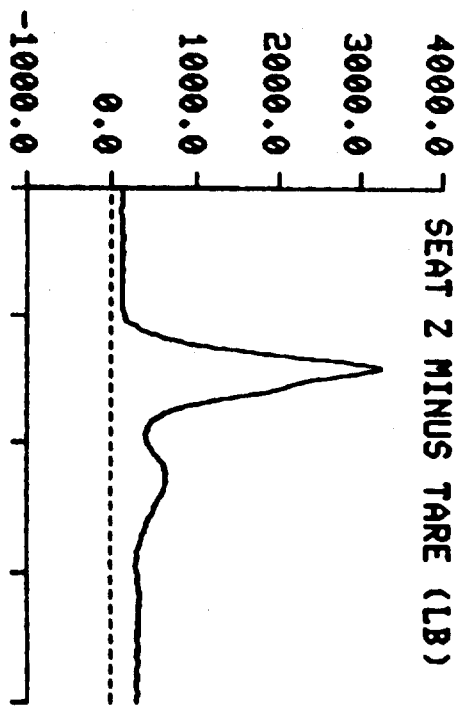
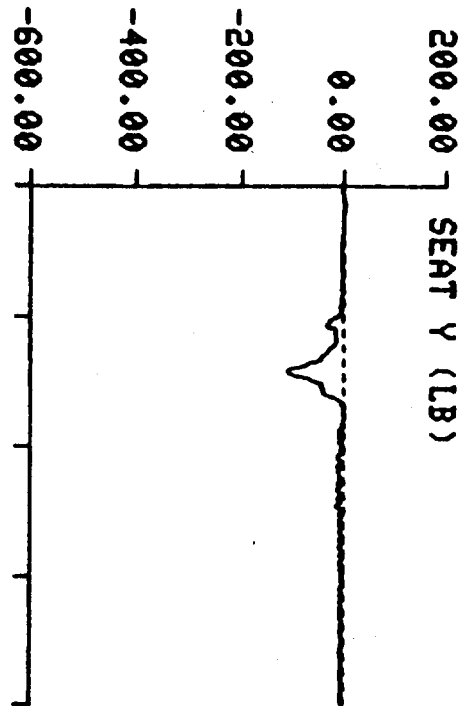


VIHAM STUDY TEST: 1467 SUBJ: ADAM-L CELL: C



TIME IN MILLISECONDS

VIHAM STUDY TEST: 1467 SUBJ: ADAM-L CELL: C



TIME IN MILLISECONDS